Aus dem Pathologischen Institut der
Ludwig-Maximilians-Universität München
Direktor: Prof. Dr. med. Thomas Kirchner
Arbeitsgruppe Experimentelle und Molekulare Pathologie
Leiter: Prof. Dr. rer. nat. Heiko Hermeking

The role of miR-34 in epithelial to mesenchymal transition and metastasis of colorectal cancer

---

Dissertation zum Erwerb des
Doktorgrades der Naturwissenschaften (Dr. rer. nat.)
an der Medizinischen Fakultät
der Ludwig-Maximilians-Universität München

vorgelegt von

Helge Siemens

aus Bad Homburg v.d.H.

2013

Gedruckt mit der Genehmigung der Medizinischen Fakultät der Ludwig-Maximilians-Universität München

Betreuer:
Prof. Dr. rer. nat. Heiko Hermeking

Zweitgutachter:
Prof. Dr. rer. nat. Peter Nelson

Dekan:
Prof. Dr. med. Dr. h.c. Maximilian Reiser, FACR, FRCR

Tag der mündlichen Prüfung:
13.02.2014

Correction: Detection of *miR-34a* Promoter Methylation in Combination with Elevated Expression of c-Met and β-Catenin Predicts Distant Metastasis of Colon Cancer

Helge Siemens, Jens Neumann, Rene Jackstadt, Ulrich Mansmann, David Horst, Thomas Kirchner, and Heiko Hermeking

In the original version of this article (1), three errors exist in Fig. 1: splice lines were missing in both Fig. 1A and B, the same gel set was used to represent lanes M0-8 to M0-14 and M1-1 to M1-7 in Fig. 1B (lanes M1-1 to M1-7 are correct), and the figure legend referred to H_2O instead of dH_2O. The errors have been corrected in the latest online HTML and PDF versions of the article. The authors regret the errors.

Reference

1. Siemens H, Neumann J, Jackstadt R, Mansmann U, Horst D, Kirchner T, et al. Detection of *miR-34a* promoter methylation in combination with elevated expression of c-Met and β-catenin predicts distant metastasis of colon cancer. Clin Cancer Res 2013;19:710–20.

Published online April 14, 2022.
Clin Cancer Res 2022;28:1739
doi: 10.1158/1078-0432.CCR-22-0505

Ehrenwörtliche Erklärung

Ich erkläre hiermit an Eides statt, dass ich die vorliegende Dissertation mit dem Thema ‚The role of miR-34 in epithelial to mesenchymal transition and metastasis of colorectal cancer' selbständig verfasst, mich außer der angegebenen keiner weiteren Hilfsmittel bedient und alle Erkenntnisse, die aus dem Schrifttum ganz oder annähernd übernommen sind, als solche kenntlich gemacht und nach ihrer Herkunft unter Bezeichnung der Fundstelle einzeln nachgewiesen habe.

Ich erkläre des Weiteren, dass die hier vorgelegte Dissertation nicht in gleicher oder in ähnlicher Form bei einer anderen Stelle zur Erlangung eines akademischen Grades eingereicht wurde.

München, den 18.09.2013

Helge Siemens

Table of contents

1) Introduction

1.1) Biogenesis and function of miRNAs

MicroRNAs (miRNAs) are small molecules consisting of about 22 nucleotides. Currently, there are 1872 miRNAs annotated according to the public microRNA database miRBase (http://www.mirbase.org; Griffiths-Jones, 2004). miRNAs were initially discovered in the nematode model organism *Caenorhabditis elegans* (Lee et al, 1993) and described as small transcripts complementary to a repeated sequence in the 3'-UTR of the *lin-14* transcript. The authors speculated about an antisense mechanism, which enables these small RNAs to regulate the translation of *lin-14*. Twenty years later this hypothesis has been validated by multiple studies elucidating the mode of action, which underlies gene regulation by miRNAs. The biogenesis of miRNA genes can be sub-divided into two pathways. While in the canonical processing pathway the miRNA encoding messenger RNA (mRNA) is transcribed from its promoter, so called miRtrons are located in introns of host genes, which also encode proteins (Kim et al, 2009; Krol et al, 2010). Transcription of miRNA-encoding RNAs is generally executed by RNA polymerase II (RNAPol II) resulting in a precursor transcript, the so called primary (pri-) miRNA. A protein-complex consisting of dsRNA-binding proteins and the RNase III family member Drosha cleaves the pri-miRNA, resulting in an approximately 70 nucleotides long precursor hairpin structure, the pre-miRNA. In case of the miRtrons the pre-miRNA is a result of post-transcriptional splicing of the host mRNA. The resulting pre-miRNA is trans-located from the nucleus to the cytoplasm via Exportin-5 (Brownawell & Macara, 2002). Once in the cytoplasm, the pre-miRNA is bound by a protein complex containing the type III RNase Dicer, which enzymatically cleaves the hairpin into two complementary, approximately 22 nucleotides long miRNAs bound to each other in a miRNA/miRNA* duplex. Following this processing, one or both of the strands are incorporated into the RNA-induced silencing complex (RISC), which can target specific mRNA molecules via a mechanism

known as RNA interference (Filipowicz, 2005; Sontheimer, 2005; Fire et al, 1998; Zamore et al, 2000).

The minimal RISC complex, sufficient for target recognition and cleavage of RNA molecules, also referred to as Slicer, was shown to consist of an Argonaute endonuclease protein bound to a small, regulatory, target-complementary RNA (Rivas et al, 2005; Pratt & MacRae, 2009). The target recognition is mediated by binding of an up to seven nucleotides long stretch, located within the 5'-portion of the miRNA, the so called seed-sequence, with a complementary sequence in the 3'-UTR of the target mRNA, the seed-matching sequence. This interaction facilitates the recruitment of the RISC/Ago2 complex to the targeted mRNA, which results in either inhibition of translation initiation, via interfering with the recruitment of the 40S small ribosomal subunit, and/or enhancement of mRNA degradation, through recruitment of a deadenylase complex, which mediates the removal of the poly adenosine tail and subsequent cleavage of the open reading frame (ORF; Bartel, 2009; Fabian et al, 2010; Huntzinger & Izaurralde, 2011).

The importance of this mechanism for the repression of gene activity is universal, since it was found to be phylogenetically conserved in all the bilaterally symmetric animals (Pasquinelli et al, 2000). Each miRNA may control the expression of hundreds of target mRNAs (reviewed in Bartel, 2009), and it has been estimated that approximately 60% of all human protein coding genes are under influence of miRNA regulation (Friedman et al, 2009).

1.2) Epigenetic silencing

The term epigenetics is defined as heritable changes in gene expression, which are not caused by changes of the underlying DNA sequence but by chemical modifications of its nucleotides and/or changes in molecules that interact with it (Bird, 2007). Epigenetic silencing consequently describes the down-regulation of gene expression by epigenetic mechanisms. Recent publications suggest that the epigenome is dynamic and reacts in response to changes of the environment, diet or aging (Feil & Fraga, 2011; Feinberg, 2007). The three major mechanisms responsible for these epigenetic changes are DNA-methylation, non-coding RNAs, and modifications of histone tails (Mulero-Navarro & Esteller, 2008). DNA-methylation occurs by a covalent modification, in which a methyl-group is transferred by DNA-methyltransferases (DNMTs) from *S*-adenosylmethionine to the C-5 position of cytosine, which is located 5' to a guanosine and forms a CpG dinucleotide (Iacobuzio-Donahue, 2009). CpG dinucleotides are under-represented in the genome, but in some regions, so called CpG islands, they cluster in high density. Often located close to the promoter regions of genes, the CpGs within these islands are mainly unmethylated (Jones & Baylin, 2002). Methylation of the CpGs negatively influences the expression of gene transcription in two ways: First, methyl-CpG-binding domain proteins (MBPs) are able to recruit chromatin modifying enzymes like histone-deacetylases (HDACs; Jones et al, 1998), which in turn initiate the condensation of chromatin and subsequent gene silencing. In cancer this mechanism was first discovered for the *Retinoblastoma* (*Rb*) tumor suppressor gene about 20 years ago (Ohtani-Fujita et al, 1993; Sakai et al, 1991). Second, the methylation of CpGs might interfere with the binding of transcription factors. This results in expression changes as well, as discovered more recently (Perini et al, 2005).

In total there are more than 100 genes known to be hyper-methylated at the promoter in association with cancer (Shames et al, 2007). Recent findings indicate that intragenic DNA-methylation exists as well, but the regulatory consequences are not well understood so far (Shenker & Flanagan, 2012).

Furthermore, there are indications that CpG-methylation is a crucial step in the progression from local tumors towards metastases (Li & Chen, 2011). The detection of these methylation events is not only important with respect to the understanding of underlying mechanisms in tumor initiation and progression, but may also serve as biomarker for several different cancer types (Mulero-Navarro & Esteller, 2008).

1.3) The miR-34 family

The following section introduces members, regulations and cancer-specific alterations of this miRNA family.

1.3.1) Members and structure

The core of the miR-34 family is represented by three members: as shown in Figure 1 the m*iR-34a* gene is located on chromosome 1p36 and is consisting of two exons connected by a ~30 kbp DNA intron (Hermeking, 2010). The sequence of the mature miR-34a resides on the second exon. *miR-34b* and *miR-34c* are encoded by a shared pri-miRNA, which resides on chromosome 11q23 and therefore have comparable levels of expression.

Due to their high homology in the seed-sequences and secondary structures miR-449a/b/c belong to the miR-34 family as well. The respective genes are organized as a cluster and embedded into a highly conserved intron region of the *CDC20B* gene on chromosome five (Lize et al, 2011).

1.3.2) Regulation

In 2007 the miR-34 family acquired wider recognition, since it was found to be up-regulated by the tumor suppressor p53, often referred to as ‘guardian of the genome’ (Lane, 1992), suggesting an anti-tumor function of this miRNA family: several laboratories reported miR-34a to be the most prominently induced miRNA upon induction of p53 (Chang et al, 2007; He et al, 2007a; Raver-Shapira et al, 2007; Tarasov et al, 2007; Tazawa et al, 2007). As shown in Figure 1, one p53 binding site was identified close to the transcription start of *miR-34a*, two additional sites reside upstream of exon 2. At the *miR-34b/c* locus two potential p53 binding sites are located upstream of the miRNA genes. Another important regulatory feature, which both loci exhibit, is a CpG island. In the *miR-34a* gene this covers the transcriptional start site and the p53 binding site upstream of it (Lodygin et al, 2008). The

miR-34b/c promoter harbors a CpG island upstream of exon 2 (Figure 1). As described in 1.2 these elements can be hyper-methylated and lead to transcriptional silencing of the respective genes. As described in more detail in 1.3.3, this is indeed the case for both *miR-34* genes.

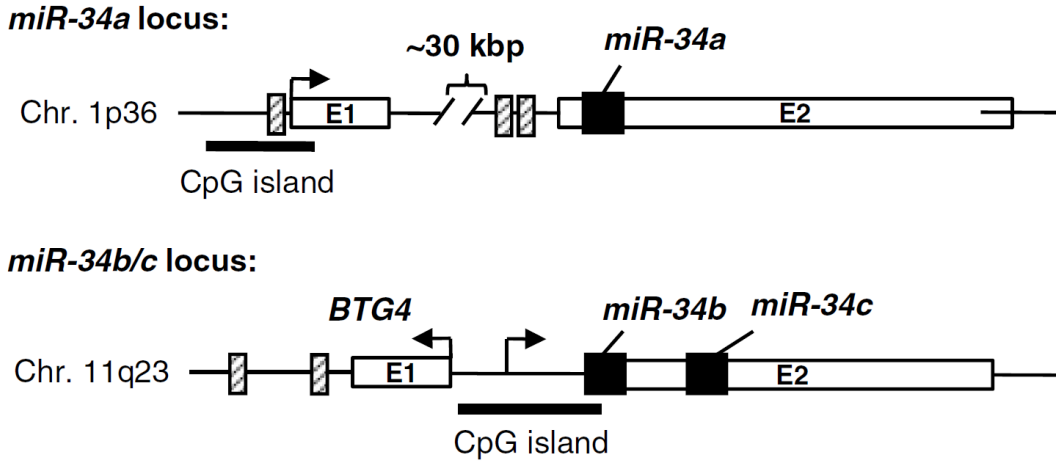

Figure 1: Structure of genomic loci of the human *miR-34a* and *miR-34b/c* genes. White and black boxes represent exons and miRNA hairpins, respectively. Hatched boxes indicate p53-binding sites; CpG islands are represented by thick black lines. The model is not shown to scale. Chromosomal (Chr) locations of the genes are provided. Figure modified from Hermeking, 2010.

Besides the well documented regulation by p53, other factors regulating miR-34 were discovered more recently: While p63, a relative of p53, represses *miR-34* genes in order to facilitate cell cycle progression, FOXO3a was recently shown to induce the expression of *miR-34b/c* (Antonini et al, 2010; Kress et al, 2011). Another study reported up-regulation of miR-34a mediated by the ETS family transcription factor ELK1 during oncogene induced senescence (Christoffersen et al, 2010). Therefore, the *miR-34* genes are not exclusively regulated by p53.

Although closely related to miR-34, the miR-449 family is neither inducible by p53 nor by DNA damage. However, a recent publication indicated that ectopic expression of miR-449 results in activation of p53 and its downstream target p21 as well as the apoptotic markers cleaved Caspase3 and poly

(ADP-ribose) polymerase (PARP; Bou Kheir et al, 2011). Moreover, the authors found that *miR-449* expression is down-regulated in gastric cancer. The role of miR-449 in apoptosis was further confirmed by another group suggesting a tumor suppressive function of miR-449 (Lize et al, 2010). Since its expression is up-regulated by the transcription factor E2F1, it is conceivable that miR-449 is a component of a failsafe mechanism against uncontrolled proliferation (Lize et al, 2010; Yang et al, 2009).

1.3.3) Role in cancer and aberrations

As depicted in Figure 2, the miR-34 family has been linked to multiple tumor suppressive effects of p53, among them induction of apoptosis, cell cycle arrest and senescence (He et al, 2007b; Hermeking, 2012). Several cancer relevant molecules can be targeted on the mRNA level by miR-34 like for instance the survival factor Bcl-2, different cyclin-dependent kinases (CDKs) or CD44, which may mediate the effects mentioned above (Bommer et al, 2007; He et al, 2007a; Liu et al, 2011). Other miR-34-targeted mRNAs encode proteins playing crucial roles in the formation and/or progression of cancer as well and are distributed over many functional classes of proteins: cell surface receptor molecules like c-Met, Axl, PDGF receptor and Notch (Bae et al, 2012; Li et al, 2009; Mudduluru et al, 2011; Silber et al, 2012), as well as transcription factors like Myc and SMAD (Christoffersen et al, 2010; Genovese et al, 2012) and regulatory elements like LEF1, MTA2 and SATB2 (Kaller et al, 2011; Wei et al, 2012) or kinase components of signaling cascades like MEK1 (Ichimura et al, 2010) are targeted. This diversity of targets makes the miR-34 family the ‘extended arm of p53’, which amplifies the inhibitory effect of p53 on various processes in malignant cells.

In line with its crucial role in tumor suppression, the miR-34 family was found to be down-regulated in different types of cancer by several mechanisms. Most frequently, methylation-dependent down-regulation of *miR-34a* was found in multiple types of cancer, among them colorectal, prostate, ovarian, pancreatic, esophageal, breast, renal cell and urothelial cancer as well as melanomas, soft tissue sarcomas and hematological

malignancies (Chen et al, 2012; Chim et al, 2010; Corney et al, 2010; Lodygin et al, 2008; Vogt et al, 2011). Methylation of *miR-34b/c* was found in colorectal, gastric, lung, ovarian, pancreatic, esophageal, breast, renal cell and urothelial cancer as well as soft tissue sarcomas (Chen et al, 2012; Corney et al, 2010; Suzuki et al, 2010; Toyota et al, 2008; Vogt et al, 2011; Wang et al, 2011). In addition, deletion of the *miR-34* gene loci was reported in colorectal cancer (Lee et al, 2000; Thorstensen et al, 2000).

Another, more cancer-specific alteration, which affects miRNA expression, is the loss or dysregulation of components of the miRNA processing machinery. Loss of Dicer1 and Drosha or mutations of *TARBP2* or *XPO5* lead to a global down-regulation of miRNAs (Lujambio & Lowe, 2012). This was shown to be associated with enhanced tumorigenic capacity in different cancer types (Melo & Esteller, 2011). One could assume that the loss of *miR-34* expression contributes to this effect.

Besides tumor suppression miR-34 is known to be involved in other physiological processes such as bone development , cardiovascular diseases and aging (Bae et al, 2012; Bernardo et al, 2012; Boon et al, 2013; Li et al, 2011; Maes et al, 2009; Xu et al, 2012). Moreover, decreased miR-34 expression is associated with asthma and T cell recruitment (Solberg et al, 2012; Yang et al, 2012a).

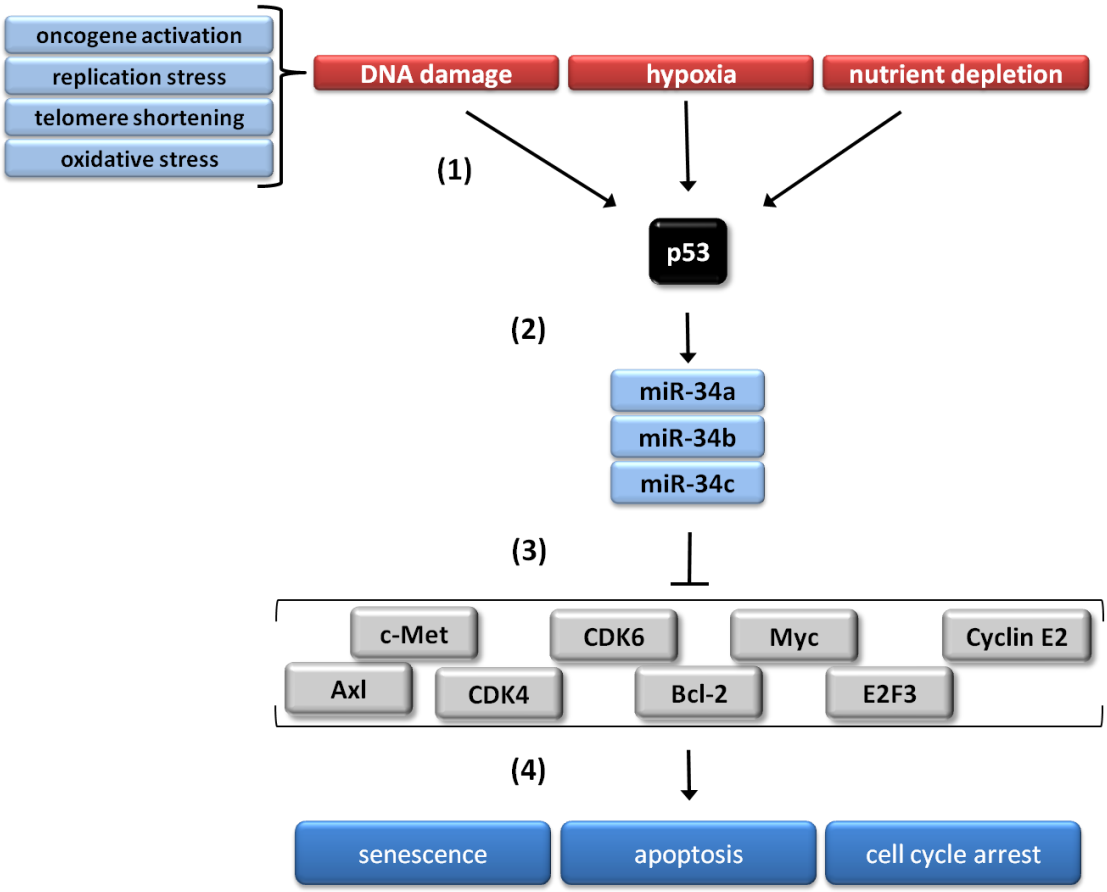

Figure 2: The miR-34 family amplifies the p53-mediated response upon cellular stresses by targeting a versatile portfolio of mRNAs. **(1)** Several different cellular stresses (shown in red) converge in an induction/activation of p53 (black). **(2)** p53 in turn induces transcription of the miR-34 family. **(3)** The miR-34 family amplifies the p53 response by targeting multiple mRNAs (some examples are shown in grey) involved in a multitude of processes. **(4)** Repression of miR-34 targets triggers several protective processes (dark blue) in response to cellular stress. Figure adapted to Hermeking, 2007.

1.4) Epithelial to mesenchymal transition in cancer progression and metastases

The term ‘epithelial to mesenchymal transition’ or short EMT describes a reversible process, initially observed in developmental biology, in which cells lose their epithelial nature and become more migratory, or in the context of cancer, more invasive (Sanchez-Tillo et al, 2012; Thiery et al, 2009). Besides that, cells undergoing EMT have been shown to acquire characteristics of cancer stem cells (CSCs) like for example self-renewal (Thiery et al, 2009). This is essential for cancer cells to metastasize from the primary tumor throughout the body (Mani et al, 2008; Polyak & Weinberg, 2009). The EMT process is characterized by expression changes of several molecular markers: cells undergoing EMT for instance express low levels of the adhesion molecule E-cadherin, while the mesenchymal-specific intermediate filament Vimentin and/or the extracellular-matrix-glycoprotein Fibronectin are expressed at elevated levels (Perl et al, 1998; Nieto, 2011). In the recent years several EMT-triggering transcription factors (EMT-TFs) could be identified, among them ZEB1 and 2, Snail (*SNAI1*) and Slug (*SNAI2*), which mediate these changes (Batlle et al, 2000; Eger et al, 2005; Thiery et al, 2009). A common structural feature of these EMT-TFs is a zinc-finger DNA binding domain, which mediates the direct binding to so called enhancer (E)-box recognition sites in the promoters of EMT effectors as for instance E-cadherin (Giroldi et al, 1997).

EMT-TFs were found to be up-regulated in a variety of solid tumor types such as breast, head and neck, ovarian and colorectal cancer (CRC; Thiery et al, 2009; Roy et al, 2005). Once arrived at metastatic sites, the invasive cells need to re-seed and grow out in order to form a solid tumor, which requires the reversal of EMT in a process called mesenchymal to epithelial transition or MET (Nieto, 2011).

Initial results obtained in our group showed that one of the EMT-TFs, namely Snail, was repressed upon DNA damage in a p53 and miR-34a-dependent manner and represents a direct miR-34 target. The functional characterization of this regulatory connection was part of this thesis.

1.5) c-Kit and the stem cell factor signaling

The type III receptor tyrosine kinase (RTK) c-Kit (also known as CD117 or stem cell factor receptor) is a central component of several signaling cascades. It was initially identified as the cellular homologue of the viral oncogene *v-Kit* encoded by the *Hardy-Zuckerman 4 feline sarcoma virus* (Besmer et al, 1986; Yarden et al, 1987). Binding of its ligand stem cell factor (SCF), also known as steel factor, leads to homo-dimerization and auto-phosphorylation of specific tyrosine residues on the intracellular domain of the c-Kit receptor and thereby results in stimulation of different pathways (Anderson et al, 1990). Among these are the PI-3, Src, Jak/Stat and MAP kinase pathways as well as Phospholipase C and D signaling (Lennartsson & Ronnstrand, 2012). Under physiologic conditions c-Kit is involved in hematopoiesis, pigmentation, gametogenesis, T cell differentiation and mast cell regulation (Galli et al, 1994; Kitamura et al, 1995; Krishnamoorthy et al, 2008; Lennartsson & Ronnstrand, 2012; Rothschild et al, 2003). However, elevated expression and mutational activation of c-Kit can cause several types of diseases among them cancer (Lennartsson & Ronnstrand, 2012).

The c-Kit signaling axis is therefore involved in different types of malignancies, such as acute myeloblastic leukemia (Ikeda et al, 1991; Wang et al, 1989), glioblastoma (Mahzouni & Jafari, 2012), melanoma (Montone et al, 1997; Natali et al, 1992), as well as lung (Hida et al, 1994; Krystal et al, 1996) and breast cancer (Hines et al, 1995). Aberrant activation of c-Kit is associated with chemoresistance of cancer cells, increased oncogenic signaling, e.g. in gastrointestinal stromal tumors (GISTs), and mediates escape from apoptotic triggers and increases invasive potential (Bellone et al, 2001; Duensing et al, 2004; Catalano et al, 2004; Luo et al, 2011; Chau et al, 2012). Expression of the c-Kit ligand SCF is often elevated in cancer as well and contributes to the autocrine/paracrine transmission of oncogenic signals (Bellone et al, 2006; Hibi et al, 1991; Martinho et al, 2008; Theou-Anton et al, 2006). Taken together, the c-Kit/SCF axis seems to play a central role in different types of malignancies.

Interestingly, several miRNAs have been described to down-regulate *c-Kit* mRNA among them miR-193a, 193b, 221, 222 and 494 (Felli et al, 2005; Gao et al, 2011a; Gao et al, 2011b; Kim et al, 2011e). Additionally, a recent study revealed a p53-dependent down-regulation of c-Kit in mice (Abbas et al, 2011). However, direct binding of p53 to the *c-Kit* promoter was not detected within 5 kbp upstream of the transcriptional start site (TSS). As mentioned above, p53 is an important tumor suppressor and amplifies the response to cellular stress by activation of target genes as the members of the miR-34 family (He et al, 2007a; Raver-Shapira et al, 2007; Tarasov et al, 2007). Based on these findings, we hypothesized that a p53-mediated up-regulation of miR-34, which might target the mRNA of *c-Kit*, would result in a decrease of c-Kit protein expression and function after DNA damage. The validation and functional characterization of a putative p53/miR-34/c-Kit axis was another topic of this thesis.

2) Aims of the thesis

The present study had the following aims:

I) Functional characterization of Snail as a miR-34a target

II) Detection and evaluation of *miR-34a* CpG-methylation and expression in combination with the detection of target expression as prognostic markers for distant metastases in colon cancer

III) Characterization of c-Kit as a new miR-34 target and the resulting consequences in cancer cells

3) Materials

3.1) Chemicals and reagents

Compound	**Supplier**
5-FU (5-fluorouracil)	Sigma-Aldrich, St. Louis, MD, USA
Ampicillin	Sigma-Aldrich, St. Louis, MD, USA
APS (ammonium peroxodisulfate)	Carl Roth GmbH, Karlsruhe, Germany
BD Matrigel™ Basement Membrane Matrix	BD Bioscience, Heidelberg, Germany
Christal violet	Carl Roth GmbH, Karlsruhe, Germany
Complete mini protease inhibitor cocktail	Roche Diagnostics GmbH, Mannheim, Germany
DAPI (2-(4-amidinophenyl)-6-indolecarbamidine dihydrochloride)	Carl Roth GmbH, Karlsruhe, Germany
dNTPs (deoxynucleotides triphosphate)	Thermo Fisher Scientific Inc., Waltham, MA, USA
DMEM	Life Technologies GmbH, Darmstadt, Germany
DMSO (dimethyl-sulfoxide)	Carl Roth GmbH, Karlsruhe, Germany
Doxorubicin	Sigma-Aldrich, St. Louis, MD, USA
Doxycycline hyclate	Sigma-Aldrich, St. Louis, MD, USA
ECL/HRP substrate	Immobilon, Merck Millipore, Billerica, MA, USA
Ethidium bromide	Carl Roth GmbH, Karlsruhe, Germany
Fast SYBR® Green Master Mix	Applied Biosystems, Foster City, CA, USA
FBS (fetal bovine serum)	Gibco®, Life Technologies GmbH, Darmstadt, Germany
FuGENE®6 Transfection Reagent	Promega, Madison, WI, USA
Gene Ruler 100bp plus DNA ladder	Fermentas GmbH, St. Leon-Rot, Germany
Gene Ruler Low Range DNA ladder	Fermentas GmbH, St. Leon-Rot, Germany
Hi-Di™ Formamide	Applied Biosystems, Foster City, CA, USA
HiPerFect Transfection Reagent	Qiagen GmbH, Hilden, Germany
Hygromycin B	Invitrogen GmbH, Karlsruhe, Germany
Immobilon-P Transfer Membrane	Immobilon, Merck Millipore, Billerica, MA, USA
LB agar (Lennox)	Carl Roth GmbH, Karlsruhe, Germany
LB medium (Luria/Miller)	Carl Roth GmbH, Karlsruhe, Germany
Lipofectamine™ 2000	Invitrogen GmbH, Karlsruhe, Germany
Mc Coy's medium	Life Technologies GmbH, Darmstadt, Germany

Compound	**Supplier**
Methyl cellulose	Sigma-Aldrich, St. Louis, MD, USA
Mitomycin C	Sigma-Aldrich, St. Louis, MD, USA
Nonidet®P40 Substitute	Sigma-Aldrich, St. Louis, MD, USA
O'Gene Ruler 1kb DNA ladder	Fermentas GmbH, St. Leon-Rot, Germany
Opti-MEM®	Life Technologies GmbH, Darmstadt, Germany
PageRuler™ Prestained Protein Ladder	Fermentas GmbH, St. Leon-Rot, Germany
Paraformaldehyde	Merck KGaA, Darmstadt, Germany
peqGOLD Universal Agarose	PEQLAB Biotechnologie GmbH, Erlangen, Germany
Phenol /C/I for RNA extraction	Promega GmbH, Mannheim, Germany
PhosSTOP Phosphatase Inhibitor Cocktail	Roche Diagnostics GmbH, Mannheim, Germany
PolyHEMA (poly(2-hydroxyethyl methacrylate)	Sigma-Aldrich, St. Louis, MD, USA
ProLong Gold Antifade	Invitrogen GmbH, Karlsruhe, Germany
Propidium iodide	Sigma-Aldrich, St. Louis, MD, USA
Puromycin dihydrochloride	Sigma-Aldrich, St. Louis, MD, USA
Rotiphorese Gel 30 (37,5:1)	Carl Roth GmbH, Karlsruhe, Germany
RPMI 1640 medium	Life Technologies GmbH, Darmstadt, Germany
SCF (stem cell factor), human recombinant	ImmunoTools, Friesoythe, Germany
SDS (sodium dodecyl sulfate)	Carl Roth GmbH, Karlsruhe, Germany
Sea Plaque® Agarose	Lonza Ltd., Basel, Switzerland
Skim milk powder	Fluka, Sigma-Aldrich, St. Louis, MD, USA
Temed (tetramethylethylendiamin,1,2-bis (dimethylamino) -ethan)	Carl Roth GmbH, Karlsruhe, Germany
Triton X 100	Carl Roth GmbH, Karlsruhe, Germany
Trypsin-neutralization solution	Lonza Ltd., Basel, Switzerland
Tween® 20	Sigma-Aldrich, St. Louis, MD, USA
Water (molecular biological grade)	Gibco®, Life Technologies GmbH, Darmstadt, Germany

3.2) Enzymes

Enzyme	**Supplier**
DNAse I (RNAse-free)	Sigma-Aldrich, St. Louis, MD, USA
FIREPol® DNA Polymerase	Solis BioDyne, Tartu, Estonia
Platinum® *Taq* DNA polymerase	Invitrogen GmbH, Karlsruhe, Germany
Proteinase K	Sigma-Aldrich, St. Louis, MD, USA
Restriction endonucleases	New England Biolabs GmbH, Frankfurt, Germany
RNAse A	Sigma-Aldrich, St. Louis, MD, USA
T4 DNA ligase	Thermo Fisher Scientific Inc., Waltham, MA, USA
Trypsin (10×, phenol-red free)	Invitrogen GmbH, Karlsruhe, Germany

3.3) Kits

Kit	**Supplier**
BCA Protein Assay Kit	Pierce, Thermo Fisher Scientific, Inc., Waltham, MA, USA
BigDye® Terminator v3.1 Cycle Sequencing Kit	Life Technologies GmbH, Darmstadt, Germany
DNeasy® Blood&Tissue Kit	QIAGEN GmbH, Hilden, Germany
DyeEx® 2.0 Spin Kit	QIAGEN GmbH, Hilden, Germany
EZ DNA Methylation Kit	Zymo Research Europe GmbH, Freiburg, Germany
High Pure miRNA Isolation Kit	Roche Diagnostics GmbH, Mannheim, Germany
High Pure RNA Isolation Kit	Roche Diagnostics GmbH, Mannheim, Germany
Pure Yield™ Plasmid Midiprep System	Promega GmbH, Mannheim, Germany
QIAamp DNA Micro Kit	QIAGEN GmbH, Hilden, Germany

Kit	Supplier
QIAprep Spin Miniprep Kit	QIAGEN GmbH, Hilden, Germany
QIAquick Gel Extraction Kit	QIAGEN GmbH, Hilden, Germany
QuikChange II XL Site-Directed Mutagenesis Kit	Stratagene, Agilent Technologies GmbH & Co.KG, Waldbronn, Germany
TaqMan® MicroRNA Reverse Transcription Kit	Applied Biosystems, Life Technologies GmbH, Darmstadt, Germany
TaqMan® qPCR Detection Kit	Applied Biosystems, Life Technologies GmbH, Darmstadt, Germany
Verso cDNA Kit	Thermo Fisher Scientific Inc., Waltham, MA, USA

3.4) Antibodies

3.4.1) Primary antibodies

Antigen	Source/Clone	Application	Supplier/Clone
α-tubulin	Mouse/ DM 1A	WB	Sigma-Aldrich, St. Louis, MD, USA
β-catenin	Mouse/ clone 14	IHC	Ventana Medical Systems, Oro Valley, AZ, USA
β-catenin	Mouse	WB	BD PharMingen, Heidelberg, Germany
β-catenin	Rabbit	IF	Epitomics, Burlingame, CA, USA
c-Kit	Rabbit	WB	Dako Deutschland GmbH, Hamburg, Germany
c-Met	Rabbit/ EP1454Y	IHC	Epitomics, Burlingame, CA, USA
E-cadherin	Mouse/ 4A2C7	WB, IF	Invitrogen GmbH, Karlsruhe, Germany
Erk	Rabbit	WB	Cell Signaling Technology, Inc., Danvers, MA, USA
p-Erk	Rabbit	WB	Cell Signaling Technology, Inc., Danvers, MA, USA
HDAC1	Rabbit	WB	Epitomics, Burlingame, CA, USA
p53	Mouse/ DO-1	WB	Santa Cruz Biotechnology, Inc., Heidelberg
p53	Mouse/ DO-7	IHC	Thermo Scientific, Lab Vision Corporation, Freemont, CA, USA

Antigen	Source/Clone	Application	Supplier/Clone
Slug	Rabbit/ H-140	WB	Santa Cruz Biotechnology, Inc., Heidelberg, Germany
Snail	Rabbit	WB, IF	Cell Signaling Technology, Inc., Danvers, MA, USA
Snail	Rabbit	IHC	Acris Antibodies, San Diego, CA, USA
VSV	Rabbit	WB, IF	Sigma-Aldrich, St. Louis, MD, USA
Vimentin	Rabbit/ EPA3776	WB, IF	Epitomics, Burlingame, CA, USA
ZEB1	Rabbit/ H-102	WB, ChIP	Santa Cruz Biotechnology, Inc., Heidelberg, Germany
ZEB2	Mouse/ E-11	WB	Santa Cruz Biotechnology, Inc., Heidelberg, Germany

WB: Western blot analysis, IF: immunofluorescence, ChIP: chromatin immuno-precipitation, IHC: immunohistochemistry

3.4.2) Secondary antibodies

Name	Source/Clone	Application	Supplier
Anti-Mouse HRP	Goat	WB	Promega GmbH, Mannheim, Germany
Anti-Mouse-Alexa Fluor-555	Goat	IF	Invitrogen GmbH, Karlsruhe, Germany
Anti-Rabbit HRP	Goat	WB	Sigma-Aldrich, St. Louis, MD, USA
Anti-Rabbit-Cy3	Donkey	IF	Jackson Immuno-Research Europe Ltd., Newmarket, Suffolk, UK
Phalloidin-Alexa-647	-	IF	Invitrogen GmbH, Karlsruhe, Germany

WB: Western blot analysis, IF: immunofluorescence

3.5) DNA constructs and oligonucleotides

3.5.1) Vectors

Name	**Insert**	**Reference**
pRTR		Jackstadt et al, 2013
pRTR-p53	human p53	
pRTR-miR-34a	human miR-34a	Kaller et al, 2011
pRTR-Snail	human Snail	
pRTR-c-Kit	human c-Kit	
pRTS-c-Kit	human c-Kit	
tTA-p53	human p53	Yu et al, 1999
pGL3-control-MCS		Welch et al, 2007
pGL3-Snail wt	human *Snail* 3'UTR	
pGL3-Snail mut	human *Snail* 3'UTR	
pGL3-c-Kit	human *c-Kit* 3'UTR	
pGL3-c-Kit mut1	human *c-Kit* 3'UTR	
pGL3-c-Kit mut2	human *c-Kit* 3'UTR	
pGL3-c-Kit mut1 + 2	human *c-Kit* 3'UTR	
pRL	Renilla	Pillai et al, 2005

3.5.2) Primers

Name	Sequence (5' – 3')	Purpose	REF
AchR fwd	CCTTCATTGGGATCACCACG	qChIP	
AchR rev	AGGAGATGAGTACCAGCAGGTTG	qChIP	
β-actin fwd	TGACATTAAGGAGAAGCTGTGCTAC	qPCR	
β-actin rev	GAGTTGAAGGTAGTTTCGTGGATG	qPCR	
β-catenin fwd	AGCTGACCAGCTCTCTCTTCA	qPCR	
β-catenin rev	CCAATATCAAGTCCAAGATCAGC	qPCR	
BMI-1 fwd	TTCTTTGACCAGAACAGATTGG	qPCR	
BMI-1 rev	GCATCACAGTCATTGCTGCT	qPCR	
CD133 fwd	TCCACAGAAATTACCTACATTGG	qPCR	Horst et al, 2009
CD133 rev	CAGCAGAGAGCAGATGACCA	qPCR	Horst et al, 2009
CD44 fwd	GCCTACTGCAAATCCAAACAC	qPCR	
CD44 rev	GAAGCTCTGAGAATTACTCTGCTG	qPCR	
CDH1 fwd	CCCGGGACAACGTTTATTAC	qPCR	Lindner et al, 2010
CDH1 rev	GCTGGCTCAAGTCAAAGTCC	qPCR	Lindner et al, 2010
c-Fos fwd	AGAATCCGAAGGGAAGGAA	qPCR	
c-Fos rev	ATCAAGGGAAGCCACAGACA	qPCR	
c-Kit 34a site1mut fwd	CCCACAGGAGTGGGAAAACAGTCGGATCTTAGT TTGGATTCT	mutagenesis	
c-Kit 34a site1mut rev	AGAATCCAAACTAAGATCCGACTGTTTTCCCACT CCTGTGGG	mutagenesis	
c-Kit 34a site2mut fwd	ACTCCCCTTCCTCAGTCGGCAATATAAAAGGCAA ATGTGTAC	mutagenesis	
c-Kit 34a site2mut rev	GTACACATTTGCCTTTTATATTGCCGACTGAGGA AGGGGAGT	mutagenesis	
c-Kit fwd	CAGGCAACGTTGACTATCAGT	qPCR	Li et al, 2007
c-Kit rev	ATTCTCAGACTTGGGATAATC	qPCR	Li et al, 2007
GAPDH fwd	GCTCTCTGCTCCTCCTGTTC	qPCR	
GAPDH rev	ACGACCAAATCCGTTGACTC	qPCR	

Name	Sequence (5’ – 3’)	Purpose	REF
hsa c-Kit 3'UTR fwd	ACCCTGGCATTATGTCCACT	Cloning	
hsa c-Kit 3'UTR rev	GGGAATATTCAAAAGACATTATTGC	Cloning	
Lgr5 fwd	GCATTTGGAGTGTGTGAGAA	qPCR	
Lgr5 rev	AGGGCTTTCAGGTCTTCCTC	qPCR	
miR-34a M fwd	GGTTTTGGGTAGGCGCGTTTC	MSP	Lodygin et al, 2008
miR-34a M rev	TCCTCATCCCCTTCACCGCCG	MSP	Lodygin et al, 2008
miR-34a qChIP fwd	TTTTCAGGTGGAGGAGATGC	qChIP	
miR-34a qChIP rev	AGGACTCCCGCAAATCTC	qChIP	
miR-34a U fwd	IIGGTTTTGGGTAGGTGTGTTTT	MSP	Lodygin et al, 2008
miR-34a U rev	AATCCTCATCCCCTTCACCACCA	MSP	Lodygin et al, 2008
miR-34b/c M fwd	TTTAGTTACGCGTGTTGTGC	MSP	Toyota et al, 2008
miR-34b/c M rev	ACTACAACTCCCGAACGATC	MSP	Toyota et al, 2008
miR-34b/c site1 fwd	CGCTGGCAGTTCATTTTAGC	qChIP	
miR-34b/c site1 rev	TCAATTCAGTGCCTTTGAAGAA	qChIP	
miR-34b/c site2 fwd	GCCAAAGCTAAAGCAGAAGGTA	qChIP	
miR-34b/c site2 rev	TCAGGAGAGACAAGGTTGATGA	qChIP	
miR-34b/c U fwd	TGGTTTAGTTATGTGTGTTGTGT	MSP	Toyota et al, 2008
miR-34b/c U rev	CAACTACAACTCCCAAACAATCC	MSP	Toyota et al, 2008
Nanog fwd	ATGCCTCACACGGAGACTGT	qPCR	
Nanog rev	AGGGCTGTCCTGAATAAGCA	qPCR	
NanogP8 fwd	TCCATCCTTGCAAATGTCTTC	qPCR	
NanogP8 rev	AGGGCTGTCCTGAATAAGCA	qPCR	
OLFM4 fwd	TGGTCATACAGCTGAAGGAGAGT	qPCR	
OLFM4 rev	GCTTCTCTACCAAGAGAGTCATATTTC	qPCR	
Oncostatin M fwd	CACACAGAGGACGCTGCTCA	qPCR	Hoermann et al, 2011

Name	Sequence (5’ – 3’)	Purpose	REF
Oncostatin M rev	ATGCTCGCCATGCTTGGAA	qPCR	Hoermann et al, 2011
pri-miR-200b fwd	CGCAGCAGTGGAACCTGT	qPCR	
pri-miR-200b rev	GTGAGGAGGTGCTGGGATG	qPCR	
pri-miR-200c fwd	CTTAAAGCCCCTTCGTCTCC	qPCR	
pri-miR-200c rev	AGGGGTGAAGGTCAGAGGTT	qPCR	
pri-miR-34a fwd	CGTCACCTCTTAGGCTTGGA	qPCR	Lodygin et al, 2008
pri-miR-34a rev	CATTGGTGTCGTTGTGCTCT	qPCR	Lodygin et al, 2008
pri-miR-34b/c fwd	GAGCTGCCTGTGCATCATC	qPCR	
pri-miR-34b/c rev	GGATGAAATCAGCATTTTCCA	qPCR	
Snail fwd	GCACATCCGAAGCCACAC	qPCR	
Snail rev	GGAGAAGGTCCGAGCACA	qPCR	
Sox2 fwd	TGCGAGCGCTGCACAT	qPCR	
Sox2 rev	TCATGAGCGTCTTGGTTTTCC	qPCR	
SP6 Promoter	TATTTAGGTGACACTATAG	(colony) PCR	
T7 Promoter	TAATACGACTCACTATAGGG	(colony) PCR	
Vimentin fwd	TACAGGAAGCTGCTGGAAGG	qPCR	
Vimentin rev	ACCAGAGGGAGTGAATCCAG	qPCR	

REF = reference, fwd = forward, rev = reverse, PCR = polymerase chain reaction, qPCR = quantitative (real time) PCR, qChIP = fast Chromatin immuno precipitation, MSP = methylation specific PCR, I = Inosine

3.5.3) MicroRNA mimics and antagomiRs

The following pre-miRNA mimics and antagomiRs were purchased from Ambion GmbH, Kaufungen, Germany:

- pre-miR-control
- pre-miR-34a
- pre-miR-34b
- pre-miR-34c
- anti-miR-control
- anti-miR-34a

3.6) Buffers and solutions

Propidium iodide staining solution:

- 800 µl propidium iodide (1.5 mg/ml)
- 1000 µl RNAse A (10 mg/ml)
- ad 20 ml PBS 0.1% Triton X.

Mini Prep buffer1 (MP1):

- 50 mM Tris-HCl (pH 8)
- 10 mM EDTA
- 100 µg/ml RNAse A

Mini Prep buffer2 (MP2):

- 200 mM NaOH
- 1% SDS

Mini Prep buffer3 (MP3):

- 3 M potassium acetate
- pH 5.5

10x ‚Vogelstein' PCR buffer:

- 166 mM NH_4SO_4
- 670 mM Tris (pH 8.8)
- 67 mM $MgCl_2$
- 100 mM β-mercaptoethanol

RIPA buffer (for protein lysates):

- 1% NP40
- 0.5% sodium deoxycholate
- 0.1% SDS
- NaCl 150 mM
- 50 mM TrisHCl (pH 8.0)

2xLaemmli buffer:

- 125 mM TrisHCl (pH 6.8)
- 4% SDS
- 20% glycerol
- 0.05% bromophenol blue (in H_2O)
- 10% β-mercaptoethanol [added right before use]

10xTris-glycine-SDS running buffer (5l, for protein gels):

- 720 g glycine
- 150 g Tris base
- 50 g SDS
- pH 8.3-8.7
- ad 5 liters ddH_2O

Towbin buffer (for protein blotting):

- 200 mM glycine
- 20% methanol
- 25 mM Tris base (pH 8.6)

10xTBST (5l):

- 500 ml 1M Tris (pH 8.0)
- 438.3 g NaCl
- 50 ml Tween20
- ad 5 liters ddH_2O

3.7) Laboratory equipment

Device	**Supplier**
5417C table-top centrifuge	Eppendorf AG, Hamburg, Germany
ABI 3130 genetic analyzer capillary sequencer	Applied Biosystems, Foster City, USA
Axiovert 25 microscope	Carl Zeiss GmbH, Oberkochen, Germany
BD Accuri™ C6 Flow Cytometer Instrument	Accuri, Erembodegem, Belgium
Biofuge *fresco*	Heraeus; Thermo Fisher Scientific, Inc., Waltham, MA, USA
Biofuge *pico* table top centrifuge	Heraeus; Thermo Fisher Scientific, Inc., Waltham, MA, USA
Boyden chamber transwell membranes (pore size 8.0 µm)	Corning Inc., Corning, NY, USA
CF40 Imager	Kodak, Rochester, New York, USA
Falcons, dishes and cell culture materials	Schubert & Weiss OMNILAB GmbH & Co. KG
Fisherbrand FT-20E/365 transilluminator	Fisher Scientific GmbH, Schwerte, Germany
Forma scientific CO_2 water jacketed incubator	Thermo Fisher Scientific, Inc., Waltham, MA, USA
GeneAmp® PCR System 9700	Applied Biosystems, Foster City, USA
Herasafe KS class II safety cabinet	Thermo Fisher Scientific, Inc., Waltham, MA, USA
HTU SONI130	G. Heinemann Ultraschall- und Labortechnik, Schwäbisch Gmünd, Germany
ME2CNT membrane pump	Vacuubrand GmbH & CO KG, Wertheim, Germany
Megafuge 1.0R	Heraeus; Thermo Fisher Scientific, Inc., Waltham, MA, USA
Mini-PROTEAN®-electrophoresis system	Bio-Rad, München, Germany
MultiImage Light Cabinet	Alpha Innotech, Johannesburg, South Africa
ND 1000 NanoDrop Spectrophotometer	NanoDrop products, Wilmington, DE, USA
Neubauer counting chamber	Carl Roth GmbH & Co, Karlsruhe, Germany
Orion II luminometer	Berthold Technologies GmbH & Co. KG, Bad Wildbad, Germany
PerfectBlue™ SEDEC 'Semi-Dry' blotting system	Peqlab Biotechnologie GmbH, Erlangen, Germany
real-time cell analyzer (RTCA)	xCELLigence RTCA SP; Roche Diagnostics GmbH, Penzberg, Germany

Device	**Supplier**
Varioskan Flash Multimode Reader	Thermo Scientific, Inc., Waltham, MA, USA
Waterbath	Memmert GmbH, Schwabach, Germany

4) Methods

4.1) Bacterial cell culture

4.1.1) Propagation and seeding

Bacterial *E.coli* XL1-blue strains, used for all conventional cloning procedures, were either cultured by agitation (225 rpm) in liquid LB-medium or on LB agar plates in an incubator at 37°C overnight. The selection for antibiotic–resistant progeny cells was achieved by addition of ampicillin [100 µg/ml] due to the resistance cassette, which is included in all plasmid vectors used in this work.

4.1.2) Transformation

In order to transform plasmid vectors into bacteria, 200 µl aliquots of competent *E.coli* XL1-blue were thawed on ice and approximately 100 ng of plasmid DNA was added. After 30 minutes of incubation on ice, the cells were heat-shocked at 42°C for 90 seconds and put back on ice for another 2 minutes. Thereafter, 1 ml of antibiotic-free LB-medium was added and cells incubated at 37°C for another hour. Next, cells were centrifuged for 5 minutes at 2000 rpm and a large proportion of the supernatant was discarded in order to reduce the volume which was to be plated. Finally, the remaining cells were resuspended and plated on nutrient LB-agar containing ampicillin for cultivation over night.

4.1.3) Purification of plasmid DNA from *E.coli*

For mini-prep of plasmid DNA, bacteria were inoculated in a volume of 5 ml of LB-medium, which was supplemented with ampicillin, and DNA was either isolated using the QIAprep Spin Miniprep Kit (Qiagen) according to the manufacturer`s protocol or via a self-made protocol:

First, cells were pelleted for 5 minutes at 3600 rpm in a table-top centrifuge. The resulting pellet was resuspended in 250 µl buffer MP1, lysed by adding 250 µl of buffer MP2 and incubated at room temperature for 5 minutes. The lysis buffer was then neutralized by adding 250 µl of buffer MP3 and the lysate was centrifuged for 10 minutes at 13000 rpm in a table-top centrifuge. Thereafter the supernatant was transferred into a new reaction tube, 700 µl of isopropanol was added and samples were vortexed. Precipitated DNA was centrifuged for 15 minutes at maximum speed, washed with 500 µl of 70% ethanol and centrifuged again for 5 minutes at maximum speed. After withdrawal of the ethanol the DNA was dried at room temperature and resuspended in 50 µl H_2O.

For midi-prep the volume of LB-medium was 150 ml and the Pure Yield™ Plasmid Midiprep System (Promega) was used according to the manufacturer`s protocol.

The small-scale purification method was used preferentially, since it yields DNA of better quality leading to a higher transfection efficiency compared to the large-scale protocol.

4.2) Mammalian cell culture

4.2.1) Propagation of human cell lines

DLD1 and HCT116 colorectal cancer cells and their derivatives were maintained in McCoy's 5A medium (Invitrogen) containing 10% fetal bovine serum (FBS). SW480, SW620, HCT15, CaCo2 and HT29 colorectal cancer cells, MiaPaCa2 human pancreatic cancer cells and human diploid fibroblasts (HDFs) were maintained in high glucose Dulbecco`s modified Eagles medium (DMEM, Invitrogen) containing 10% FBS. Colo320 colorectal cancer cells were propagated in RPMI 1640 medium supplemented with 10% FBS. All media were further supplemented with penicillin [100 U/ml] and streptomycin [100 µg/ml]. All cell lines were maintained at 37°C in a humidified atmosphere at 5% CO_2. Cells were passaged every two to four days in order to avoid confluency.

4.2.2) Transfection of oligonucleotides, vectors and constructs

For the transfection of oligonucleotides, cells were trypsinized and seeded in the desired format, mostly into six-well plate wells. During trypsin treatment the transfection mix was set up. For transfection of oligonucleotides in a six-well format the mix contained 100 µl Opti-MEM, 10 µl HiPerFect and 10 µl of oligonucleotide [10 µM] in order to achieve a final concentration of 100 nM. For the transfection of plasmids, the transfection mix consisted of 150 µl Opti-MEM, 4 µg DNA and 5 µl FuGENE. For efficiency reasons the DNA was added to the Opti-MEM first, the transfection reagent was added last.

Before adding the mix drop-wise to the cells, it was incubated at room temperature for oligonucleotides 15, for plasmids 25 minutes. In case cells were selected in antibiotics, cells were incubated for 24 hours without the respective antibiotic first, to avoid additional stress, which could lead to cell death of successfully transfected cells.

4.2.3) Cryo-preservation of mammalian cells

For cryo-preservation, sub-confluent, exponentially growing cells were trypsinized, pelleted by centrifugation at 300xg for 5 minutes and resuspended in 50% FBS, 40% growth medium and 10% DMSO (Roth). Aliquots in cryo-vials were stored at -80°C for up to six months or, for long term storage, transferred into a liquid nitrogen tank.

For recovery, cells were rapidly thawed in a 37°C water bath and transferred into a 15 ml tube of pre-warmed growth medium. Cells were pelleted by centrifugation and resuspended in the respective growth medium for further cultivation.

4.3) Isolation of DNA

Genomic DNA from paraffin sections was isolated after overnight proteinase K digestion [0.1 mg/ml] in 0.1% SDS (Sigma) at 58°C with subsequent phenol/chloroform extraction (pH 8) and precipitation. Cellular DNA was isolated using the Blood & Tissue Kit (Qiagen) according to manufacturer's instructions.

4.4) Bisulfite treatment

For subsequent methylation analyses 200-1000 ng of DNA were treated with sodium bisulfite using the EZ DNA methylation kit (Zymo Research) according to the manufacturer's instructions. This treatment converts unmodified cytosine residues to uracil, while methylated cytosine residues remain unaffected. These methylation-specific changes of the DNA sequence can be detected by different methods such as methylation specific PCR (see below) or bisulfite sequencing.

4.5) PCR methods

4.5.1) Colony PCR

For detection of insert positive transformants a bacterial culture tube containing selective medium was prepared in parallel with a 20 µl PCR master mix containing vector-specific primers (e.g. T7 fwd and SP6 rev for T-easy vectors), dNTPs, PCR buffer and FIREPol® DNA polymerase. A single colony was picked from the plate, transferred into the PCR tube and thereafter inoculated in the culture tube over night. If needed a replica-plate was used as well.

Representative PCR cycling conditions were the following: 95°C for 5 minutes, followed by 25 cycles of 95°C for 20 seconds, 58°C for 30 seconds

and 72°C for 1 minute or longer, depending on the size of the insert. PCR results were controlled on a 1% agarose gel.

4.5.2) Methylation specific PCR (MSP)

For the detection of DNA-methylation at the promoter sites of the *miR-34* genes, MSPs were performed using bisulfite treated DNA as a template (see above). MSP analyses were performed in a total volume of 20 µl using 1.5 units Platinum Taq-polymerase (Invitrogen) per reaction and 30 ng of bisulfite converted DNA as template. The reaction conditions for *miR-34a* were the following: 95°C for 10 minutes, followed by 35 cycles of 95°C for 30 seconds, 64°C for 30 seconds and 72°C for 30 seconds. The final elongation step was performed for 5 minutes at 72°C. Amplification conditions for *miR-34b/c* were: 95°C for 10 minutes, followed by 40 cycles of 95°C for 30 seconds, 65°C for 30 seconds and 72°C for 30 seconds. The final elongation step was performed for 5 minutes at 72°C.

Amplified fragments were separated by electrophoresis on 10% polyacrylamide gels and visualized by staining with ethidium bromide. Pictures were taken using a MultiImage Light Cabinet (Alpha Innotech). The oligonucleotide sequences used in this study are provided in the materials section. Addition of two inosines at the 5'-end of the miR-34a primer was used to increase the annealing temperature and hence achieve a decrease in unspecific PCR products. The MSP amplicon used for detection of *miR-34a* CpG-methylation is located within the only CpG island, which is present in the promoter and transcribed region of *miR-34a*. Therefore, it is likely that results obtained with this setup comprehensively represent relevant CpG-methylation affecting miR-34a expression.

In addition, it was previously shown in the Hermeking lab that the methylation detected by use of this PCR amplicon corresponds to results obtained with bisulfite sequencing of the promoter region and de-methylation of this region resulted in de-repression of *miR-34a* (Lodygin et al, 2008).

4.6) Isolation of RNA and reverse transcription

Total RNA was isolated using High Pure RNA Isolation Kit (Roche) according to the manufacturer's protocol and eluted in 50 µl elution buffer. Amount and quality of the RNA were determined using a Nanodrop spectrophotometer. For analysis of mRNA levels cDNA was generated with the Verso cDNA Kit (Thermo Fisher Scientific) from 1 µg of total RNA using anchored oligo-dT primers.

For isolation of the RNA fraction enriched for small RNAs the High Pure miRNA Isolation Kit (Roche) was used according to the manufacturer's instructions - either for cell lines or for FFPE tissue sections. cDNA was synthesized from 15 to 20 ng of RNA template using the TaqMan MicroRNA Reverse Transcription Kit (Applied Biosystems).

4.7) qPCR/TaqMan

Real-Time PCR for analysis of mRNA levels was performed using a Light Cycler 480 System (Roche) and the Fast SYBR Green Master Mix (Applied Biosystems). Results were normalized to the mRNA levels of 'house keeping genes' like *β-actin* or *GAPDH*. A list of qPCR-primers used for this study is provided in the materials section.

For detection of mature miR-34a expression, the TaqMan qPCR Detection Kit (Applied Biosystems) was used according to the manufacturer's instructions. The measurement was performed in a Light Cycler 480 System (Roche) and results were normalized to *RNU48* expression.

4.8) Protein isolation and Western blot analysis

Cells were incubated and/or treated under the respective conditions, washed with ice-cold PBS and harvested on ice by using a plastic cell scraper and ice-cold RIPA buffer, which was supplemented with protease- and

phosphatase inhibitors (Roche) immediately before use. The cell suspension/lysate was further transferred into a new reaction tube and sonicated using a HTU SONI130 (G. Heinemann Ultraschall- und Labortechnik) for three consecutive five-second pulses with an intensity of 85%. Thereafter remaining cells and debris were separated by centrifugation for 20 minutes at 14.000xg and 4°C and the supernatant, containing the protein lysate, was transferred subsequently into a new reaction tube. Unless used immediately, protein lysates were stored at -80°C.

Depending on the size of the analyzed proteins gels were prepared with polyacrylamide concentrations ranging from 7.5 to 12% and overlaid with a 4% stacking gel.

Protein concentrations were determined using the BCA Protein Assay Kit (Pierce, Thermo Scientific) according to manufacturer's protocol and concentration was determined in a Varioskan Flash Multimode Reader using the SkanIt RE for Varioskan 2.4.3 software (Thermo Scientific). 25-100 µg of protein were then diluted in an equal volume of 2xLaemmli buffer and denatured at 95°C for 5 minutes prior to loading on the gel together with a pre-stained protein ladder (Fermentas). Separation by electrophoresis was performed at 60-130 V in a Mini-PROTEAN®-electrophoresis system (Bio-Rad) with Tris-glycine-SDS running buffer.

After separation the proteins were transferred from the Gel to an Immobilon-P PVDF membrane (Millipore) in Towbin buffer using the PerfectBlue™ SEDEC 'Semi-Dry' blotting system (Peqlab) and a EPS 600 power supply (Pharmacia Biotech) at a constant amperage of 120 mA per gel and a maximum voltage of 10 V for 25-70 minutes, depending on the size of the analyzed protein.

To avoid non-specific binding during the subsequent antibody treatment the protein-containing membranes were incubated for one hour in 5% skim milk/TBS-T before. Thereafter primary antibodies were diluted in TBS-T and applied at 4°C over night or three hours at room temperature. Before and after incubation for one hour with the horseradish-peroxidase (HRP)-conjugated respective secondary antibody, membranes were washed in three 10-minute-

steps in TBS-T. Detection of proteins was performed using a CF40 Imager (Kodak) and ECL/HRP substrate (Immobilon).

4.9) Migration/Invasion assay in Boyden chambers

DLD1 and SW480 cells harboring doxycycline (DOX)-inducible pRTR vectors were cultured for 96 hours in presence or absence of DOX [100 ng/ml]. Serum was deprived (0.1% FBS) for the last 24 hours before starting the assay. To avoid serum stimulation after trypsination, Trypsin was inactivated with Trypsin-neutralization solution (Clonetics) before seeding of the cells.

For a migration assay $5x10^4$ cells were seeded in the upper compartment of a Boyden chamber (pore size 8.0 µm; Corning) containing serum-free medium and allowed to migrate towards the lower compartment, containing medium supplemented with 10% FCS as a chemo-attractant.

For invasion assays $7x10^4$ cells were used and membranes were coated with Matrigel (BD Bioscience), which was solved in serum-free medium at a concentration of 3.3 ng/ml. After 48 hours the assay was stopped by fixing cells in ice-cold methanol for 10 minutes. After removing cells from the upper compartment, migrated cells were stained with DAPI [1 µg/ml] and pictures were taken using an Axiovert Observer Z.1 microscope connected to an AxioCam MRm camera in combination with the Axiovision software (Zeiss). For each condition three individual membranes were analyzed, five pictures were taken per membrane at random positions and cell number determined using fluorescence microscopy. The relative invasion/migration was expressed as the number of treated cells to control cells.

4.10) Wound healing assay

Cells were seeded in medium with or without DOX [100 ng/ml] at high density one day before starting the experiment in order to obtain a confluent cell layer. Mitomycin C [10 µg/ml medium] was added to inhibit proliferation

two hours before scratching, using a 200 µl pipette tip or a culture insert (Ibidi). To remove floating cells, debris and Mitomycin C cells were washed twice with HBSS containing Ca^{2+} and Mg^{2+} (HBSS+/+). Thereafter, medium with or without DOX [100 ng/ml] was added and the cells were allowed to close the wound for 48 hours, while pictures were taken at regular intervals using an Axiovert Observer Z.1 microscope connected to an AxioCam MRm camera in combination with the Axiovision software (Zeiss). Per biological state three different measurements were performed per scratch in three independent wells.

4.11) Sphere formation assay

For induction of sphere formation, adherent DLD1 cells were trypsinized and $1x10^5$ cells were seeded into a six-well coated with attachment preventing PolyHEMA (Sigma) using 5 ml sphere-medium (Yu et al, 2007). Right after seeding, the cells were transfected with either a control oligo or miR-34a [200 nM] and treated with either water or SCF [10 ng/ml]. For all states experiments were carried out in triplicates. Resulting spheres were trypsinized again and quantified as well as employed for a second generation. For quantification, $1x10^4$ cells/well were seeded in sphere-medium containing 1% methyl cellulose (Sigma) into PolyHEMA (Sigma) coated 96-well plates, at least six wells per unicate. The number of colonies larger than 50 µm in diameter was determined after seven days. Representative pictures were taken using an EOS 400D camera (Canon) at a 40-fold magnification.

4.12) Soft agar colony formation assay

To measure anchorage-independent cell growth, the bottom of a 12-well was coated with 700 µl base agar containing 0.8% low melt agarose (Lonza), which was then covered with 700 µl 0.4% agarose containing $2x10^3$ SW480 cells, either transfected with miR-34a or control oligos 24 hours before, and incubated for 24 hours at 37°C and 5% CO_2. 24 hours later 250 µl medium

was added, supplemented with either 10% FBS and either DOX [100 ng/ml] or water. Cells were incubated for 14 days changing the media every 3 days. For determination of colony numbers cells were stained with 50 µl of 0.005% crystal violet per well for two hours and de-stained in PBS over night at 4°C. Pictures were taken using an EOS 400D camera (Canon) and colonies were counted using image J software (http://rsbweb.nih.gov/ij/).

4.13) Luciferase assay

To study binding of miRNAs to potentially matching sequences on the respective target mRNAs, a luciferase assay was performed. For this purpose the respective 3'-UTR was cloned down-stream of a luciferase gene. In case of successful binding, the luciferase gene transcription was targeted by the miRNA interaction and thereby upon addition of luciferase substrate the luciferase signal was lower than for a control oligonucleotide.

First, $3x10^4$ H1299 or $1x10^6$ SW480 cells were seeded into 12-well-plate wells. After 24 hours, cells were transfected with 100 ng empty pGL3 firefly luciferase reporter plasmid or molar equivalent of pGL3 containing the potential target sequence. Additionally, 20 ng of Renilla reporter plasmid were co-transfected as a normalization/transfection control together with the respective miRNA [25 nM], negative control oligonucleotide [25 nM] or antagomiR [50 nM].

After 48 hours of incubation the Dual Luciferase Reporter assay (Promega) was performed according to manufacturer's instructions. Luminescence intensities were measured with an Orion II luminometer (Berthold) in 96-well format and analyzed with the SIMPLICITY software package (DLR).

4.14) Site directed mutagenesis

To confirm the binding of miRNAs to the respective seed matching sequences, these had to be mutated in order to abolish the binding reaction. For this purpose site-directed mutagenesis was performed using the

QuickChange Mutagenesis Kit (Stratagene) according to manufacturer's instructions. Cytosine and guanine residues were exchanged by mutagenesis preferentially, since the base pairing between these and their counter-bases is predicted to be stronger than binding between adenine and thymine. Oligonucleotides used for cloning and mutagenesis are provided on page 20.

4.15) Flow cytometry

4.15.1) Analysis of transfection efficacy

In order to control the transfection efficiency of the pRTR and pRTS vectors, both harbor either a *green fluorescent protein* (*GFP*) or *red fluorescent protein* (*RFP*) gene, respectively. The percentage of GFP/RFP-positive cells was determined after 72 hours without or following addition of DOX [100 ng/ml]. A BD Accuri^{TM} C6 Flow Cytometer instrument (Accuri) and the corresponding CFlow® software was used to determine the proportion of fluorescent cells.

4.15.2) Cell cycle analysis using propidium iodide

To analyze cell cycle distribution, cells were seeded and/or treated before transferring the supernatant, which includes dead and/or swimming cells, into a new falcon tube. The remaining, attached cells were washed with HBSS-/- and trypsinized at 37°C. Thereafter trypsin activity was abolished using the respective supernatant and the cell suspension was centrifuged for 4 minutes at 300xg. The cells were resuspended and fixed in one milliliter of ice-cold 70% ethanol at -20°C overnight. After spinning down the pellet for 5 minutes at 4000 rpm in a table-top centrifuge, cellular DNA was then stained for one hour at 37°C using 400 µl propidium iodide (PI) staining solution, which had been passed through 0.22 µm sterile filter units (Millipore). DNA content was analyzed via PI fluorescence using a BD Accuri^{TM} C6 Flow Cytometer Instrument (Accuri) and the corresponding CFlow® software. 1x10^4 cells were analyzed per sample.

4.16) Real-time cell analysis (xCELLigence)

A real-time cell analyzer (RTCA) was used to assess cell proliferation according to manufacturer's instructions (xCELLigence Roche). $5x10^3$ cells were seeded into each well of an E-plate 16. The seeded cells were allowed to equilibrate for at least 30 minutes in the tissue culture incubator, then transfected or treated with DOX [100 ng/ml] respectively before impedance was recorded every 60 minutes. After 24 hours 5-FU was administered. Cell growth monitoring was continued every 60 minutes for up to 48 hours. The electrical impedance was represented as a dimension/unit-less parameter termed cell-index which represents relative change in electrical impedance that occurs in the presence and absence of cells in the wells. This change is calculated based on the following formula: CI = (Zi −Z0)/15, where Zi determines the impedance at an individual experimental time point and Z0 is the impedance measured at the beginning of the experiment. The impedance is measured at three different frequencies (10, 25 or 50 kHz) and a specific time (Reference: Roche Diagnostics GmbH. Introduction of the RTCA DP Instrument. RTCA DP Instrument Operator's Manual, A. Acea Biosciences, Inc.; 2008.).

4.17) Immunofluorescence

In order to analyze the localization/expression of cellular proteins, cells were seeded on glass cover-slides and cultivated under the desired conditions. For fixation cells were first washed three times with PBS, then treated with 4% paraformaldehyde, which was solved in PBS, for 10 minutes, washed with PBS and permeabilized in 0.2% Triton X in PBS for 15 minutes.

After blocking 30 minutes with 100% filtered FBS, cell slides were incubated with the pre-blocked first antibody in a solution of 0.05% Tween20 (Sigma) and 50% FBS in PBS for one hour in a humidity/dark chamber. The respective antibodies are listed in the materials section. Thereafter, slides were washed three times in PBS-T (0.05%) and pre-blocked secondary antibody was applied in a solution of 0.05% Tween20 and 50% FBS in PBS for 30 minutes

in the humidity/dark chamber. Finally, cells were washed again three times in PBS-T (0.05%) and nucleic chromatin was counter-stained by adding DAPI (Roth) in the last washing step, before covering the slides using ProLong Gold antifade (Invitrogen). As a control each staining was carried out without primary antibody.

For the detection of stress-fiber forming F-actin, Alexa Fluor 647-labeled Phalloidin (Invitrogen) was used. This is a heptapeptide which specifically binds at the interface of adjacent F-actin subunits.

Pictures were taken using laser scanning microscopy (LSM). For this purpose a confocal LSM 700 (Zeiss) was used with a Plan Apochromat 20x/0.8 M27 objective, the ZEN 2009 software (Zeiss) and the following settings: image size 2,048 x 2,048 and 16 bit; pixel/dwell of 25.2 µs; pixel size 0.31 µm; laser power 2%; master gain 600-1000.

4.18) Scoring of immunohistochemistry signals

For quantification of the c-Met expression the previously published *H*-score was applied (Camp et al, 1999; Uddin et al, 2010). Each region of the tumor was assigned an intensity score from 0 to 3: 0 indicates no staining, 1 an incomplete and 2 and 3 complete staining with ascending intensity. The proportion of the tumor staining for the respective intensity was recorded as 5% increments from a range of 0–100. A final *H*-score with a possible range from 0 to 300 was obtained by adding the sum of scores obtained for each intensity and proportion of area stained. Cases showing an *H*-score above the median (median=176.5) were categorized as high grade expression, whereas cases with a lower score were classified as low grade expression.

Nuclear Snail expression was evaluated using the following score: 0 no, 1 weak, 2 moderate and 3 strong staining. Subsequently, the samples were assigned to two groups with either low (scores 0 and 1) or high Snail expression (scores 2 and 3). Since transcriptionally active Snail is only localized in the nucleus, the detection of cytoplasmic Snail expression was not considered in this analysis.

The staining score for nuclear expression of β-catenin was assigned as published previously (Neumann et al, 2012a).

For detection of p53, nuclear staining was evaluated for both, frequency and intensity of stained nuclei. Intensity values were categorized as follows: 0-no staining, 1-weak, 2-moderate, and 3-strong staining. When more than 70% of tumor cell nuclei were stained and the intensity was at least moderate (score 2) or strong (score 3), p53 expression was considered to be “high”. Cytoplasmic p53 staining was not included in further statistical analysis.

All immunohistochemical detections were evaluated independently by two observers (Dr. med. Jens Neumann and Helge Siemens for c-Met, Dr. med. Jens Neumann and Rene Jackstadt for Snail and Prof. Dr. med. Thomas Kirchner and Dr. med. Jens Neumann for p53). Discrepant evaluations were discussed and a consensus was reached.

4.19) Statistical analysis

During this study different tests were applied in order to qualitatively evaluate statistical significant differences for different types of data constellation: For analysis of patient data calculations were conducted using SPSS software 19 (SPSS Inc.). For instance, a paired t-test was applied when comparing continuous outcomes (e.g. IHC scores) from two groups, e.g. case and control. Classification of cases into ‘high’ and ‘low’ populations, e.g. miR-34a expression, was conducted using the median of the total population as a cut-off. For illustration purposes box plots were generated using the SPSS chart builder tool and data were reported as median, first and third quartile while whiskers indicate maximum and minimum and single dots indicate outliers. For the comparison of two continuous variables the Pearson correlation algorithm was applied for the generation of Pearson correlation coefficient (r) and statistical significance (p-value). A p-value of ≤ 0.05 was considered as statistically significant. Correlations were illustrated by the generation of a scatter/dot plot using the SPSS chart builder tool. In some cases a partial regression line was added in order to emphasize the respective correlation.

Conditional logistic regression was used to quantitatively determine the simultaneous prognostic potential of several factors with respect to distant metastases. Age and gender were added as nuisance parameters to adjust for corresponding influences (Breslow & Day, 1987). The algorithms for Cox regression were used to calculate the conditional logistic regression as described previously (Krailo & Pike, 1984). The significant regression coefficients determined by multivariate analysis were further used to derive a prognostic score. A log-linear model was used to assess the relevance of the score with respect to case–control matching. These analyses were performed with the help of Prof. Dr. rer. nat. Ulrich Mansmann.

For evaluation of the remaining data like *in vitro* assays, qPCR results and other non-patient-related results a t-test was performed using the TTEST function in EXCEL (Microsoft Office). In all analyses a p-value of ≤ 0.05 was considered significant.

4.20) Sequencing

In order to verify DNA sequences, e.g. of miR- or protein-coding vectors, a Sanger sequencing reaction was performed using the BigDye® Terminator v3.1 Cycle Sequencing Kit (Life Technologies) according to the manufacturer's protocol. One µg of DNA was supplemented with 5 pmol of primer and kit components were added to a total reaction volume of 10 µl. Amplification was carried out in 15 cycles, with ten seconds at 96°C, followed by 90 seconds at 60°C each. Thereafter, samples were cooled down to 25°C.
To remove dye terminators from sequencing reactions, the DyeEx 2.0 Spin Kit (Qiagen) was used according to the manufacturer's protocol in a 5417C centrifuge (Eppendorf). Purified DNA was then diluted in Hi-Di formamide (Applied Biosystems), incubated at 90°C for 3 minutes and loaded onto an ABI3130 genetic analyzer capillary sequencer (Applied Biosystems). Data evaluation was then performed using the 3130 Data Collection Software v3.0 and the sequencing analysis software 5.2 (Applied Biosystems).

5) Results

5.1) miR-34 and Snail form a double-negative feedback loop controlling EMT

The results presented in this section are part of the publication: Siemens H*, Jackstadt R*, Hünten S*, Kaller M*, Menssen A*, Götz U and Hermeking H (2011). miR-34 and SNAIL form a double-negative feedback loop to regulate epithelial-mesenchymal transitions. Cell Cycle 10 (24), 4256-71. (* These authors contributed equally to this work). Contributions of the co-workers are indicated in the text and in the figures legends.

5.1.1) *Snail* is directly targeted by miR-34 during p53-mediated MET

Recent reports described that p53 inhibits EMT (Chang et al, 2011; Kim et al, 2011d). Since *miR-34a* and *miR-34b/c* are well known p53 target genes, we hypothesized that they could likewise be involved in this process. In order to investigate these putative regulations, my colleague Sabine Hünten, another Dr. rer. nat. student in our group, analyzed the colorectal cancer cell line HCT116 and an isogenic clone, which carried a homozygous deletion of *p53* (Bunz et al, 1998). In order to activate p53, the cells were treated using Nutlin-3a, which inhibits MDM2 (mouse double minute 2 homolog). The MDM2 ubiquitin-protein ligase inhibits p53 function by mediating its degradation (Vassilev et al, 2004). When the levels of the zinc-finger EMT-TF Snail were analyzed in the aforementioned cells, Western blot analyses revealed that it was expressed at higher levels in the p53-deficient background (Figure 3). Upon induction of p53 with Nutlin-3a, Snail levels decreased, while the epithelial marker protein and Snail target E-cadherin showed increased levels.

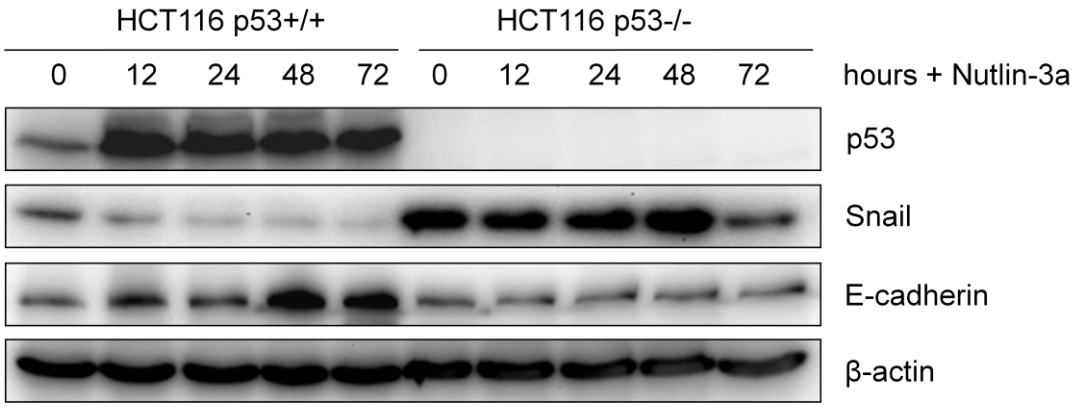

Figure 3: p53-dependent regulation of Snail protein in HCT116 colorectal cancer cells. HCT116 *p53+/+* and HCT116 *p53-/-* cells were treated with Nutlin-3a for the indicated periods. The indicated proteins were detected by Western blot analysis. β-actin served as a loading control. Sabine Hünten performed the analysis and generated the figure.

These results confirmed that expression of p53 negatively influences the expression of Snail protein. In a subsequent experiment, Sabine Hünten isolated RNA from cells treated as in Figure 3. By qPCR analysis she found that the *miR-34* family was induced on level of the primary transcript upon induction of p53 (Figure 4). In accordance with the results obtained before, the mRNA levels of *E-cadherin* were up-, the levels of *Snail* and *Vimentin* down-regulated. In the p53-deficient HCT116 cells, these genes did not show significant expression changes after Nutlin-3a treatment.

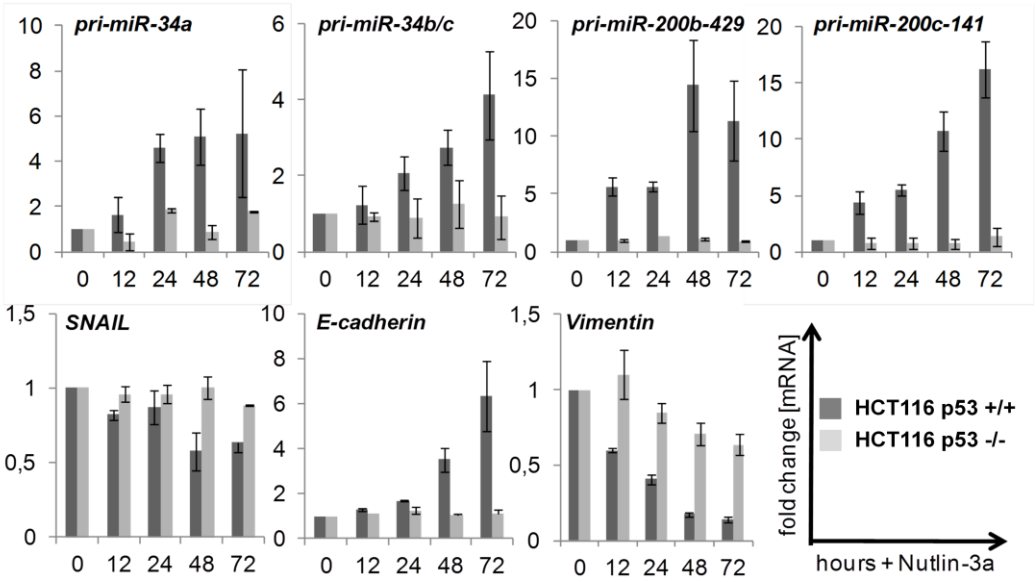

Figure 4: p53-dependent regulation of *Snail* mRNA, miRNAs and EMT-related factors in HCT116 colorectal cancer cells. *p53+/+* and *p53-/-* HCT116 cells were treated with Nutlin-3a for the indicated periods. Expression of the indicated mRNAs was determined by quantitative real-time PCR (qPCR) analyses. Fold changes represent mean values of triplicate analyses of Nutlin-3a vs. DMSO treated cells normalized to *β-actin* expression. Data are represented as mean ± SD (n=3). Sabine Hünten performed the analyses and generated the figure.

Similar results were obtained by Sabine Hünten using cells pools of the colorectal cancer cell line SW480 transfected with the DOX-inducible p53 expression vector pRTR (Figure 5): induction of ectopic p53 led to a pronounced reduction of Snail protein levels. This effect could be abolished by transfection of the cells using a miR-34a-specific antagomiR, showing that the p53-mediated Snail down-regulation was dependent on and mediated, at least in part, by miR-34a.

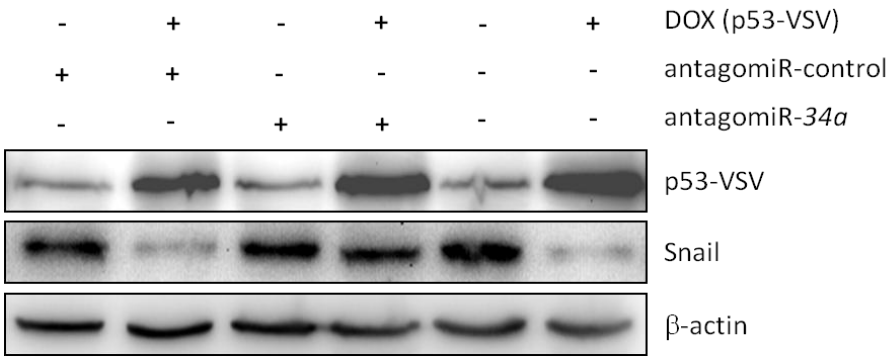

Figure 5: Regulation of Snail by p53 in SW480 colorectal cancer cells depends on miR-34a. Protein lysates of SW480 cells harboring a pRTR-p53-VSV vector were subjected to Western blot analysis. Cells were transfected with the indicated oligonucleotides for 48 hours in the presence or absence of DOX for the last 24 hours prior to lysis. antagomiR-34a and antagomiR-control represent oligonucleotides specifically targeting miR-34a and the respective control. β-actin served as a loading control. Sabine Hünten performed the analyses and generated the figure.

To study, whether this regulation was direct or indirect, my colleague Dr. rer. nat. Markus Kaller analyzed the *Snail* 3'-UTR for potential miR-34 binding sites using the targetSCAN and Miranda algorithms (Grimson et al, 2007; John et al, 2004). This revealed a conserved miR-34 seed-matching site, which was further confirmed by Dr. rer. nat. Markus Kaller in a dual-reporter luciferase reporter assay with a *Snail* 3'-UTR harboring either a wild-type or a mutated miR-34 site (Figure 6). While luciferase activity of the construct harboring the wild-type *Snail* 3'-UTR was diminished upon transfection of the miR-34 family members, the construct carrying the mutated miR-34 site in the *Snail* 3'-UTR was not responsive to ectopic miR-34.

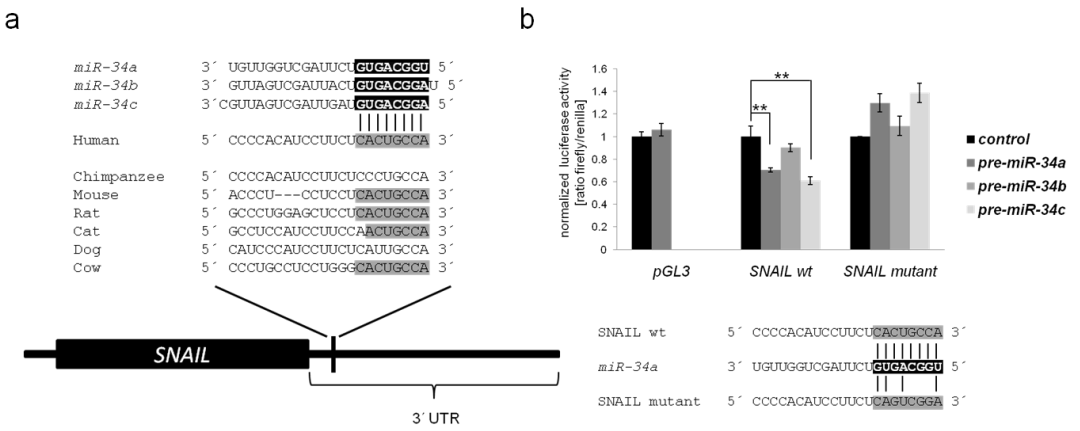

Figure 6: miR-34a/b/c regulates *Snail* via a conserved seed-matching site. a) Schematic depiction of the miR-34 seeds and seed-matching sequences in the 3'-UTR of the *Snail* mRNA and phylogenetic conservation among species. The position of the miR-34 seed-matching sequence in the *Snail* 3'-UTR is depicted as a black vertical bar. b) Dual reporter assay in H1299 cells transfected with miR-34a/b/c mimics (pre-miR-34a/b/c) or control oligos and the indicated reporter constructs for the human *Snail* 3'-UTR. The targeted mutation of the *Snail* 3'-UTR is shown below. Data are presented as mean ± SD (n=3). Student's t-test was used for comparisons, with $p \leq 0.05$ considered significant. Dr. rer. nat. Markus Kaller performed the analyses and generated the figure.

These results confirmed that miR-34 directly binds to the *Snail* mRNA and thereby negatively regulates its expression. Subsequently, I addressed the question, whether this regulation leads to an epithelial phenotype and MET of mesenchymal CRC cell lines.

5.1.2) miR-34a inhibits EMT

In order to determine, whether miR-34a expression alone is sufficient to mediate MET in the CRC cell line SW480, which has a mesenchymal phenotype, miR-34a was ectopically expressed in SW480 cell pools transfected with the DOX-inducible pRTR vector. Similar to ectopic p53 expression, expression of miR-34a resulted in a down-regulation of Snail protein (Figure 7a) and mRNA (Figure 7b). Accordingly, the Snail target E-cadherin showed higher expression levels in cells with miR-34a induction compared to untreated cells. This was accompanied by decreased expression of the mesenchymal marker Vimentin on mRNA and protein level.

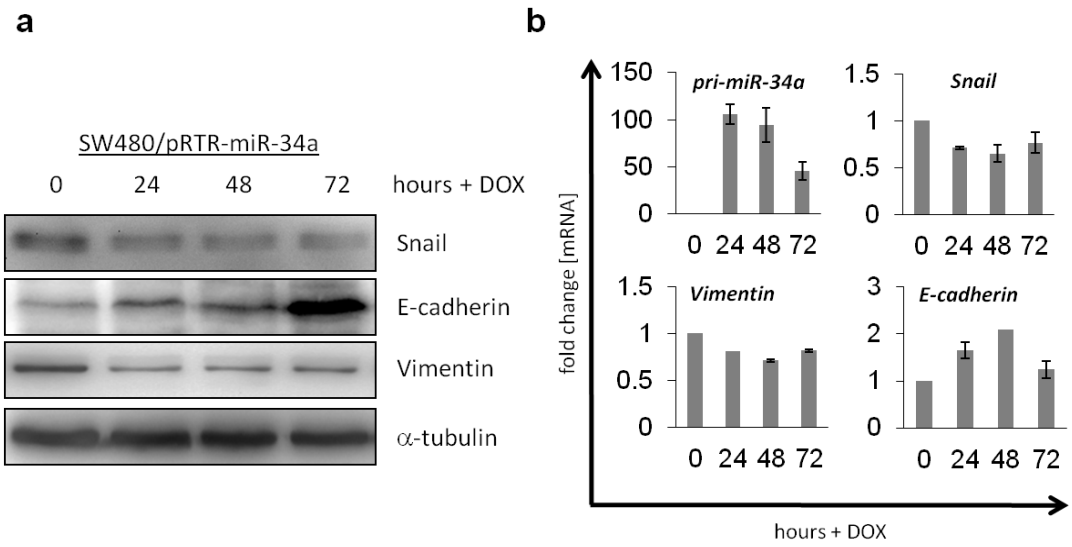

Figure 7: Ectopic expression of miR-34a in SW480 cells causes down-regulation of Snail and mesenchymal markers. a) SW480 cell pools carrying the pRTR-miR-34a vector were treated with DOX for the indicated periods. The indicated proteins were detected by Western blot analysis. α-tubulin served as a loading control. b) qPCR analysis of mRNAs corresponding to cells and proteins described in a). Bar charts and error bars represent mean and standard deviation of three independent experiments for each time point. Expression changes were normalized to *β-actin* mRNA.

Moreover, ZEB1, β-catenin and HDAC1 were repressed on the protein level (Figure 8a) and less nuclear β-catenin was detected by immunofluorescence (Figure 8b) upon induction of miR-34a compared to untreated SW480 cells. Besides the direct down-regulation of Snail by miR-34a, these effects may also contribute to miR-34a-mediated MET, since the TCF4/β-catenin signaling pathway is able to induce Snail expression and HDAC1 has previously been shown to serve as a co-repressor for Snail (reviewed by Peinado et al, 2007).

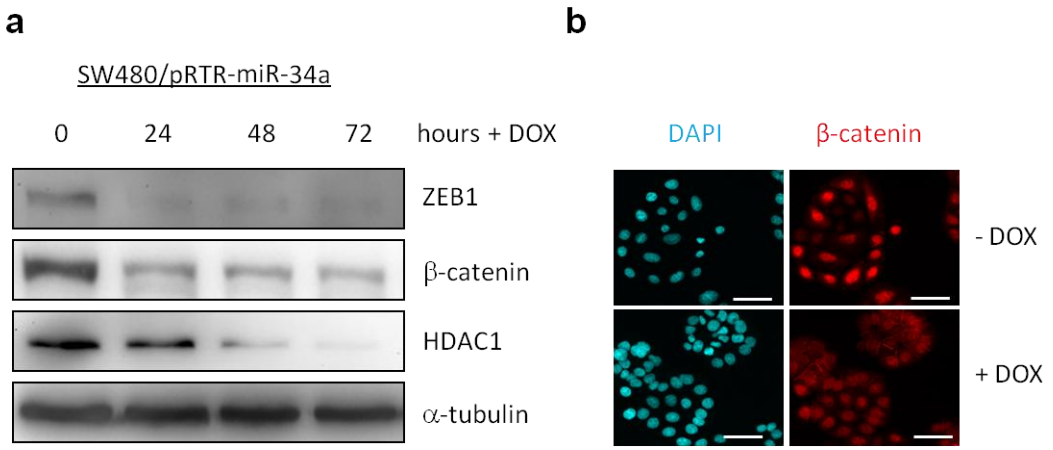

Figure 8: Ectopic expression of miR-34a causes down-regulation of ZEB1, β-catenin and HDAC1 in SW480 cells. a) Detection of the indicated proteins using Western blot analysis of SW480 cells carrying the pRTR-miR-34a vector and treated with DOX for the indicated periods. α-tubulin served as a loading control. b) Immunofluorescence analysis of β-catenin in SW480/pRTR-miR-34a cells either untreated (upper panel) or treated with DOX for 48 hours (lower panel). Nuclei were counter-stained with DAPI. Pictures were taken at a 200-fold magnification. Scale bars represent 50 µm.

Since EMT has been linked to the induction of tumor cell stemness (Thiery et al, 2009), different markers and mediators of stemness were analyzed on mRNA level under the conditions described above (Figure 9). Upon ectopic expression of miR-34a, the expression of *CD133*, *OLFM4*, *BMI-1, CD44* and *c-Myc* mRNAs was repressed. The latter two represent previously published miR-34a targets (Christoffersen et al, 2010; Liu et al, 2011).

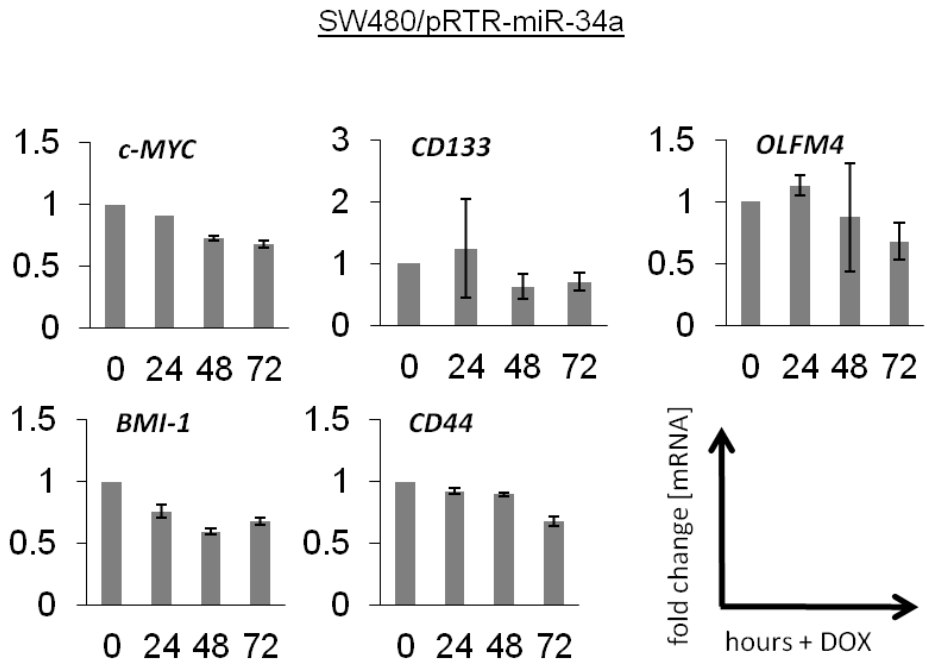

Figure 9: Regulation of stemness-related mRNAs upon miR-34a induction in SW480 cells. SW480 cells carrying the pRTR-miR-34a vector were treated with DOX for the indicated periods. Bar charts and error bars represent the mean and standard deviations of three independent experiments for each time point. Results were normalized to *β-actin* mRNA expression.

Taken together, these changes indicated an inhibition of mesenchymal properties and potential loss of stemness upon ectopic expression of miR-34a. Next, the question was addressed, whether the molecular changes, observed after induction of miR-34a in SW480 cells, had an impact on EMT-associated cellular functions. For this purpose SW480/pRTR-miR-34a cells were subjected to three different assays: wound closure, migration and invasion were determined in the presence or absence of DOX. Wound closure

was significantly diminished by addition of DOX, as well as migration and invasion, which were reduced about 80% (Figure 10). Therefore, miR-34a is sufficient to induce MET and diminish wound closure, cellular migration and invasion.

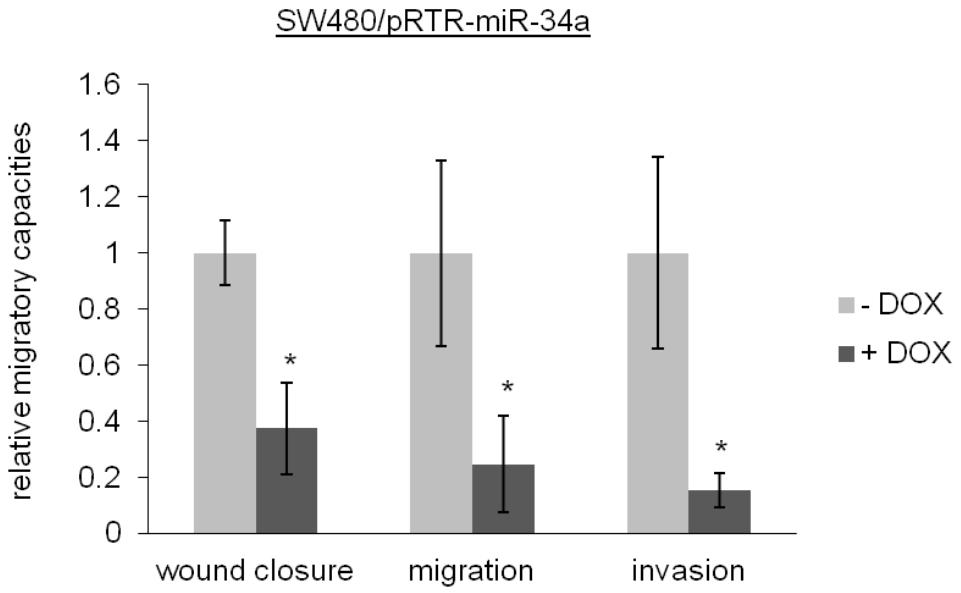

Figure 10: Decreased migratory capacities upon induction of miR-34a in SW480 cells. SW480 cells carrying the pRTR-miR-34a vector were subjected to wound closure-, migration- and invasion assays without or following stimulation with DOX. Bar charts and error bars represent mean and standard deviation of three independent experiments for each assay and condition. Statistical relevance was calculated using the Student's t-test considering $p \leq 0.05$ significant and indicated by *.

These results raised the question, whether the observed inhibitory effects on cellular migration were dependent on the miR-34a-mediated reduction of Snail expression. To address this issue, a *Snail* cDNA sequence, which was tagged with VSV and lacking the 3'-UTR, and therefore was miR-34a resistant, was cloned into the DOX-inducible expression vector pRTR and transfected into SW480 cells.

Next, cells were transfected with miR-34a oligonucleotides in the presence or absence of DOX and protein expression was analyzed (Figure 11). Similar to vector-driven miR-34 expression (Figure 7) transfection with the miR-34a oligonucleotides resulted in a decrease of Snail protein, while transfection with a control oligonucleotide did not. In contrast, addition of DOX significantly increased the Snail protein level even in the presence of the miR-34a oligos.

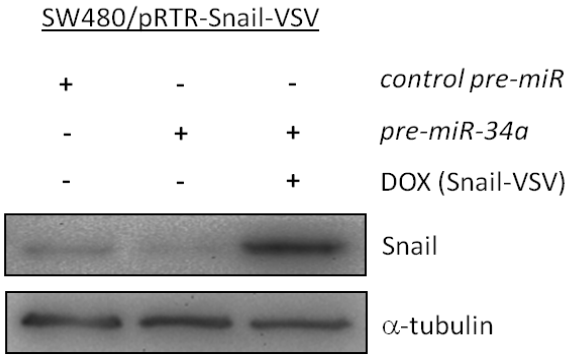

Figure 11: Ectopic Snail expression is not affected by miR-34a mimics in SW480 cells. Western blot analysis of Snail protein in SW480 cells carrying the pRTR-Snail construct either transfected with control- or miR-34a oligo for 48 hours and treated with or without DOX for the last 24 hours. α-tubulin served as a loading control.

Next, these cells were subjected to wound closure and migration analyses (Figure 12). The inhibitory effect of miR-34a oligonucleotide transfection on wound closure was less pronounced when compared with ectopic expression from the pRTR vector (Figure 10) but still significant. As shown in Figure 12, the effect on migration was almost identical to the results obtained with pRTR-miR-34a. However, when adding DOX to the cells, and thereby ectopically expressing miR-34-resistant Snail protein, these effects could be reverted and migration was significantly restored.

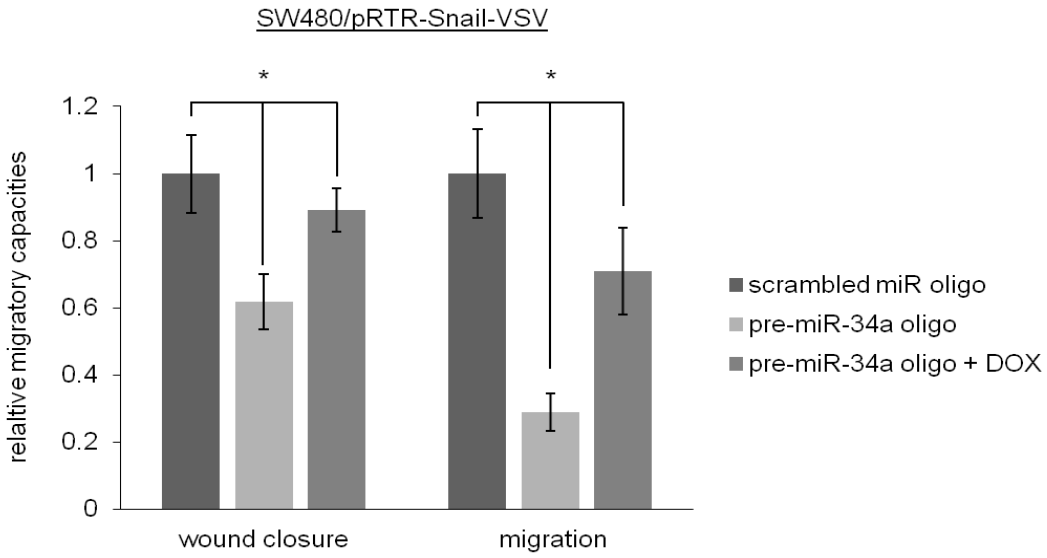

Figure 12: Restoration of migratory properties in miR-34a treated SW480 cells by ectopic Snail expression. SW480 cells carrying the pRTR-Snail vector were transfected with either scrambled (control) or miR-34a oligo and treated with or without DOX (as described for Figure 11) and subjected to wound closure- and migration assays. Bar charts and error bars represent mean and standard deviation of three independent experiments for each assay and state. Statistical relevance was calculated using the Student's t-test with $p \leq 0.05$ considered to be significant and indicated by *.

Consequently, the down-regulation of Snail seems to be a key mediator of miR-34a-mediated suppression of migration in SW480 colorectal cancer cells.

5.1.3) Snail binds to the *miR-34a* promoter and represses its expression

Previous studies had reported a negative feedback-loop between ZEB1/2 and the p53-induced miR-200 family (Bracken et al, 2008; Burk et al, 2008). While the miRNAs down-regulate the EMT-TFs via binding to seed-matches in the 3'-UTR, their own transcription is targeted by ZEB proteins, which bind to E-boxes in the promoter regions of the miRNAs. This was reminiscent of what was found in this study: the miR-34 family is induced by p53 as well and Snail is also a Zinc-finger EMT-TF. Therefore, Dr. rer. nat. Antje Menssen hypothesized that miR-34 may also be suppressed by Snail and therefore

form a negative feed-back loop. To prove this hypothesis, the inducible expression vector pRTR-Snail was used to induce EMT in the colorectal cancer cell line DLD1, which has an epithelial phenotype. First, Snail expression and initiation of EMT was confirmed on molecular level by loss of E-cadherin shown by Western blot analysis (Figure 13).

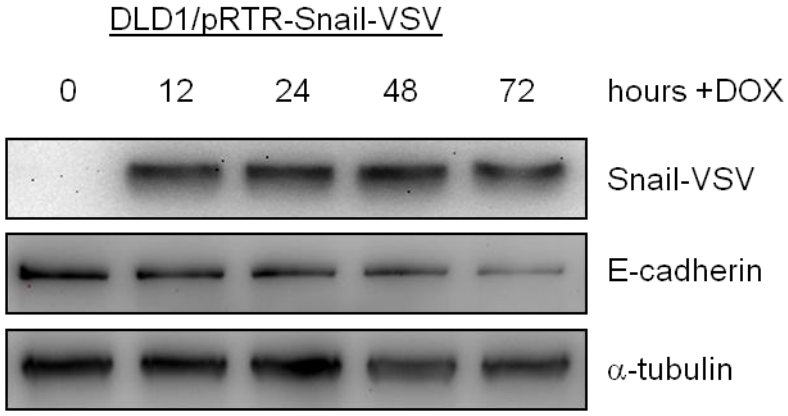

Figure 13: Characterization of a DLD1 cell pool conditionally expressing Snail. DLD1 cells carrying a pRTR-Snail-VSV construct were treated with DOX for the indicated periods. The indicated proteins were detected by Western blot analysis. Ectopic expression of Snail was controlled using an antibody directed against the VSV-tag. E-cadherin expression served as a marker for Snail-induced EMT in the cells. α-tubulin served as a loading control.

Furthermore, phase contrast microscopic evaluation revealed a transition from an epithelial and clustered morphology to a more mesenchymal, spindle- or fibroblast-like cell shape upon induction of Snail expression (Figure 14, left panel). This was accompanied by the disappearance of E-cadherin from the cellular junctions and stress-fiber formation, as shown by immunofluorescence for E-cadherin and F-actin (Figure 14, right panels).

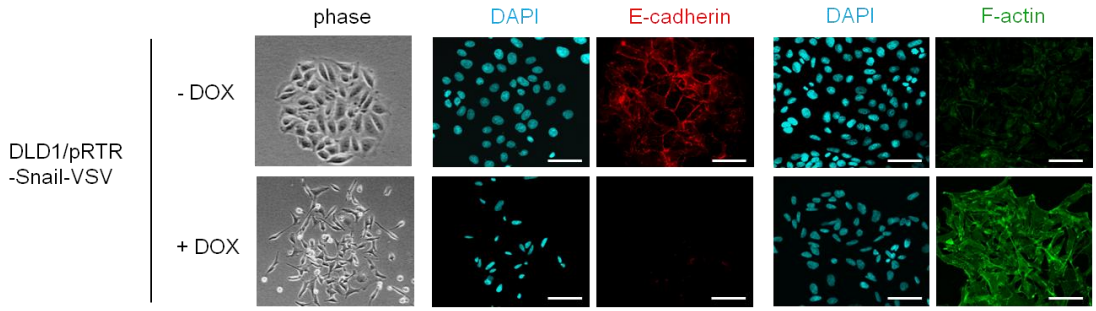

Figure 14: Ectopic expression of Snail leads to EMT-like changes in DLD1 cells. DLD1 cells carrying the pRTR-Snail-VSV vector were either treated for 96 hours with DOX or left untreated. Morphological differences were determined using phase contrast microscopy (left panel). Confocal immunofluorescence analysis (other panels) was performed for the epithelial marker protein E-cadherin and the stress fiber-forming F-actin, which is associated with mesenchymal traits. Nuclei were counter-stained with DAPI. Pictures were taken at a 200-fold magnification and the scale bars represent 50 µm.

In accordance to the previous findings (Figure 12), ectopically induced Snail resulted in significantly increased migration, invasion and wound closure of the cells. This was measured by means of wound closure capabilities as well as in Boyden chamber assays for migration and invasion, all depicted in Figure 15. While the effect of ectopic Snail expression on the wound healing assay was less pronounced, it led to a severe increase of migration and invasion.

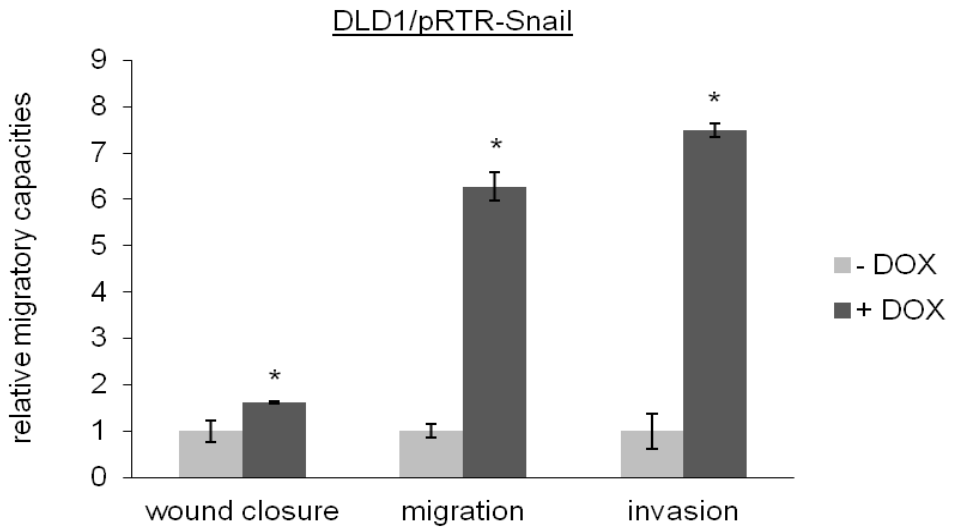

Figure 15: Analysis of EMT-associated processes after ectopic expression of Snail in DLD1 cells. DLD1 cells carrying the pRTR-Snail-VSV vector were subjected to the indicated assays in the presence absence of DOX. Bar charts and error bars represent mean and standard deviation of three independent experiments for each assay and state. The statistical significance of the results was determined using Student's t-test, with data considered significant when $p \leq 0.05$ and indicated by *.

In order to test whether Snail negatively regulates miR-34a expression, as Dr. rer. nat. Antje Menssen hypothesized, the levels of the primary *miR-34a* transcript were measured after adding DOX to DLD1 cells carrying the pRTR-Snail vector. Interestingly, *pri-miR-34a* levels were reduced up to 95% after 96 hours, which was accompanied by repression of the primary *miR-200c* transcript and *E-cadherin* mRNA as well as an increase in *Vimentin* and *ZEB1* (Figure 16). Since *ZEB1* was previously shown to be a target of miR-200c the induction of *ZEB1* by Snail may be due to the decreased expression of miR-200c (Gregory et al, 2008). These regulatory loops may also explain the repression of ZEB1 protein by miR‑34a, depicted in Figure 8.

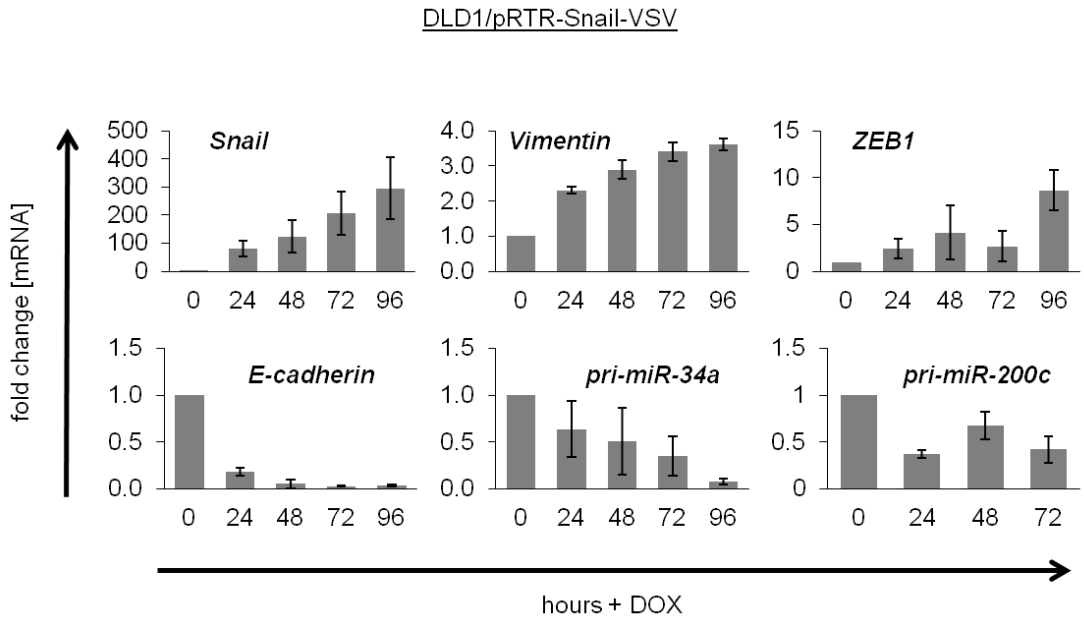

Figure 16: Ectopic Snail affects mRNA expression of EMT markers and primary miRNA transcripts. DLD1 cells carrying the pRTR-Snail-VSV vector were treated with DOX for the indicated periods. Bar charts and error bars represent the mean and standard deviations of three independent experiments for each time point. Changes in expression were normalized to *β-actin* mRNA.

To confirm that the repression of miR-34a was specifically mediated by Snail and to exclude secondary effects, my colleague Rene Jackstadt, another Dr. rer. nat. student in our group, transfected SW480 cells with *Snail*-specific siRNAs. This resulted in a marked decrease of Snail protein (Figure 17a) and additionally in a pronounced de-repression of the primary transcripts of *miR-34a* and *b/c* (Figure 17b).

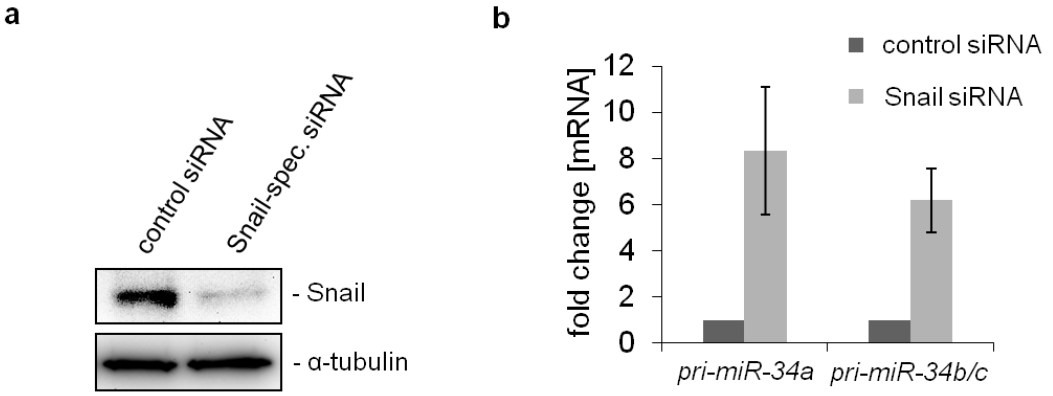

Figure 17: Inhibition of Snail restores expression of the primary *miR-34* transcripts. a) SW480 cells, naturally expressing relatively high levels of Snail, were transfected with a siRNA directed against *Snail* and decrease of the Snail protein was confirmed by Western blot analysis. α-tubulin served as loading control. b) Expression levels of the primary transcripts of *miR-34a* and *miR-34b/c* were measured by qPCR analysis with the indicated siRNAs for 48 h using *β-actin* mRNA for normalization. Mean values ± SD (n=3) are represented as bar charts and error bars. Rene Jackstadt performed the analysis and generated the figure.

To analyze, if Snail represses the *miR-34* genes, Rene Jackstadt screened the region around the two *miR-34* TSSs for Snail binding sites (SBS). As depicted in Figure 18, two these were located in each of the *miR-34* promoter regions and had high sequence homologies with the sites characterized for the *E-cadherin* promoter (Peinado et al, 2007).

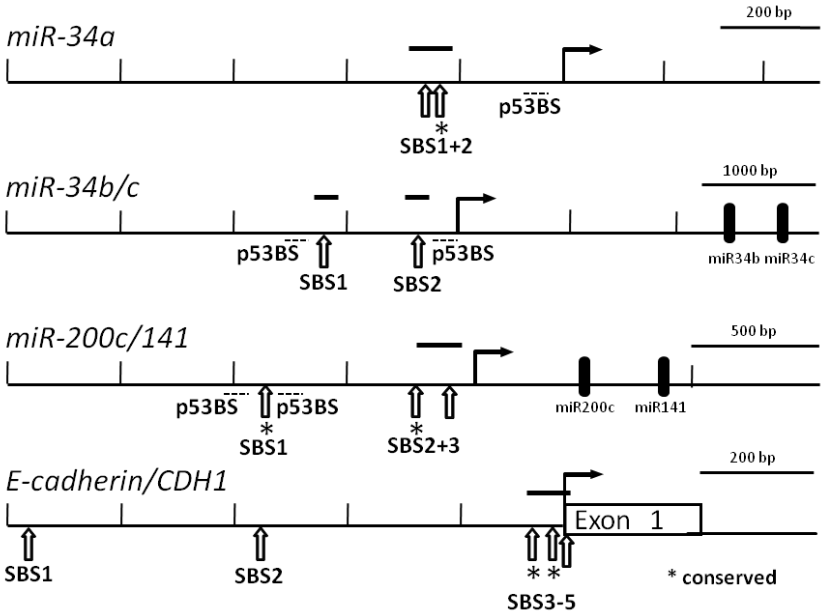

miR-34a

```
            SBS1                        SBS2
Human GCCCCCACCTGGTCCTC--TTTCCTTTTCAGGTGGAGGA
Rat   TCGCCCACCTTGACCCACTTTTTCTTTTCAGGTGACGGA
Mouse TCGCCCACCTTGACCCACTTTTTCTTTTCAGGTGACAGA
```

miR-34b/c

```
            SBS1                        SBS2
Human AGGTTCAGGTGCAGTAC//CTGGGATTACAGGTGTGAGC
Rat   ------------------//--------------------
Mouse ------------------//--------------------
```

miR-200c/141

```
            SBS1                    SBS2                SBS3
Human GCAATCACCTGTCGGGC//GGACACACCTGTGCGC//GGGGGCAGGTGGGCC
Rat   GCCTTCACCTGT-GTGC//GGACACACCTGTGCGC//GGGGTCAGGCGGGTC
Mouse GCCATCACCTGT-GTGC//GGACACACCTGTGCGC//GGGGTCAGGCGGGTC
```

E-cadherin/CDH1

```
            SBS1                        SBS2
Human GCTCACACCTGAAATCC//GGTGGTGTGCACCTGTACTC
Rat   ------------------//--------------------
Mouse ------------------//--------------------
            SBS3                    SBS4                SBS5
Human GCCGGCAGGTGAACCCT//GGGCTCACCTGGCTGC//AAAGCACCTGTGAGC
Rat   ACCTGCAGGTGCGTCCC//GG-CTCACCTGGCGGC//GGCGCACTACTGAGT
Mouse ACCTGCAGGTGCGTCCC//GG-CTCACCTGGCGGC//GGCGCACTACTGAGT
```

Figure 18: Snail binding sites are located in the promoters of *miR-34a/b/c* and *miR-200c.* The location of predicted Snail binding sites (SBS) in the human *miR-34a/b/c* promoters is indicated by vertical arrows in the upper panel and dotted lines indicate previously characterized p53 binding sites (p53BS). qChIP amplicons (see next figure) are indicated by horizontal bars, transcriptional start sites (TSSs) by horizontal arrows. Detailed sequences are given below including phylogenetic sequence alignment of the SBS in the *miR-34a*, *miR-34b/c*, *miR-200c/141* and *CDH1/E-cadherin* promoters. Rene Jackstadt performed the analysis and generated the figure.

As proof for the direct binding of Snail to these sites, Rene Jackstadt demonstrated the Snail occupancy of the promoters by chromatin immuno-precipitation (ChIP). The binding to the *E-cadherin* promoter served as a positive control and was even more pronounced than for *miR-34a*, which was more prominent than Snail binding to both sites in the promoter of *miR-34b/c* (Figure 19).

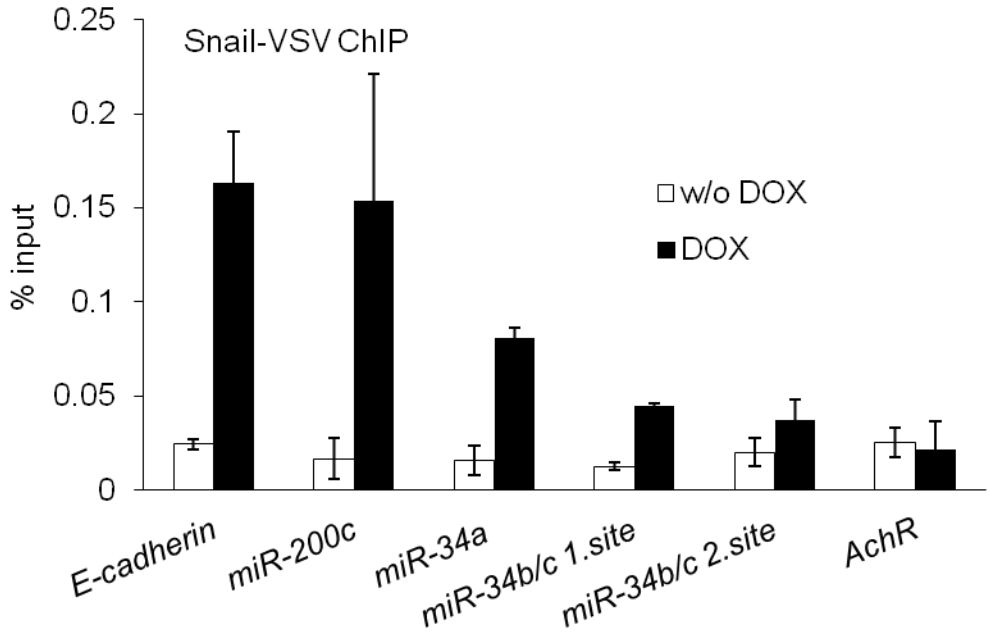

Figure 19: Direct regulation of *miR-34a/b/c* and *miR-200c* by Snail. qChIP analysis of DLD1 cells 24 hours after activation of Snail-VSV expression by addition of DOX [100 ng/ml] using anti-VSV and anti rabbit IgG for ChIP. Binding to the *E-cadherin* promoter was used as a positive control. Binding to the *Acetylcholine receptor* promoter (*AchR*) served as a negative control. Experiments were performed comparing DOX-induced with untreated cells. Results represent the mean ± SD (n=3). Rene Jackstadt performed the analyses and generated the figure.

Taken together these data establish a negative feedback loop consisting of the EMT-TF Snail and miR-34. These regulations could be of importance in cancer, since their deregulation may shift cells to the mesenchymal state and thereby promote metastasis.

5.2) Epigenetic silencing of *miR-34a* and expression of its targets can predict distant metastases in colon cancer

The results presented in this section have been published: Siemens H*, Neumann J*, Jackstadt R, Mansmann U, Horst D, Kirchner T and Hermeking H (2013). Detection of miR-34a promoter methylation in combination with elevated expression of c-Met and β-catenin predicts distant metastasis of colon cancer. Clinical Cancer Research 19 (3), 710-20. (* These authors contributed equally to this work). Contributions of the respective co-workers are indicated in the text and the figure legends.

5.2.1) *miR-34a* is down-regulated via CpG-methylation in colon cancer with distant metastases

As previously mentioned, EMT is known to play an important role for the development of metastasis and according to the present literature, low levels of miR-34a are associated with elevated risk for metastases in breast cancer, as well as advanced stages and relapse in several types of solid tumors (Brabletz, 2012b; Corney et al, 2010; Gallardo et al, 2009; Peurala et al, 2011; Tanaka et al, 2011). Since previous studies identified promoter hyper-methylation as frequent mode of *miR-34* silencing in colorectal cancer samples and *miR-34b/c* methylation was associated with metastases in several cancer types including colon cancer, the question was addressed, whether there was a connection between these results and the regulatory events observed in this study so far (Lujambio et al, 2008; Vogt et al, 2011). As a hypothesis, silencing of *miR-34a* in the primary tumor was assumed to lead to an up-regulation of its target genes, among them the EMT-TF Snail. As a result, the primary tumor cells would undergo EMT and gain mesenchymal properties like increased migration and invasion abilities, stemness or resistance to apoptosis, which would then lead to formation of metastases at distant sites throughout the body.

To address this question, a patient sample collection, consisting of 94 adenocarcinoma samples from resected colorectal tumors, was generated by

Dr. med. Jens Neumann. The collection was grouped into 47 pairs, matched for tumor grade, localization and extent (T classification). Each pair was composed of a case and a control sample. The case samples represented a primary tumor sample from a patient with distant metastases to the liver within five years after resection of the primary tumor (M1). The control counterpart represented a primary tumor sample from a patient with disease-free survival for at least five years after surgery (M0).

First, tumor DNA was isolated, treated with bisulfite and subjected to a methylation-specific PCR (MSP), in order to determine the methylation pattern of the *miR-34a* and *b/c* promoters (Figure 20). 93 and 86 samples showed a MSP product for the *miR-34a* and *b/c* promoter amplicon, respectively. Possible explanations for non-detectable PCR products in one and eight cases may be insufficient amounts of template and/or loss of the chromosomal loci as published before (Fijneman et al, 2007; Lee et al, 2000). The positive MSP results were as follows: methylation of the *miR-34a* promoter was detected in approximately 45% (42 of 93), methylation of *miR-34b/c* in approximately 92% (79 of 86) of the cases, respectively.

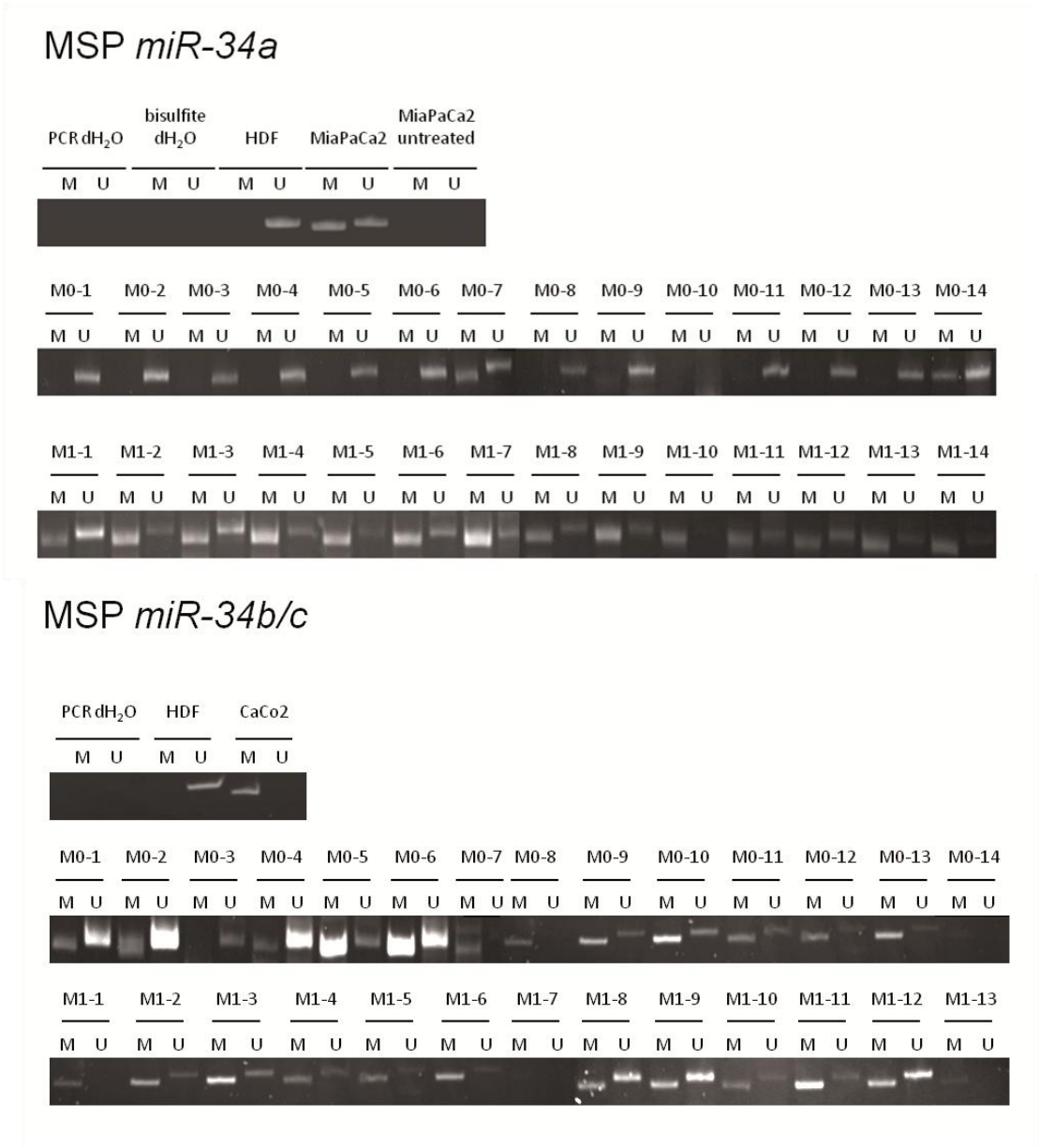

Figure 20: MSP analysis of *miR-34a* and *b/c* promoters in colorectal cancer samples with and without distant metastases. DNA was isolated from colon cancer samples either with (M1) or without (M0) distant metastases, treated with bisulfite and used as template for methylation specific PCR. Representative results are shown for *miR-34a* (upper panel) and *miR-34b/c* (lower panel). M and U represent methylated or unmethylated alleles, respectively. Water was used instead of a template in a negative control reaction, and genomic DNA from human diploid fibroblasts (HDF) served as biological negative control. MiaPaCa2 and CaCo2 DNA served as positive controls for *miR-34a* and *miR-34b/c* methylation, respectively (Lodygin et al, 2008; Toyota et al, 2008).

Notably, the proportion of hyper-methylated *miR-34a* promoters was significantly elevated in M1 samples (30 of 46) compared to M0 samples (12 of 47), summarized in Table 1. Additionally, *miR-34a* methylation significantly correlated with the status of lymph node metastases. About 54% of cases with lymph node metastases (N+) showed a methylation of the *miR-34a* promoter, while this was only the case in about 31% of the lymph node metastases-free (N0) samples. Other parameters like gender, tumor size or -grade were not significantly associated with *miR-34a* or *miR-34b/c* methylation according to a first analysis using the Pearson correlation algorithm.

Characteristics	No. of patients	*miR-34a* methylation -	+	%	p-value
Gender					
Male	49	23	25	51.0	0.170
Female	45	28	17	37.8	
Tumor size					
T2	8	5	3	37.5	
T3	72	36	35	48.6	0.465
T4	14	10	4	28.6	
Nodal status					
N0	39	26	12	30.8	0.029
N+	55	25	30	54.5	
Distant metastases					
M0	47	35	12	25.5	< 0.001
M1	47	16	30	63.8	
Tumor grade					
G2	34	21	13	38.2	
G3	56	26	29	51.8	0.838
G4	4	4	0	0.0	

Table 1: Association of *miR-34a* promoter methylation events with clinico-pathological parameters. Results obtained by MSP were correlated with several clinical parameters. *miR-34a* promoter methylation significantly correlated with distant and lymph node metastases. N+ indicates the presence of one or more lymph node metastases. p-values of ≤ 0.05 were regarded as statistically significant.

Methylation of *miR-34b/c* did not associate with any of the parameters analyzed in this study. As mentioned above the overall methylation frequency was relatively high (approximately 92%). This corresponds to previous

studies, which showed that *miR-34b/c* methylation is a very frequent event in colorectal cancer in general (Kalimutho et al, 2011; Toyota et al, 2008; Vogt et al, 2011). Therefore, the use of *miR-34b/c* methylation as a biomarker was not further analyzed in this study.

Next, I addressed, whether the *miR-34a* promoter CpG-methylation results in lower expression levels of the mature miRNAs. Since *miR-34b/c* promoter methylation was almost ubiquitously present in our collection and miR-34c expression was shown to be about 300-fold lower than miR-34a in a small subset of tumor samples (n=6; data not shown) and in previous studies, the further analyses were focused on the silencing of *miR-34a* (Kalimutho et al, 2011; Toyota et al, 2008; Vogt et al, 2011). Expression of the mature miRNA was measured by a probe-based TaqMan assay specific for miR-34a. The expression of miR-34a showed a significant inverse correlation with the methylation of its promoter in the respective tumor samples (Figure 21).

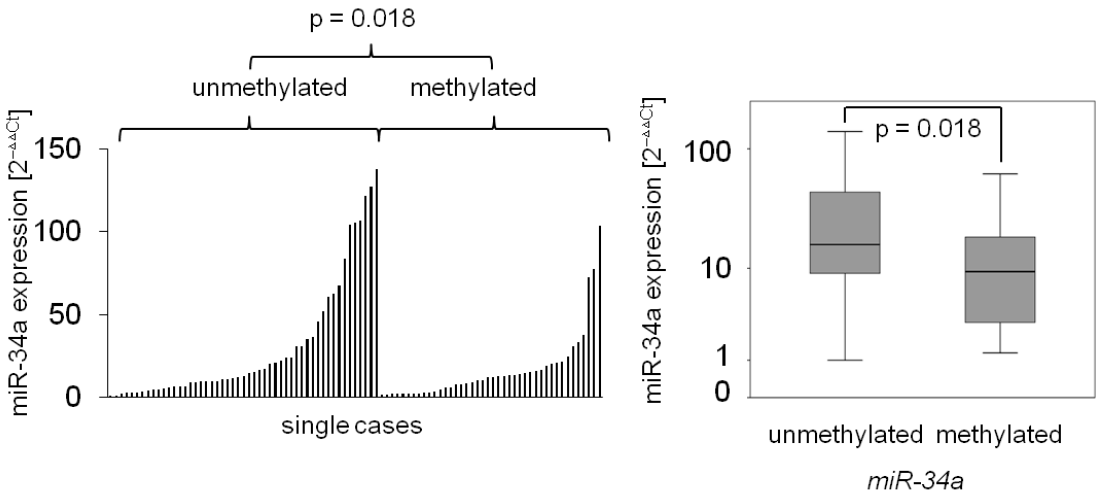

Figure 21: Correlative analysis of miR-34a expression and methylation of its promoter. Small RNAs were isolated from primary colon cancer samples either with (M1) or without (M0) distant metastases to the liver and employed as template in a miR-34a specific TaqMan assay. The left panel shows single bars representing miR-34a expression of each single case. The right panel shows box plots representing the entire populations of the methylated or unmethylated subgroups, respectively. Y-axis in the right panel is given in $\log_{10}$ scale. The p-values were calculated with a paired t-test.

In accordance to the correlation between *miR-34a* methylation and distant spread, elevated miR-34a expression showed a significant correlation with the absence of metastases to the liver (M0, Figure 22).

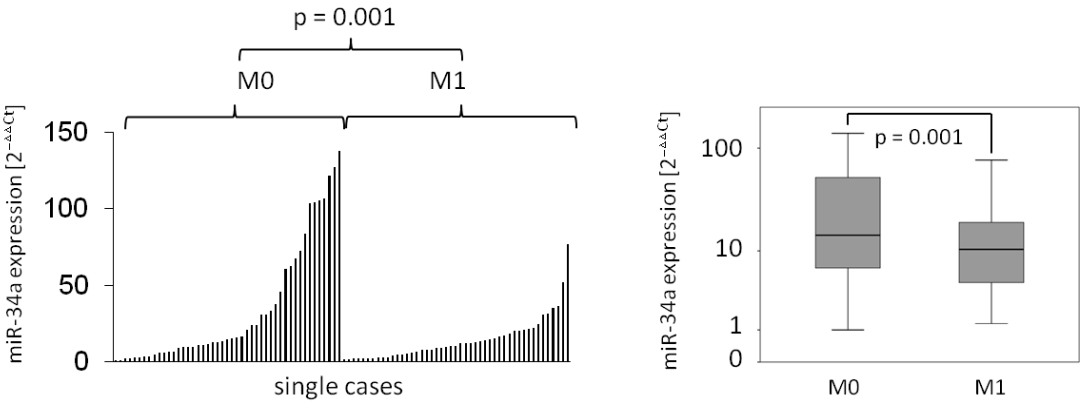

Figure 22: Detection of mature miR-34a in colorectal cancer populations with and without distant metastases. Small RNAs were isolated from colon cancer samples either with (M1) or without (M0) distant metastases to the liver and used as a template in a miR-34a specific TaqMan assay. Left panel shows single bars representing miR-34a expression of each single case. The right panel shows box plots representing the entire populations of the respective subgroups. Y-axes in both panels are given in $\log_{10}$ scale. The p-values were calculated with a paired t-test.

Analyzing the population on the basis of the matched pairs confirmed the previous results: miR-34a expression was increased in the M0 samples when compared to the respective M1-counterparts in ~68% (32 of 47) of the matched pairs (Figure 23).

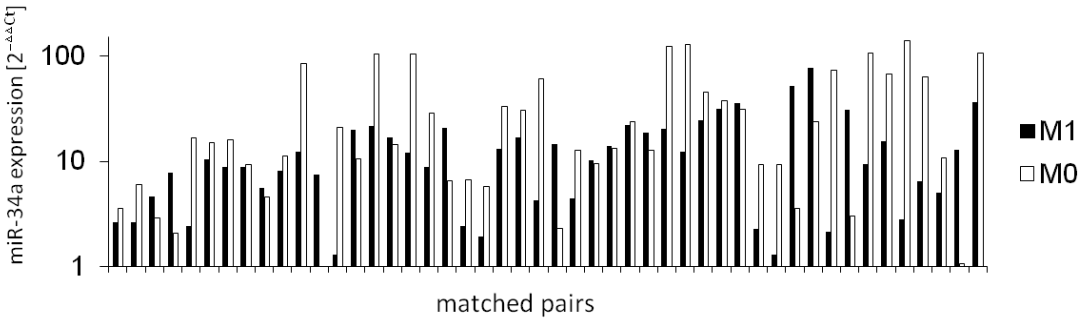

Figure 23: Detection of mature miR-34a in single colorectal cancer cases with and without distant metastases. Small RNAs were isolated from colon cancer samples either with (M1) or without (M0) distant metastases to the liver and used as a template in a miR-34a specific TaqMan assay. The single bars represent miR-34a expression of each case as single bar arranged according to matched pairs. Black bars indicate the M1 samples; white bars represent the corresponding M0 counterparts. Y-axis is given in a $\log_{10}$ scale.

Therefore, *miR-34a* expression is epigenetically silenced preferentially in primary colon cancers, which give rise to distant metastases. The subsequent analyses were aimed to determine, whether low miR-34a expression results in elevated expression of pro-metastatic miR-34-targets.

5.2.2) miR-34a expression inversely correlates with expression of its targets and clinico-pathological features

To clarify, whether the miR-34-mediated regulation of its downstream targets, like for instance Snail, was detectable in primary CRC as well and correlated with formation of metastases, immunohistochemical (IHC) analyses were performed on the tumor collection described in 5.2.1. The receptor tyrosine kinase c-Met as well as the transcription factors Snail and β-catenin were examined, all of which are targeted by miR-34a and have previously been associated with distant spread in colorectal cancer (Brabletz et al, 2005; Fujita & Sugano, 1997; Hwang et al, 2011a; Kim et al, 2011b; Kim et al, 2011c; Kudo-Saito et al, 2009; Li et al, 2009; Siemens et al, 2011). First, it was analyzed whether the expression of the proteins correlates with the miR-34a expression data obtained before. While low miR-34a expression significantly correlated with elevated levels of c-Met and β-catenin ($p=0.031$ and 0.004; Figure 24, upper and lower panel), Snail expression did not correlate with miR-34a according to the Pearson algorithm ($p=0.132$; Figure 24, middle panel). However, a weak correlation was determined using the Spearman algorithm ($p=0.044$, data not shown).

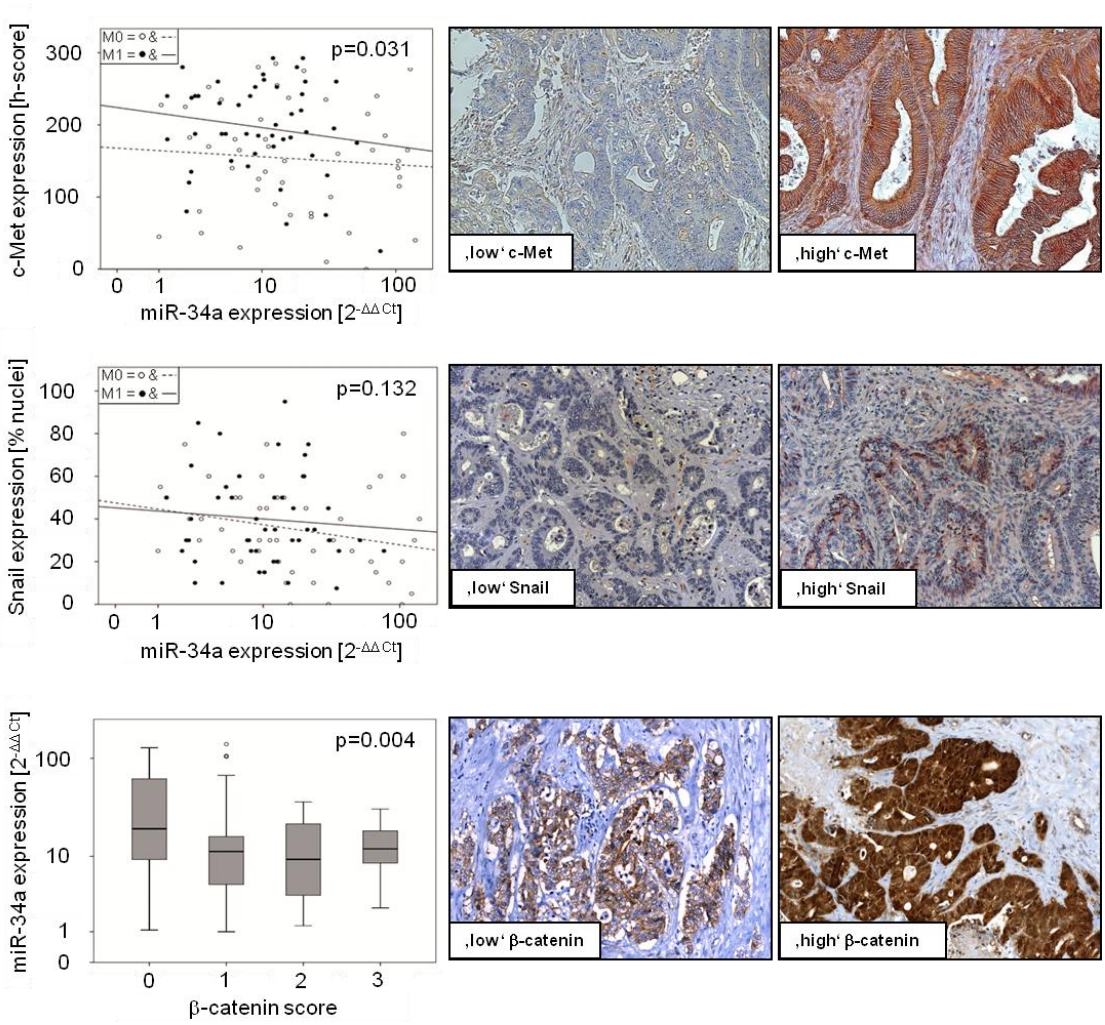

Figure 24: Correlation of the expression of miR-34a and its target proteins c-Met, Snail and β-catenin. Tissue sections of colorectal cancer samples were stained in order to determine protein expression of miR-34a targets and results were compared with miR-34a expression. In every panel the correlation between the respective target and miR-34a expression is plotted on the left. The consecutive pictures show representative immunohistochemical detections of either low or high expression of the respective protein. The upper panel shows results for c-Met, the middle panel shows results for Snail and β-catenin results are represented in the lower panel. The p-values were calculated applying the Pearson correlation algorithm.

Though inverse correlations between miR-34a and its targets were relatively weak, the expression of the respective proteins alone displayed significantly increased levels in the M1 samples in all three cases (p=0.001, 0.017 and 0.005), as shown in Figure 25.

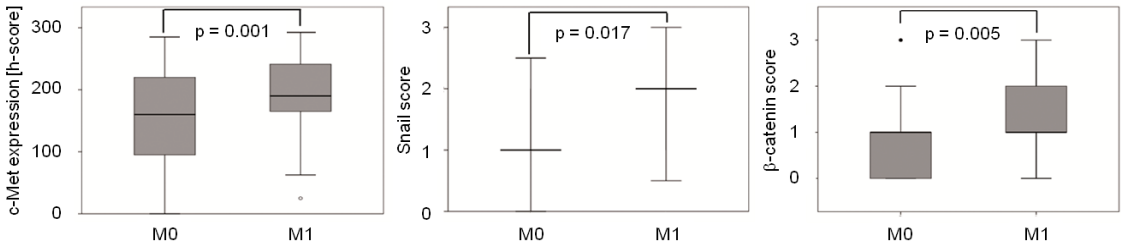

Figure 25: Correlation of miR-34a targets with distant metastases in colorectal cancer. Tissue sections of colorectal cancer samples were stained in order to determine protein expression of miR-34a targets and results were correlated with the presence of metastases. Y-axes represent expression levels of the respective miR-34a targets and boxes represent M0 and M1 subgroups. All p-values were calculated applying a paired t-test.

Additional analyses regarding the presence or absence of lymph node metastases were performed (Table 2), revealing strong correlations between the occurrence of metastases and the presence of *miR-34* methylation and low miR-34 expression. However, miR-34a targets did not reach significant differences between the two groups.

marker	analyzed parameter	mean difference N+ - N0	95% CI	p-value
miR-34a methylation	no methylation = 0 methylation = 1	0.289	[0.089 - 0.49]	0.006
miR-34a expression	$2^{-\Delta\Delta Ct}$	-19.105	[-32.649 - -5.562]	0.007
c-Met expression	H-score IHC c-Met	26.41	[-5.202 - 58.023]	0.099
Snail expression	score IHC Snail	0.231	[-0.062 - 0.523]	0.118
β-catenin expression	score IHC β-catenin	0.487	[0.088 - 0.887]	0.018

Table 2: Lymphatic spread correlates with the expression of markers analyzed in this study. N0 indicates the absence, N+ the presence of one or more lymph node metastases. Mean differences, 95% confidence interval (CI) and p-values were calculated using a paired t-test. Calculations were performed with the help of Prof. Dr. rer. nat. Ulrich Mansmann.

Thereafter, the miR-34a expression data described before (see 5.2.1) were compared with clinical features previously evaluated in this tumor sample collection (Neumann et al, 2012a). This revealed significant correlations between miR-34a expression and loss of the protein encoded by the DNA repair gene *hMLH1* as well as with microsatellite instability (MSI-H), shown in Figure 26. This is in line with the observation that the loss of hMLH1 expression causes MSI-H in colon cancer (Bronner et al, 1994; Papadopoulos et al, 1994).

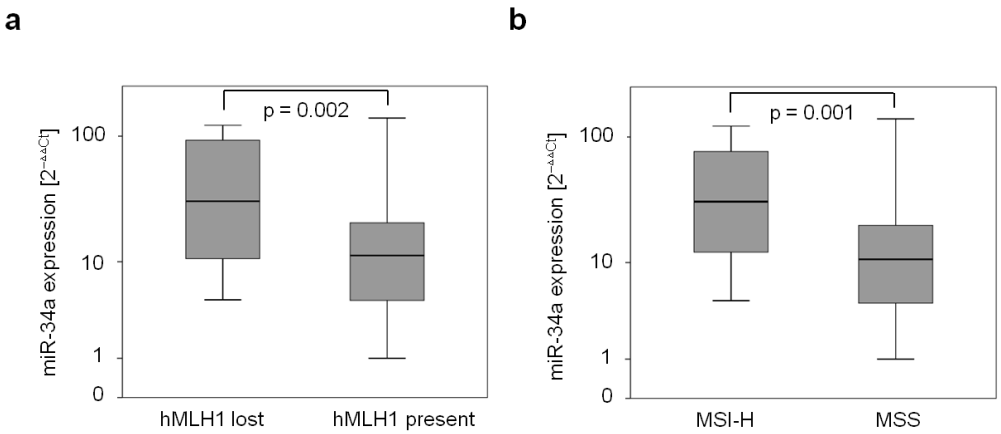

Figure 26: Correlation of miR-34a expression with hMLH1 and microsatellite instability. Expression of mature miR-34a in colorectal cancer samples was assigned to a) expression of hMLH1 and b) microsatellite instability. Data are presented as box plots. Y-axes are given in $\log_{10}$ scale and p-values were calculated with a t-test.

Additionally, the miR-34a expression data were analyzed for correlations with activated BRAF, namely V600E mutation, and advanced age, which was previously found in model organisms (Christoffersen et al, 2010; Li et al, 2011; Liu et al, 2012). The V600E mutation affects the activating loop of the mature BRAF protein reaching from codon 596 to 600. It results in the permanent activation of BRAF and occurs in a subset of colorectal cancer (Cantwell-Dorris et al, 2011).

According to the increased miR-34 expression in BRAF induced senescence (Christoffersen et al, 2010), miR-34a expression was significantly elevated in tumors with activating BRAF mutation (p=0.008, Figure 27a).

Moreover, elevated miR-34a expression in the tumor sample was associated with high age of the patients (p=0.013, Figure 27b).

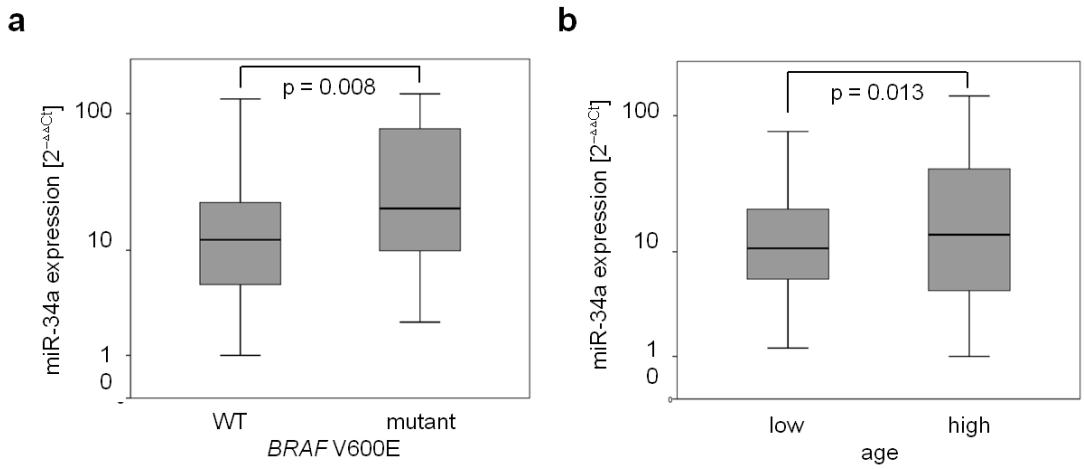

Figure 27: **Correlation of increased expression of mature miR-34a with the activating BRAF mutation V600E and advanced age in colorectal carcinomas.** Panels show box plots representing miR-34a expression of the entire population stratified either for a) BRAF mutation versus wild-type or b) age (using the median of the overall age as a cutoff for high and low age). Y-axes are given in $\log_{10}$ scale and p-values were calculated applying a t-test.

Interestingly, neither expression nor methylation of miR-34a was associated with the IHC expression pattern of p53 protein (data not shown).

5.2.3) A new marker combination is highly predictive for the risk of distant metastases in colon cancer

Finally, the prognostic value for predicting the risk of distant metastases was evaluated for the markers, which were analyzed in this study. For this purpose, sample data were sub-divided into high- and low-expressing populations, using the total median as threshold, and subjected to conditional logistic regression (Table 3). As described for the Pearson algorithm, Snail did not significantly correlate with distant spread (M1), whereas *miR-34a* methylation, c-Met- and β-catenin expression showed significant associations with metastases and exhibited comparatively high odds ratios (ORs).

Unexpectedly, miR-34a expression did not show a correlation with the absence of metastases, probably due to the simplifying assignment of the cases into high and low subpopulations.

marker	analyzed parameter	categorization	no. of patients	M0	M1	odds ratio	95% CI	p-value
			n=94	n=47	n=47			
miR-34a methylation	PCR product for methylated *miR-34a* promoter	no product = 0	42	12	30	3.571	[1.544 - 8.264]	0.003
no *miR-34a* methylation		product = 1	51	35	16			
miR-34a low	qPCR for mature miR-34a	value < median = 1	46	20	26	2	[0.751 - 5.328]	0.166
miR-34a high		value > median = 0	48	27	21			
c-Met high	H-score IHC c-Met	value > median = 1	55	20	35	4	[1.501 - 10.655]	0.006
c-Met low		value < median = 0	39	27	12			
Snail high	score IHC Snail	value > median = 1	39	16	23	1.636	[0.725 - 3.253]	0.198
Snail low		value < median = 0	54	31	23			
β–catenin high	score IHC β-catenin	value > median = 1	33	11	22	3.2	[1.173 - 8.728]	0.023
β–catenin low		value < median = 0	61	36	25			

Table 3: Univariate correlation analysis of distant metastases with clinico-pathological variables analyzed for qualitative parameters in the matched case-control collection. After categorization, based on the respective overall median of expression, data were separated into populations with low (below the median) and high (above the median) populations. A multivariate conditional logistic regression was applied to calculate the respective odds ratios, p-values and the 95% confidence intervals (CI). Calculations were performed with the help of Prof. Dr. rer. nat. Ulrich Mansmann.

In order to exclude an influence of the confounding factors gender and patient's age, a multivariate regression model was generated (Table 4). The results indicated a significant association of distant metastases with methylation of the *miR-34a* promoter and high expression of c-Met. However, β-catenin expression was not significantly associated with M1 state but nevertheless exhibited a strong trend as indicated by a p-value of 0.058.

name	categorization	odds ratio	95% CI	p-value	adjusted odds ratio	95% CI	p-value
miR-34a methylation	no product = 0 product = 1	3.182	[1.117 - 9.058]	0.03	3.522	[1.286 - 9.645]	0.014
low miR-34a expression	value < median = 1 value > median = 0	1.835	[0.456 - 7.379]	0.393			
c-Met expression	value > median = 1 value < median = 0	3.992	[1.044 - 15.191]	0.043	3.685	[1.125 - 12.059]	0.031
Snail expression	value > median = 1 value < median = 0	1.113	[0.406 - 3.048]	0.834			
β-catenin expression	value > median = 1 value < median = 0	3.519	[0.899 - 13.765]	0.71	3.762	[0.954 - 14.835]	0.058
gender	male = 1 female = 0	2.316	[0.732 - 7.334]	0.154			
age	value > median = 1 value < median = 0	1.155	[0.333 - 4.001]	0.82			

Table 4: Confounder-adjusted multivariate regression model for quantitative analysis of factors associated with metastasis formation in colon cancer. Unmatched confounding factors age and gender were added to the multivariate analysis to estimate their potential effects on the analyzed data. A multivariate conditional logistic regression was applied to calculate the respective ORs, p-values, and the 95% confidence intervals (CI). Calculations were performed with the help of Prof. Dr. rer. nat. Ulrich Mansmann.

Remarkably, *miR-34a* methylation, c-Met expression, and β-catenin expression displayed similar ORs, indicating a similar prognostic power for distant metastases. Consequently, we evaluated the prognostic value of combinations of the markers analyzed here by generating an additive score, ranging from zero to three, which sums up the value of one or zero assigned for the presence or absence of *miR-34a* methylation, high c-Met and β-catenin expression (Figure 28).

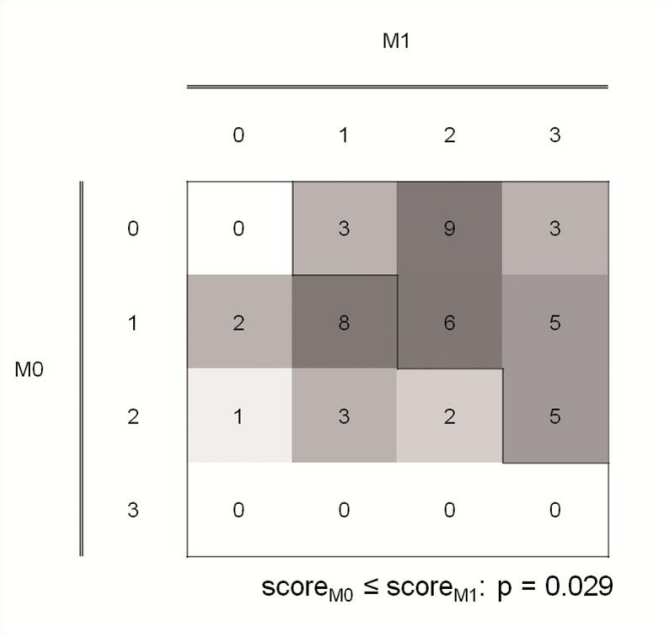

Figure 28: Combinatorial distribution of markers within the matched M0/M1 pairs. Numbers in the fields indicate number of pairs with the respective M0 and M1 score. Increased darkening indicates elevated abundance of the respective combination; white fields indicate the absence of adequate pairs. Calculations were performed with the help of Prof. Dr. rer. nat. Ulrich Mansmann.

In 31 of the 47 (approximately 66%) matched pairs, the M1 sample displayed a higher score value than the respective M0 counterpart, whereas in only six of the 47 studied pairs (12.8%), the M0 patient showed a higher marker score. For 10 pairs, no difference between case and control was determined. The difference of the combined score between case and control samples was statistically significant with a p-value of 0.029. Noteworthy, none of the M0 samples displayed a score larger than two and only three M1 samples had a score of zero. Notably, 13 of the 94 (13.8%) primary tumor samples showed the maximum score of three, thereby representing the group of patients with the highest risk of distant metastases.

To determine the practical relevance of combined marker detections, we conducted a hypothetical calculation of the risk for distant metastasis (Table 5). Assuming a baseline risk of 0.2 (20%) if none of the markers is positive, the risk increases to about 0.48 (48%) if only one of the three markers is positive, to about 0.77 (77%) when two of the three markers are positive, and to about 0.92 (92%) if all three markers are detected.

miR-34a methylation	c-Met high	β-catenin high	OR by components	OR total	Odds	Risk
no	no	no	1	1	0.25	0.20
yes	no	no	3.522	3.522	0.881	0.47
no	yes	no	3.685	3.685	0.921	0.48
no	no	yes	3.762	3.762	0.941	0.49
yes	yes	no	3.522x3.685	12.98	3.245	0.76
yes	no	yes	3.522x3.762	13.25	3.313	0.77
no	yes	yes	3.685x3.762	13.86	3.465	0.78
yes	yes	yes	3.522x3.685x3.762	48.83	12.208	0.92

Table 5: Theoretical evaluation of the prognostic value of the marker combination for the prediction of metastases in colon cancer. Odds ratios (ORs) of single markers (see Table 4) and ORs for combinations of 2 or 3 markers are listed. The risk column represents the result of a hypothetical calculation estimating the risk for distant metastases in dependence of expression of the markers analyzed in this study. For this, the baseline risk for metastases in the absence of detection of any of the 3 markers was set to 20% (=0.2). The increasing darkness of grey shading indicates the increasing risk due to the number of detected markers (0–3). Calculations were performed with the help of Prof. Dr. rer. nat. Ulrich Mansmann.

Taken together, the combined detection of *miR-34a* CpG-methylation, elevated c-Met and β-catenin expression emerged as the combination with the highest prognostic power for distant metastasis in this cohort of patients with colon cancer.

5.3) *c-Kit* is directly targeted by miR-34 upon p53 activation

The results presented in this chapter have been published: Siemens H, Jackstadt R, Kaller M and Hermeking H (2013). Repression of c-Kit by p53 is mediated by miR-34 and is associated with reduced chemoresistance, migration and stemness. Oncotarget 4 (9), August 6, advance online publications. The respective contributions of the co-workers are indicated in the text.

5.3.1) c-Kit is repressed by ectopic expression of p53 and miR-34a in colorectal cancer cell lines

According to a recent study, the RTK c-Kit is repressed by p53 in murine hematopoietic stem cells (Abbas et al, 2011). However, the authors did not detect a direct binding of p53 to the *c-Kit* promoter. This led us to the hypothesis, that miR-34 may mediate the down-regulation of c-Kit expression after p53 activation. To analyze the potential regulation of c-Kit by p53, two different conditional systems were employed to express p53: SW480 cell pools transfected with the DOX-inducible vector pRTR expressing the *p53* ORF and a DLD1 single cell clone harboring a *p53* allele under control of the tet-off system (Siemens et al, 2011; Yu et al, 1999). Although the endogenous levels of c-Kit were lower in SW480 cells than in DLD1 cells, in both cellular systems c-Kit protein expression was down-regulated following activation of p53 for 48 hours (Figure 29).

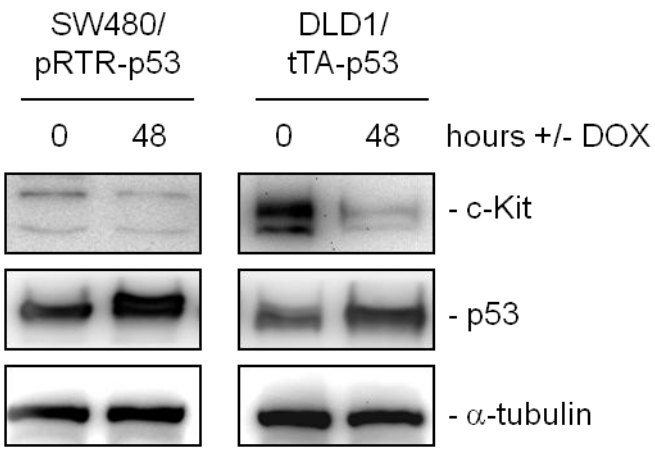

Figure 29: c-Kit protein levels are repressed after ectopic p53 in colorectal cancer cell lines. p53 was ectopically induced in the CRC cell lines SW480 and DLD1 for 48 hours. The indicated proteins were detected by Western blot analysis. α-tubulin served as a loading control.

Since miRNAs were shown to mediate gene repression by p53, we examined the *c-Kit* 3'-UTR using the Target-Scan algorithm (Lewis et al, 2005). Thereby two potential miR-34 seed-matching sequences were identified in the 3'-UTR of c-*Kit*, which are depicted in Figure 30. While the first site, which is a perfect match to the miR-34a 8-mer seed-sequence, is relatively conserved among different species, the second site was less conserved.

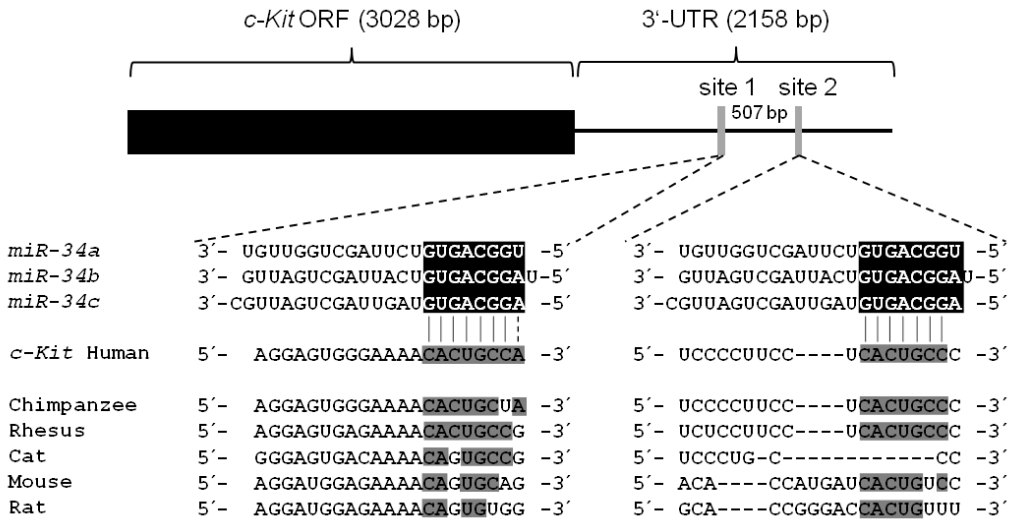

Figure 30: Scheme of the *c-Kit* mRNA and conservation of the putative miR-34 seed-matching sequences among species. miR-34-seed matches are represented as grey vertical bars in the *c-Kit* 3'-UTR (thin black line)**.** Detailed sequences of the two sites and phylogenetic homologies are shown below. Potential base pairing is shaded in grey.

To determine whether the differences in c-Kit protein were due to changes on mRNA level, and therefore potentially caused by miRNA activity, p53 was induced in SW480 and DLD1 cells for 72 hours, total RNA was isolated and employed as template for qRT-PCR (Figure 31). As expected, expression of the primary *miR-34a* transcript was induced. Furthermore, repression of the *c-Kit* mRNA was observed after p53 activation in both SW480 and DLD1 cells.

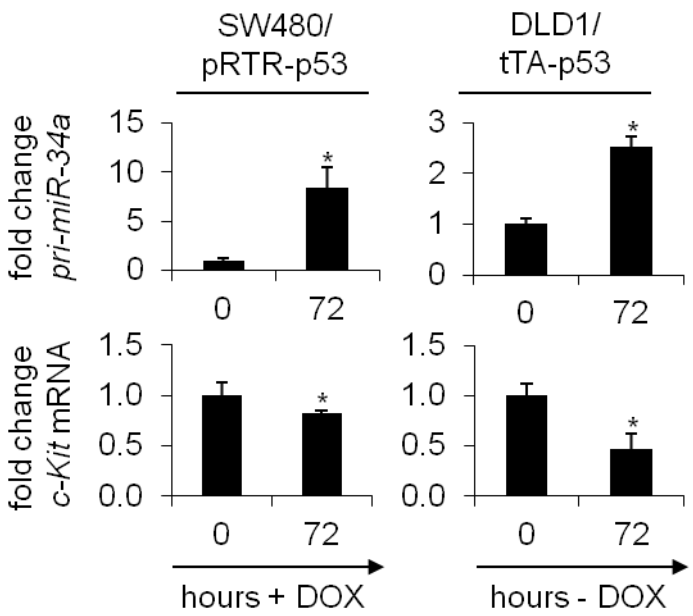

Figure 31: qPCR analysis of *pri-miR-34a* and *c-Kit* mRNA levels in the colorectal cancer cell lines SW480 and DLD1 after p53 induction. p53 was induced by addition or withdrawal of DOX for 72 hours. Results were normalized to *β-actin* mRNA. Results represent the mean +/- SD (n=3) and significance was calculated applying a Student's t-test. p-values ≤ 0.05 are indicated by *.

Since the basal levels of miR-34b and c expression have been shown to be relatively low in colon cancer and therefore seem to be of minor functional relevance, we focused our further studies on miR-34a (Kalimutho et al, 2011; Toyota et al, 2008; Vogt et al, 2011). In order to test whether miR-34a expression alone is sufficient to down-regulate c-Kit, *pri-miR-34a* was expressed in SW480 and DLD1 cells using the conditional pRTR expression system. Indeed ectopic miR-34a reduced *c-Kit* mRNA levels in both cell lines (Figure 32).

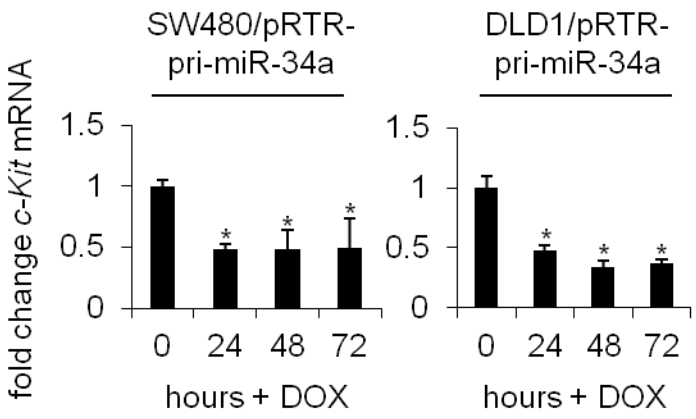

Figure 32: qPCR analysis of *c-Kit* mRNA levels in the colorectal cancer cell lines SW480 and DLD1 upon ectopic miR-34a expression. miR-34a was induced by addition of DOX for the indicated periods. Results were normalized to *β-actin* mRNA. Results represent the mean +/- SD (n=3) and significance was analyzed by a Student's t-test. p-values ≤ 0.05 are indicated by *.

To confirm that the regulation of *c-Kit* mRNA by miR-34a was accompanied by a decrease of the protein, corresponding protein lysates of DOX-treated SW480 and DLD1 cells were generated and subjected to Western blot analysis (Figure 33).

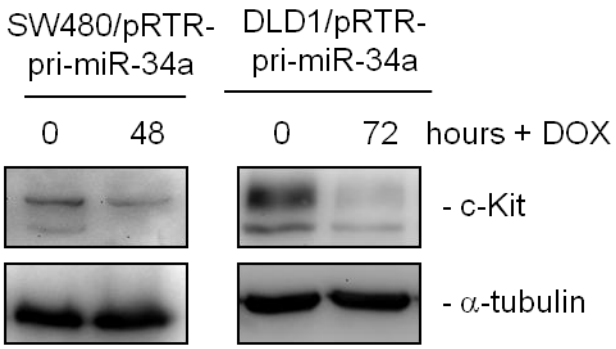

Figure 33: Down-regulation of c-Kit protein expression upon induction of ectopic miR-34a in colorectal cancer cells. miR-34a was induced by addition of DOX for the indicated time points. The indicated proteins were detected by Western blot analysis. α-tubulin served as a loading control.

This revealed a concomitant decrease of the c-Kit protein after addition of DOX. Therefore, elevated miR-34a expression is sufficient to decrease c-Kit protein and mRNA levels.

5.3.2) miR-34 directly targets *c-Kit* and mediates c-Kit down-regulation by p53

To determine whether the miR-34 family members bind to the predicted target sites in the *c-Kit* 3'-UTR, a dual luciferase reporter assay was performed. For this a 1245 bp fragment of the *c-Kit* 3'-UTR, including the two potential binding sites, was cloned downstream of a *luciferase* ORF. To additionally analyze whether one of the two sites is preferred by miR-34a, either both or one of the seed-matching sites were mutated (Figure 34).

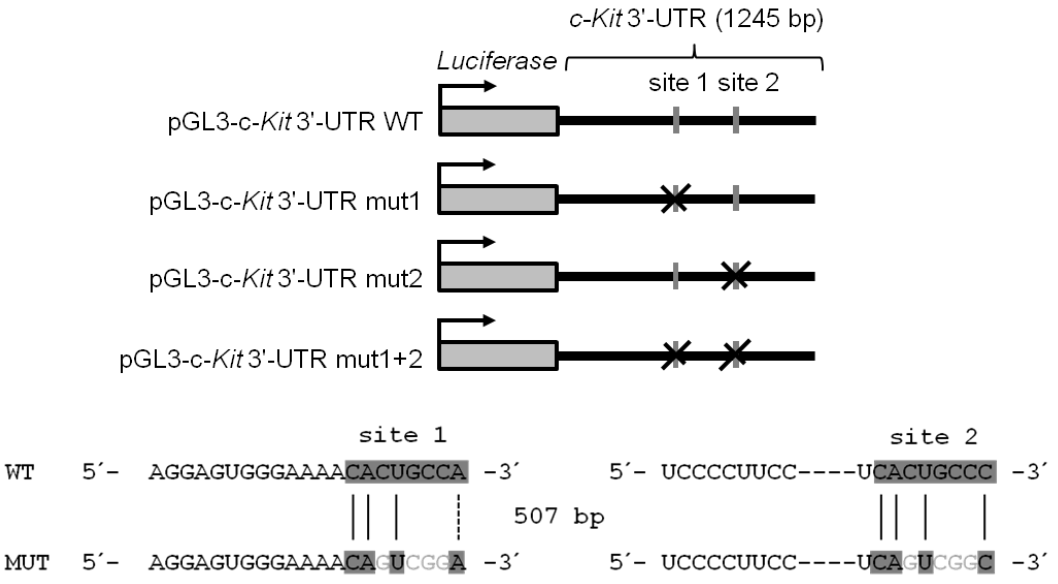

Figure 34: Schematic depiction of constructs used for dual luciferase assay. The luciferase gene is presented as grey box, the *c-Kit* 3'-UTR is presented as black horizontal bar and the positions of the miR-34 seed-matching sequences in the *c-Kit* 3'-UTR are depicted as a grey vertical bars. The targeted mutation of the potential miR-34 sites are expressed as crossed out. Detailed base exchanges of the respective targeted mutations are given below.

In the dual-reporter luciferase assay miR-34a as well as miR-34b and c significantly decreased the activity of the reporter representing the wild-type *c-Kit* 3'-UTR compared to the empty control vector (Figure 35). When site 1 was mutated, we observed a strong de-repression, whereas mutation of site 2 could not prevent the down-regulation of the luciferase activity. Mutation of both sites led to resistance against miR-34a regulation, but not to a de-repression.

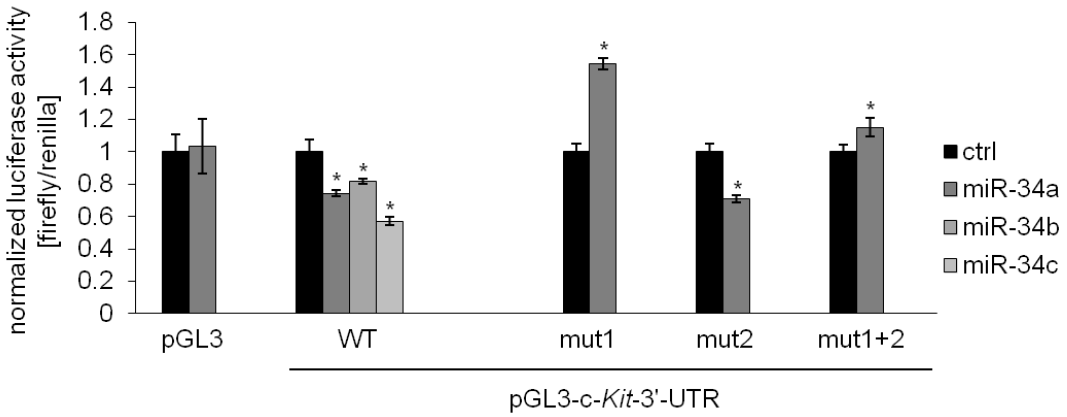

Figure 35: miR-34 oligonucleotides repress a *c-Kit* reporter in a dual-luciferase assay. Dual reporter assay in SW480 cells transfected with miR-34a/b/c mimics or control oligonucleotide and the indicated reporter constructs for the human *c-Kit* 3'-UTR. Data are represented as mean ± SD (n=3) and significance was calculated applying a Student's t-test. p-values ≤ 0.05 are indicated by *.

These results indicate that the miR-34 family targets the *c-Kit* mRNA using the first of the two tested binding sites and additionally substantiate the assumption that the first site is the preferred target sequence, since it is highly conserved among species.

In addition, p53-mediated down-regulation of c-Kit in DLD1 cells could be prevented by simultaneous transfection of an antagomiR directed against miR-34a (anti-miR-34a), while additionally transfected miR-34a further enhanced the repression of c-Kit when p53 was activated concomitantly (Figure 36).

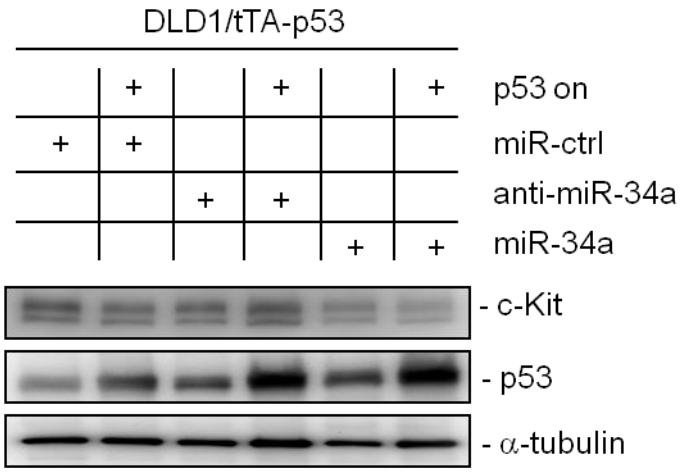

Figure 36: Inhibition of miR-34a attenuates the p53-mediated degradation of c-Kit. DLD1/tTA-p53 cells were either transfected with a control oligonucleotide, miR-34a or an anti-miR directed against miR-34a for 24 hours and kept either in the presence or absence of DOX (without or with ectopic p53). The indicated proteins were detected by Western blot analysis. α-tubulin served as a loading control.

Taken together, miR-34a therefore mediates the repressive effects of p53 on c-Kit expression by directly targeting the *c-Kit* 3'-UTR via a single conserved seed-matching site.

5.3.3) Ectopic expression of c-Kit overrides miR-34a-mediated inhibition of Erk signaling and colony formation in DLD1 cells

In order to determine the effects of the miR-34a-mediated decrease in c-Kit protein, we analyzed its impact on downstream signaling pathways. While phosphorylated Stat3 did not seem to be affected (data not shown), phosphorylated Erk levels were significantly decreased after miR-34a induction and the concomitant reduction of c-Kit in DLD1 cells, while un-phosphorylated Erk levels remained unchanged (Figure 37).

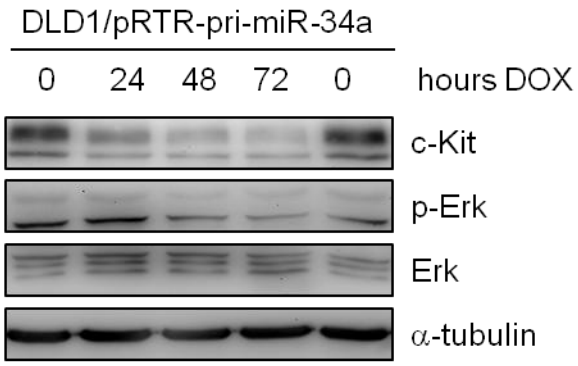

Figure 37: Down-regulation of c-Kit by miR-34a negatively influences Erk signaling in DLD1 cells. DLD1 cells carrying the DOX-inducible vector pRTR-pri-miR-34a were treated with DOX for the indicated time-points and cell lysates subjected to Western blot analysis using antibodies against the indicated proteins. α-tubulin served as a loading control.

Next, it was determined whether the miR-34a-mediated decrease in Erk phosphorylation was dependent on the down-regulation of c-Kit. Therefore, DLD1 and SW480 cell pools were generated carrying a conditional expression vector for c-Kit lacking its original 3'-UTR. Without the miR-34 seed-matching sequence, ectopic c-Kit was expected to be resistant to degradation by miR-34a. In line with the vector-driven miR-34a expression (Figure 37), transfection of these cells with a miR-34a oligonucleotide resulted in decreased levels of Erk phosphorylation in both cell lines, while the control oligo had no effect (Figure 38). Notably, induction of ectopic c-Kit largely reversed the effect of miR-34a on phosphorylated Erk, whereas the amount of total Erk was not affected. Collectively, these results show that the down-regulation of c-Kit is necessary for the inhibitory effects of miR-34a on Erk signaling.

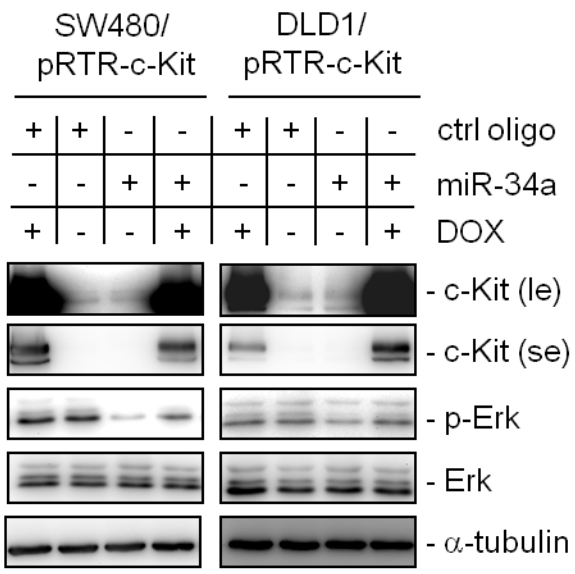

Figure 38: Ectopic (miR-34a-resistant) c-Kit prevents miR-34a-mediated repression of Erk phosphorylation in CRC cell lines. SW480 and DLD1 cells were transfected with oligonucleotides for 48 hours and DOX was added for 24 hours. Subsequently, Western blot analysis of the indicated proteins was performed. α-tubulin served as a loading control. le: long exposure, se: short exposure. The cell pools of SW480/pRTR-c-Kit were generated by Rene Jackstadt.

To test, whether these regulations would affect the capacity of SW480 cells to grow anchorage-independent in soft agar, which is known to be affected by Erk signaling (Wiesenauer et al, 2004), cells treated as in Figure 38 were seeded into soft agar and colony formation was measured (Figure 39). miR-34a transfection severely reduced the number of colonies. The induction of ectopic c-Kit expression led to a slight but significant increase in the number of colonies, at least partially reflecting the results observed on the level of Erk phosphorylation.

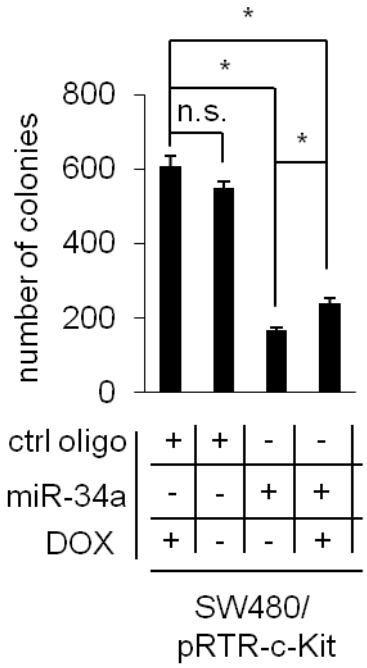

Figure 39: The interplay of c-Kit and miR-34a influences colony formation of CRC cells. SW480 cells were treated as described in Figure 38 and subjected to a colony formation assay. Results represent the mean +/- SD (n=3) and significance was calculated applying a Student's t-test. p-values ≤ 0.05 are indicated by *. The cell pools of SW480/pRTR-c-Kit were generated by Rene Jackstadt.

In conclusion, Erk signaling downstream of c-Kit contributes to colony formation and can be suppressed by miR-34a. As demonstrated, this effect of miR-34a seems to depend, at least in part, on the down-regulation of the c-Kit receptor expression by miR-34a.

In a subsequent qPCR analysis, the EMT markers *Vimentin* and *CDH1* as well as the primary transcript of *miR-34a* were not affected on mRNA level upon the ectopic expression of c-Kit in either SW480 (Figure 40a) or DLD1 cell pools (Figure 40b).

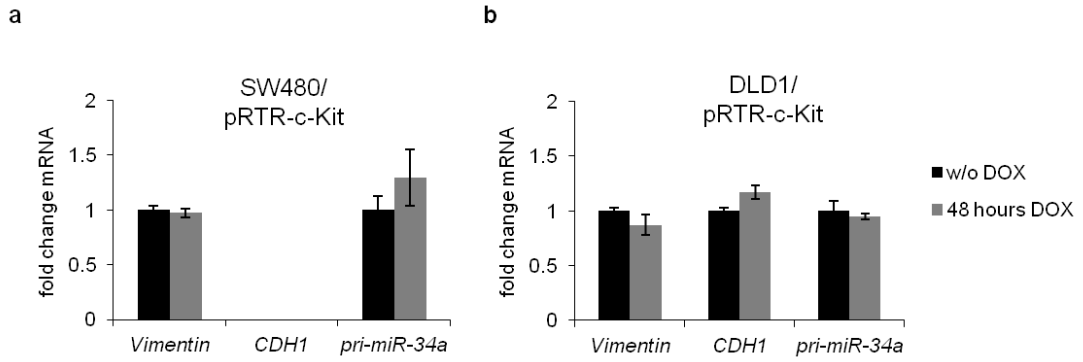

Figure 40: EMT markers and the primary *miR-34a* transcript are not regulated upon induction of c-Kit. SW480 a) and DLD1 cells b) carrying the DOX inducible vector pRTR-c-Kit were treated with DOX for 48 hours or left untreated. qPCR was applied to measure the mRNA expression of the EMT markers *Vimentin*, *CDH1* and the primary *miR-34a* transcript. Each bar represents the mean +/- SD (n=3).

This is worth mentioning, since former publications linked c-Kit with EMT (Peparini et al, 2009). This assumption was further supported by the finding that two crucial EMT-TFs, namely Snail and Slug, induce a stemness gene signature and increase the numbers of $CD44^{+}/CD117^{+}$ cells (Kurrey et al, 2009). However, according to our data, no mRNAs of EMT-specific-markers, such as *CDH1* or *Vimentin,* were regulated by ectopic c-Kit expression.

5.3.4) miR-34a enhances the response of cancer cells to 5-fluorouracil by down-regulation of c-Kit

Recently, c-Kit was shown to mediate chemoresistance in ovarian tumor initiating cells (Chau et al, 2012). Therefore, we asked whether c-Kit might play a similar role in colorectal cancer. To address this issue DLD1 cells, expressing relatively high basal levels of c-Kit, and SW480 cells, expressing relatively low basal levels, were employed (Figure 41a). Both cell lines were treated either with 5-fluorouracil (5-FU) [20 µg/ml], Doxorubicin (=Adriamycin) [0.25 µg/ml] or left untreated for 48 hours. Subsequently, apoptosis and cell cycle distribution was determined by DNA content analysis

using flow cytometry. SW480 cells, which express lower basal c-Kit levels than the respective DLD1 counterparts, showed a much stronger response to both chemotherapeutics (Figure 41b). Apoptosis, as indicated by cells in the sub-G1 phase, was elevated about 3-fold after treatment with the anti-metabolite 5-FU and about 4-fold using the anthracycline antibiotic Doxorubicin compared to DLD1 cells. Noteworthy, the apoptosis rates of untreated cells were increased in SW480 cells as well, compared to DLD1 cells.

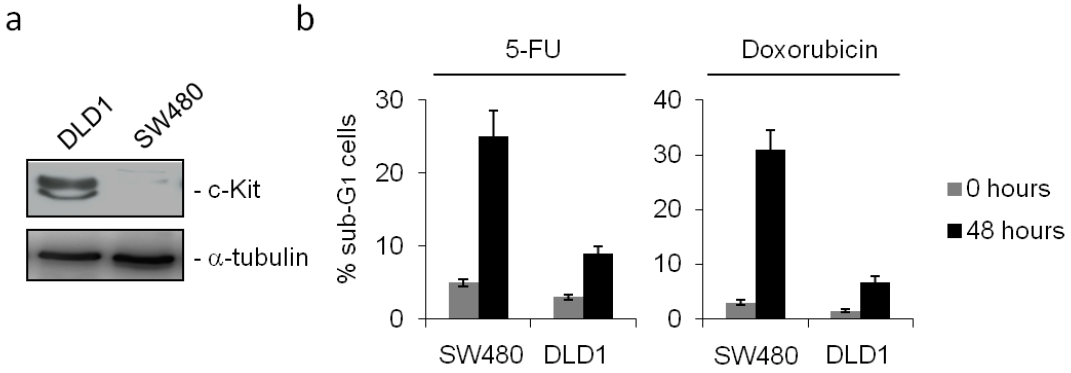

Figure 41: High levels of c-Kit are associated with a decreased apoptotic response to chemotherapy treatment. a) Western blot analysis of parental DLD1 and SW480 colorectal cancer cells comparing endogenous c-Kit levels. α-tubulin served as loading control. b) Cells characterized in a) were treated with either 5-FU or Doxorubicin for 48 hours or left untreated. Results represent the mean +/- SD (n=3) for each cell line and treatment.

To prove whether this low chemosensitivity can be influenced by miR-34a, DLD1 cells were either transfected with miR-34a or control oligos for 24 hours to achieve c-Kit down-regulation. Subsequently, the cells were treated with either 5-FU [20 µg/ml] or left untreated and the cell index was measured every hour over two days using the xCELLigence real-time cell analyzer (RTCA). This revealed an additive effect of miR-34a and 5-FU on DLD1 cells (Figure 42a): while cells transfected with the control oligo appeared unaffected, transfection with miR-34a resulted in a lower cell index over time. Treatment with 5-FU negatively influenced the survival of the cells comparably stronger

but the most significant response resulted from additive treatment with miR-34a and 5-FU at the same time.

As demonstrated by Western blot analysis in Figure 42b, transfection of DLD1 cells with miR-34a resulted in a decrease of c-Kit protein levels. The control oligo did not influence the c-Kit protein.

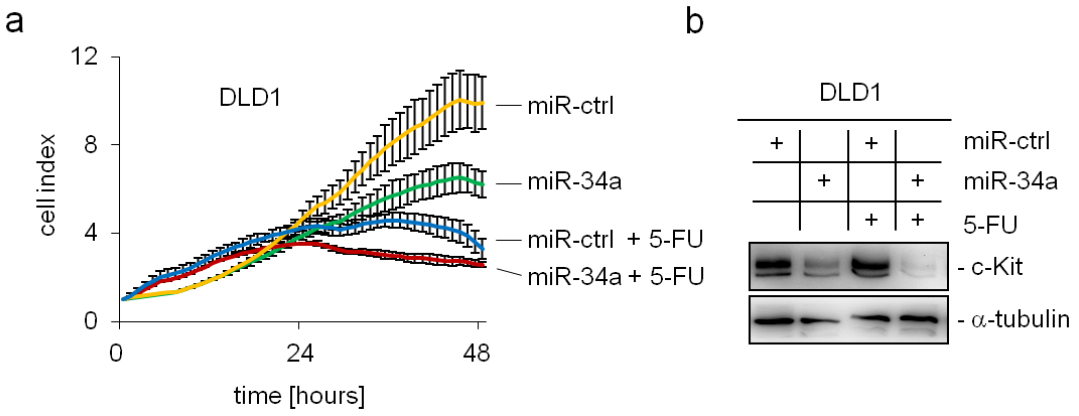

Figure 42: Ectopic expression of miR-34a enhances response of cancer cells to 5-FU by down-regulation of c-Kit. a) DLD1 cells were seeded into wells of an E-plate 16 and either transfected with miR-34a or control oligos. Thereafter, the cells were treated with either 5-FU or left untreated and the cell index was measured using the xCELLigence RTCA. b) Cells treated as described in a) were lysed to validate miR-34a-mediated c-Kit regulation. The indicated proteins were detected by Western blot analysis. α-tubulin served as loading control.

5.3.5) miR-34a inhibits SCF-induced migration and invasion in Colo320 colorectal cancer cells

Another function of the SCF/c-Kit axis is an enhancement of migration, which was previously observed after treatment of the CRC cell line Colo320 using SCF (Yasuda et al, 2007). Based on this report it was analyzed whether transfection with miR-34a may interfere with the effects of SCF. First, regulation of c-Kit by miR-34a was confirmed on mRNA and protein level to prove, that c-Kit regulation by miR-34a also occurs in this cellular background (Figure 43a/b). As expected, transfection of Colo320 cells with miR-34a

oligonucleotides for 48 hours led to a decrease of c-Kit on the mRNA and protein levels.

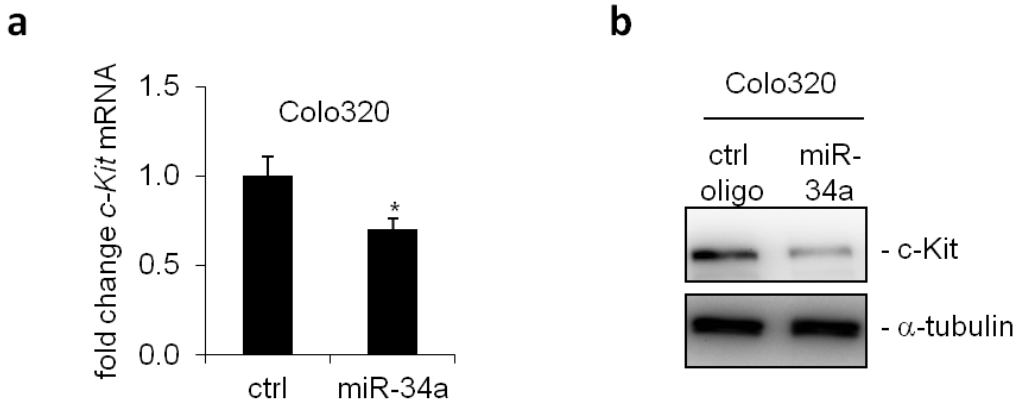

Figure 43: Treatment of Colo320 colorectal cancer cells with miR-34a oligonucleotides reduces *c-Kit* mRNA and protein levels. a) Colo320 cells were transfected either with a control oligo (ctrl) or miR-34a [50 nM each]. qPCR analysis was used to study *c-Kit* mRNA levels, *β-actin* mRNA served as normalization. Results represent the mean +/- SD (n=3) and significance was calculated applying a Student's t-test. * indicates a p-values ≤ 0.05. b) Protein lysates of cells treated as described in a) were subjected to Western blot analysis in order to compare c-Kit protein levels of transfected cells. α-tubulin served as loading control.

Our results confirmed that miR-34a interferes with the expression of c-Kit in Colo320 cells and therefore potentially affects SCF-mediated signaling and cellular down-stream effects.

In order to analyze the migratory behavior, Colo320 cells were transfected with either miR-34a or a control oligo [100 nM each] and treated with SCF [10 ng/ml] or water. After 24 hours cells were seeded into Boyden chambers either coated (invasion) or uncoated (migration) with Matrigel. Media were supplemented with SCF for stimulated cases. Cells were allowed to migrate for 48 hours and pictures of DAPI stained cells (see methods) were taken. As shown in Figure 44, transfection of the cells with miR-34a reduced migration and invasion compared to the control oligo. In accordance to the previous study mentioned above, administration of SCF and control oligo resulted in a two to three-fold increase of the migration in both assays. Strikingly, administration of SCF and concomitant transfection with miR-34a reduced migration and invasion of the cells almost to basal levels. These data suggest

that miR-34a interferes with SCF signaling by depletion of the receptor and thereby makes the cells refractory to SCF.

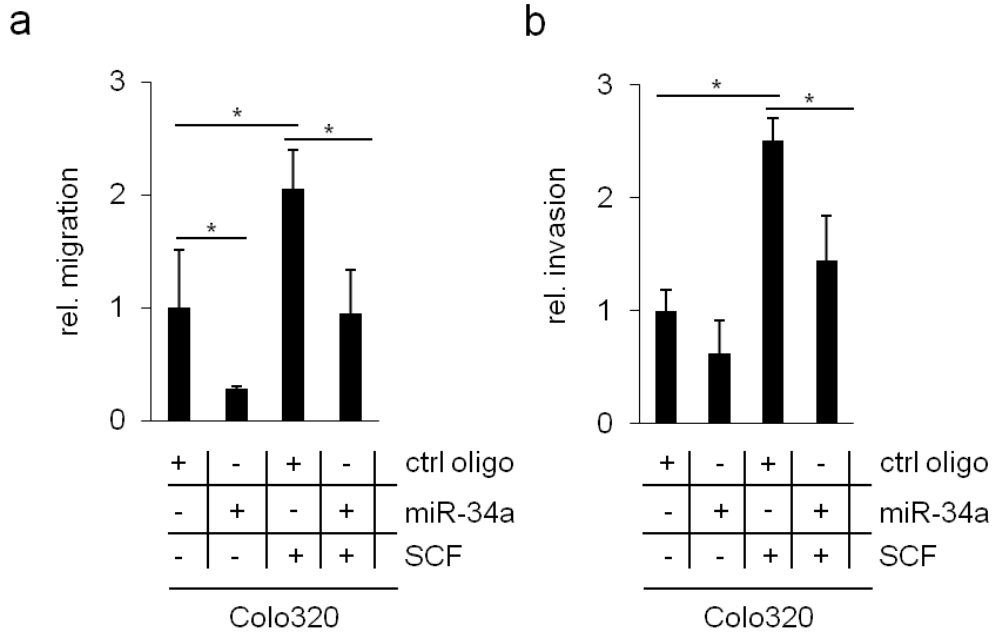

Figure 44: miR-34a transfection abolishes increased cell mobility of Colo320 cells upon stimulation with SCF. Colo320 cells were treated with and without SCF and transfected at the same time for 24 hours with the indicated oligonucleotides. Thereafter cells were seeded into Boyden chambers and allowed to migrate for two days to study migration and invasion. Migration results are given in a) results of invasion assay are given in b). Each bar represents the mean +/- SD (n=3) and significance was calculated applying a Student's t-test. p-values ≤ 0.05 are indicated by *.

An SCF-dependent increase of proliferation rates in Colo320 cells, as described by Yusada and colleagues, was not detected and therefore no experiments related to proliferation were performed.

Since SCF is involved in the regulation of hematopoietic stem cells and recent studies indicated a role for c-Kit in stemness in ovarian cancer, the role of c-Kit in the regulation of stemness markers was investigated in colorectal cancer cells (Kent et al, 2008; Chau et al, 2012). Therefore, c-Kit was ectopically expressed in DLD1 cells and changes in mRNA expression of several stemness markers were determined by qPCR. As positive control for c-Kit-mediated gene regulation, the expression of its downstream effectors *c-*

Fos and *Oncostatin M*, was analyzed (Hoermann et al, 2011; Lennartsson et al, 1999). As markers for CRC stemness the following genes were chosen: *CD44*, *CD133*, *Lgr5*, *Nanog*, *Nanog P8*, *β-catenin*, *Sox2*, *BMI-1* and *OLFM4* (Horst et al, 2012; Kemper et al, 2010; Ma et al, 2012; Wellner et al, 2009; Zhang et al, 2012). *c-Fos* and *Oncostatin M* were significantly induced after 48 hours of c-Kit activation by the addition of DOX (Figure 45). While *CD44* was repressed and *BMI-1* expression remained unchanged, all other analyzed stemness markers were significantly up-regulated by ectopic c-Kit. These data supported the assumption that c-Kit plays a role in colorectal cancer stem cells.

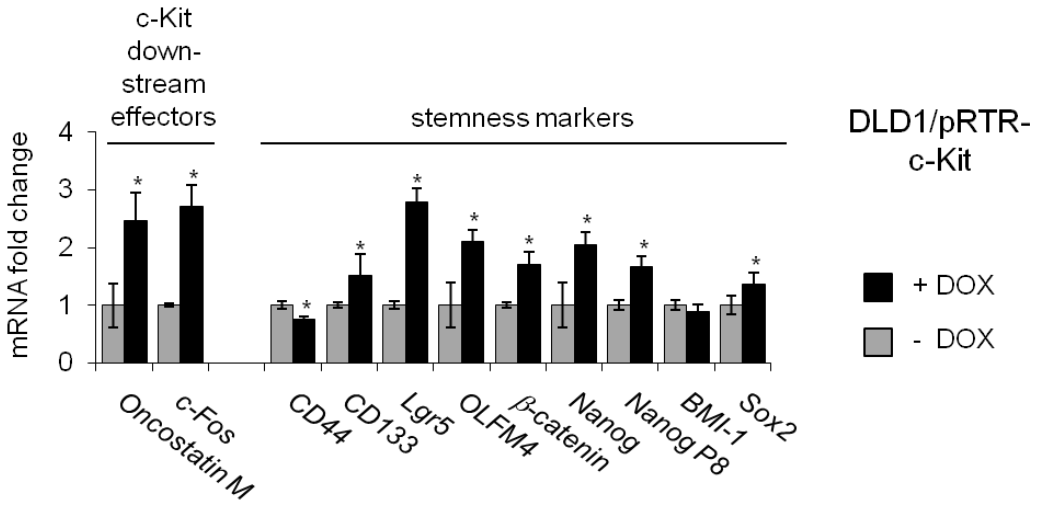

Figure 45: c-Kit expression induces expression of stemness CRC cells. DLD1/pRTR-c-Kit cells were treated with DOX for 48 hours. Expression levels of different mRNAs were measured via qPCR. Results represent the mean +/- SD (n=3). * indicates a p-value of ≤ 0.05, calculated using a Student's t-test.

To determine whether an association between c-Kit and stemness markers is also found in clinical samples as well, expression data of 196 colorectal tumors from the public database TCGA (the cancer genome atlas; Muzny, 2012) was analyzed (Figure 46). Within this collection, the expression of *OLFM4, CD44, β-catenin, BMI-1* and *Lgr5* mRNA emerged as significantly associated with elevated *c-Kit* mRNA expression ($p \leq 0.05$). Additionally, elevated *SCF* mRNA expression correlated with increased expression of its

receptor. This supports the assumption that an auto-regulatory loop exists between receptor and ligand (Bellone et al, 2006; Hibi et al, 1991; Martinho et al, 2008; Theou-Anton et al, 2006). Taken together, these data suggest that c-Kit plays a role in the regulation of stem cell markers in human colorectal tumors as well as in colorectal cancer cell lines. Therefore, the regulation of c-Kit by miR-34 might be relevant for suppressing colorectal cancer stem cells.

.

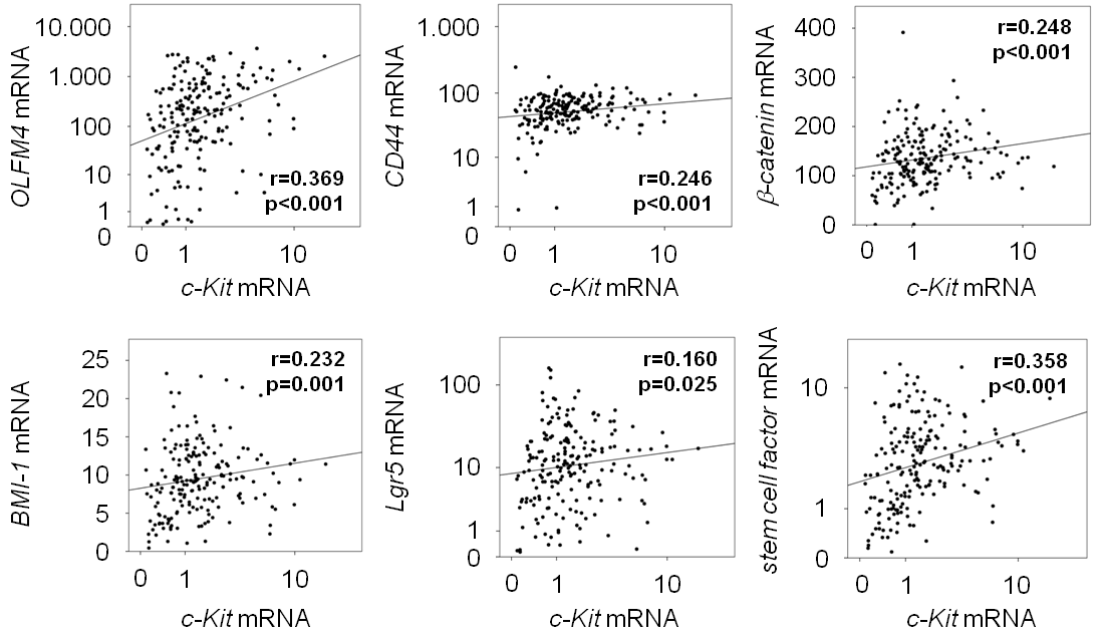

Figure 46: high *c-Kit* expression is associated with elevated expression of stemness marker mRNA in CRC patients. mRNA expression data derived from primary CRC samples (n=196) were obtained from the public database TCGA (Muzny, 2012). Correlation coefficients and p-values were calculated applying the Spearman correlation algorithm. Scatter plots show the respective correlations. Both, the c-*Kit* levels on the x-axes and the y-axes corresponding to *OLFM4, CD44, Lgr5* and *SCF* are provided as $\log_{10}$ scale.

To investigate whether miR-34a-dependent regulation of c-Kit might interfere with stemness markers in CRC cell lines, the same mRNA expression levels were analyzed in previously described DLD1 cells carrying a pRTR/pri-miR-34a vector. Upon induction of ectopic miR-34a expression, the mRNA levels of *c-Kit* and the published down-stream effectors *c-Fos* and *Oncostatin M* were strongly diminished (Figure 47). However, the stemness marker mRNAs showed only weak down-regulation compared to the un-induced state. Most significant changes occurred in the expression of *CD44* and *BMI-1*.

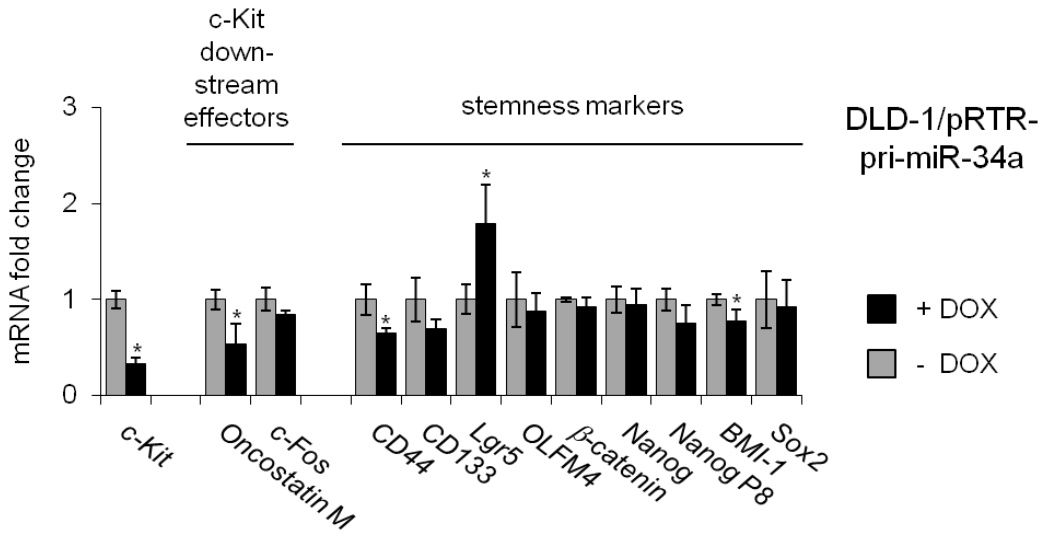

Figure 47: Ectopic miR-34a expression down-regulates stemness marker genes in CRC cells. DLD1 cells carrying the pRTR/pri-miR-34a vector were treated with DOX for 48 hours. Expression of the indicated mRNAs was analyzed by qPCR. Results represent the mean +/- SD (n=3). * indicates a p-value of ≤ 0.05.

To determine whether these regulations are functionally relevant for stemness, DLD1 cells were subjected to a sphere formation assay, in which cells are kept in suspension under non-adherent conditions.

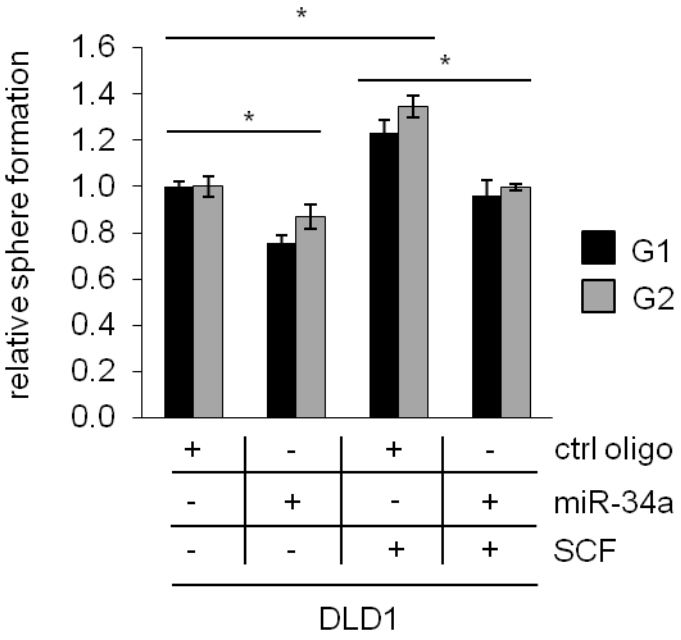

Figure 48: miR-34 interferes with SCF-induced sphere formation in CRC cells. DLD1 cells were transfected with the indicated oligonucleotides, treated with SCF (or water) and subjected to a sphere formation assay. Sphere numbers were determined after seven days for the first generation (G1) and after additional seven days for G2. Treatment with oligonucleotides and SCF was repeated when cells were passaged. Results represent the mean +/- SD (n=3) and significance was calculated applying a Student's t-test. * indicates a p-value of ≤ 0.05. G1: first generation, G2: second generation

This assay is widely used to assess self-renewing capacities in cancer stem cells. In line with previous publications (Bellone et al, 1997), treatment with SCF significantly stimulated sphere formation of DLD1 cells (Figure 48). The treatment with ectopic miR-34a oligos reduced the number of resulting spheres and moreover reduced sphere formation in presence of SCF to baseline levels. These effects were stable over two consecutive generations. Representative pictures of the spheres are shown in Figure 49.

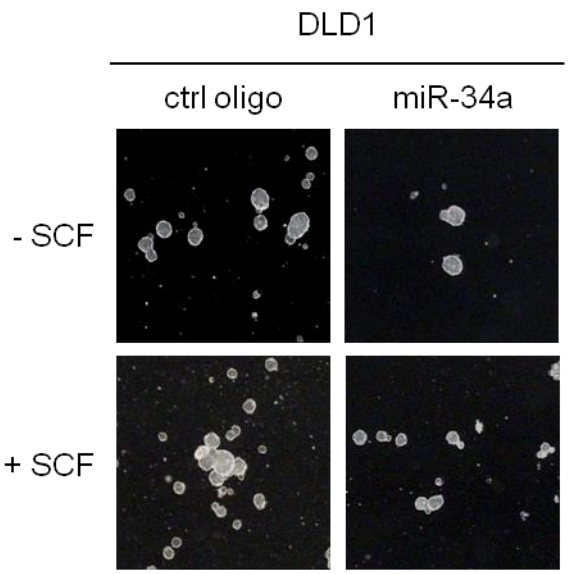

Figure 49: miR-34 interferes with SCF-induced sphere formation in CRC cells. DLD1 cells were treated like described in Figure 48. Representative pictures of DLD1 derived G1 spheres, magnification: 40-fold.

These results indicate that miR-34 negatively affects the sphere formation abilities of colorectal cancer cells by targeting c-Kit. Taken together the results show that repression of c-Kit by p53 is mediated via miR-34a. This in turn leads to suppression of mitogenic Erk signaling, chemoresistance, migration/invasion and stemness. Thereby, and presumably via additional effector mechanisms, the p53/miR-34a axis may contribute to tumor suppression.

6) Discussion

6.1) miR-34a in EMT

In the first part of this thesis a double-negative feedback loop between miR-34 and Snail was identified. In the following section the results and their respective consequences for the understanding of EMT regulation are discussed.

6.1.1) miR-34a mediates p53-mediated suppression of EMT and stemness via Snail

During this study, the role of miR-34 as an important mediator of p53-mediated tumor suppression was further substantiated: the direct regulation of the EMT-TF Snail by miR-34a was characterized in detail. The down-regulation of Snail led to a reduction of mesenchymal traits in terms of migratory capacities as well as reduction of stemness markers, thereby leading to suppression of EMT and induction of MET. These effects underline the role of miR-34 as the 'extended arm of p53', as it was already shown before to induce apoptosis and senescence (reviewed in Hermeking, 2012). By employing miR-34 as a down-stream effector, p53 regulates several additional targets. This in turn influences different pathways and cellular properties. For instance, migration and invasion of CRC cells was heavily diminished by p53 in a miR-34-dependent manner. Moreover, the results show that miR-34 down-regulates the expression of stemness markers like *BMI-1*, *c-Myc*, *CD44*, *CD133* and *c-Kit*, which is particularly discussed in section 6.3.2. Some of the miR-34-targeted markers were published before (c-Myc, CD44), others are novel (c-Kit) and additional ones probably represent indirect targets (BMI-1).

However, the repression of Snail might also lead to a decrease of stemness related genes, since elevated Snail has been implicated in stemness induction previously: in immortalized mammary epithelial cells, for instance, the

formation of mammospheres, a property associated with mammary epithelial stem cells, was elevated by increased Snail expression (Mani et al, 2008). In addition, colorectal cancer derived colonospheres displayed high expression of Snail and its ectopic expression promoted the formation of colonospheres from colorectal cancer cell lines (Hwang et al, 2011b). Furthermore, Snail is expressed in the nuclei of crypt base columnar stem cells in the small intestine in mice and loss of APC resulted in increased expression of Snail in polyps of *MIN* mice (Horvay et al, 2011).

A recent study identified *Notch1* mRNA as direct target of miR-34a in colon cancer stem cells (Bu et al, 2013). The authors reported that down-regulation of Notch by miR-34 led to diminished colonosphere formation and tumorigenicity. This supports the results of this thesis, which show that miR-34 is involved in stemness and sphere formation by down-regulation of Snail and c-Kit. Therefore, multiple miR-34 targets potentially contribute to the suppression of stemness, presumably in a cell-type dependent manner.

This was also found in another study, which shows that in mouse embryonic fibroblasts derived from *miR-34a* deficient mice induced pluripotent stem cell (iPSC) generation was elevated compared to wild-type mice (Choi et al, 2011). The suppression of somatic reprogramming by miR-34a was due, at least in part, to repression of several pluripotency genes, including *Nanog*, *Sox2* and *N-Myc*. miR-34b/c similarly repressed reprogramming and all three miR-34 members acted cooperatively in this process. This study is presumably cancer-relevant as well, since induced pluripotency and oncogenic transformation were recently found to be similar, interrelated processes (Riggs et al, 2013; Suva et al, 2013).

The down-regulation of BMI-1 by miR-34 might occur in an indirect manner, since *BMI-1* and *KLF4* have been characterized as miR-200 targets, which might be induced after miR-34-mediated repression of Snail (Wellner et al, 2009). Besides the miR-34-mediated down-regulation of Snail itself, further indirect inhibition of Snail functions may be mediated by the down-regulation of the miR-34 target HDAC1 (Kaller et al, 2011; Zhao et al, 2013). Since it was shown to be an important co-repressor of Snail, loss of HDAC1 might negatively affect Snail-mediated gene regulations (Peinado et al, 2004).

All together the data presented here demonstrate that miR-34 is mediating a decrease of stemness and other cellular properties like migration and invasion upon induction of p53. Therefore one could describe its role as ‘the extended arm of p53’, since it exerts many additional functions, which all result in a thorough cancer opposing function, once it is activated by p53.

6.1.2) The transition between epithelial and mesenchymal states is controlled by several double-negative feedback loops

The miR-34-dependent regulation of Snail adds another layer of complexity to the regulation of MET by p53, since another analogous feedback loop between a p53 induced miRNA and an important EMT-TF was described by others before (Brabletz & Brabletz, 2010; Chang et al, 2011; Shimono et al, 2009): the miR-200 family was shown to target transcription factors of the ZEB family, which in turn down-regulate the expression of the *miR-200* genes and thereby form a bi-stable, double-negative feedback loop, which might be important for the cellular plasticity of cancer cells. Several studies have shown that a shift towards elevated miR-200 expression concomitantly promotes a shift to an epithelial phenotype (Shimono et al, 2009; Wellner et al, 2009). Thus, the miRNAs of the miR-200 and the miR-34 family seem to maintain and stabilize an epithelial state, while the EMT-TFs antagonize this by promoting mesenchymal traits (Brabletz, 2012a).

The depicted model (Figure 50) gives a simplified overview of the findings made in this sub-project combined with recent publications and emphasizes the interplay between molecules determining epithelial and mesenchymal states and stemness. Once this equilibrium is out of balance, e.g. by hyper-methylation of the miRNA promoters or by constitutive activation of the transcription factors, and a critical threshold is reached, the EMT-regulators can endow tumor initiating cells not only with an increased invasiveness, but also with stemness and resistance to apoptosis (Mani et al, 2008; Thiery et al, 2009). These findings suggest that the two loops have evolved as amplifiers of p53-mediated MET and differentiation by controlling several important EMT-TFs in parallel. These parallel circuits represent a safety mechanism,

which might be important for tumor suppression in case one of the loops is inactivated during tumor initiation or progression. According to this model, loss of p53, however, seems to be fatal with regards to EMT. Both loops would be affected and shifted to the mesenchymal state at the same time by a strong induction of Snail and the ZEB family. The presence of intact p53 therefore is crucial for the prevention of EMT.

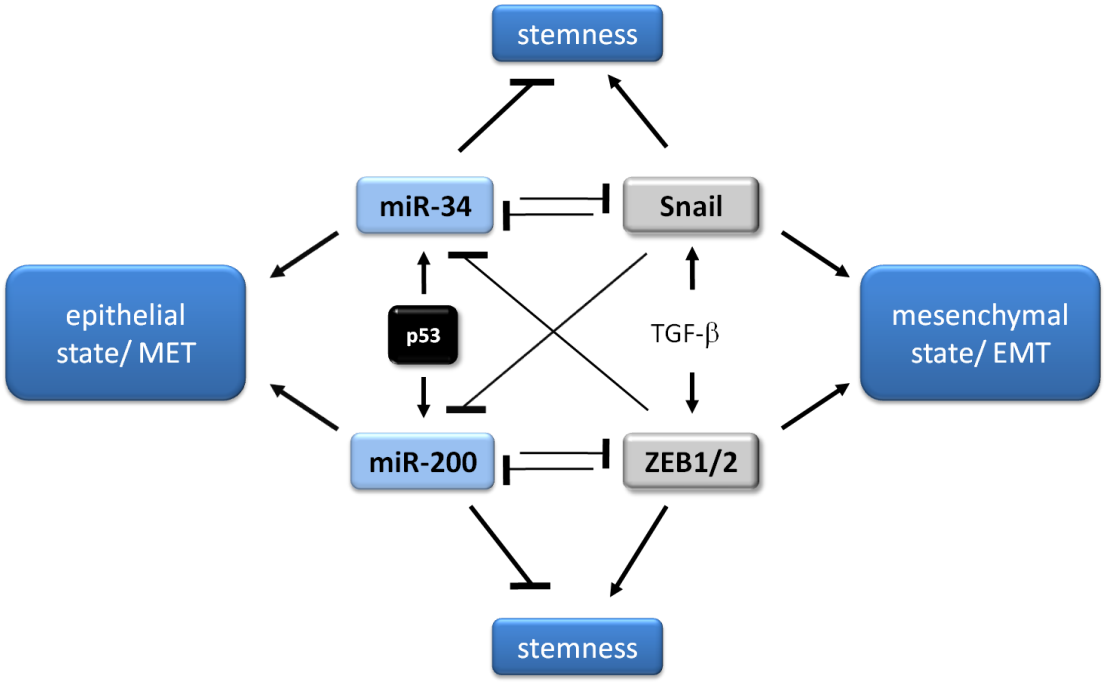

Figure 50: Two reciprocal feedback loops control cellular plasticity. Certain extracellular stimuli, such as TGF-β, stimulate expression of EMT activators, which induce EMT, stemness and survival (dark blue). The EMT-TFs ZEB and Snail (grey) are linked in double-negative feedback loops to the miR-200 and miR-34 families (light blue), respectively. p53 (black) activates the expression of both miRNA families, thereby shifting the feedback loops towards MET (dark blue), epithelial differentiation and apoptosis. The close interconnections between *miR-200* and *miR-34* genes via co-regulated, common repressors may stabilize the transcriptional programs in place in either epithelial or mesenchymal cells. Thereby, the immediate response to minor signals and aberrant cellular reactions may be suppressed.

Moreover, the involvement of two or potentially more almost identically organized loops is presumably no coincidence. Interestingly, a similar loop-like mechanism, involving the miRNA let-7, was recently discovered to serve as a bi-stable switch in embryonic stem cells and guards the decision

between pluripotency and differentiation (reviewed in Gunaratne, 2009). These data suggest that the loop-like organized regulation of genes involving miRNA activity is a recurring mechanism to control the transitions between alternative cellular states.

In the context of this study, the role of other important EMT-TFs, besides Snail and ZEB, remained unclear. Among the prototypical EMT regulators Snail seems to be the only factor, which is directly targeted by miR-34. Nevertheless other factors like ZEB1, ZEB2 and Slug might be indirectly regulated by miR-34, since they are miR-200 targets and the loss of Snail occupancy at the *miR-200* promoters might lead to a de-repression of these miRNAs. This in turn would result in a down-regulation of their respective targets. This is supported by findings in pancreatic acinar cells from mice with a deletion of *p53*, which therefore presumably express low levels of miR-34 and miR-200 members: Snail, Slug, Twist and ZEB1/2 and several stemness markers are highly expressed in these cells, which undergo EMT upon subculture and show enhanced sphere formation (Pinho et al, 2011).

Due to the similarity of the DNA-binding motifs of Snail and Slug it is likely that Slug also regulates the expression of *miR-34a/b/c*. Noteworthy, Slug expression is significantly associated with distant metastases in CRC and had a significant impact on patient overall survival (Shioiri et al, 2006). This is at least similar to what was found for Snail in the present study and suggests an analogous role for Slug in CRC.

6.2) Role and potential clinical application of miR-34a in metastatic colorectal cancer

In the second part of this thesis the role of miR-34 and its targets in metastatic colon cancer was investigated. The following section contains a discussion of the results that were obtained and their potential clinical implications in the future.

6.2.1) *miR-34* silencing and expression are independent of the p53 status in metastatic colorectal cancer specimen

The present study revealed a strong correlation of *miR-34* promoter-methylation in primary colon cancer with metastatic spread to the liver, whereas *miR-34b/c* seems to be methylated at high frequencies, irrespective of tumor stage or outcome. The data confirm previous findings, which indicate that methylation-mediated gene silencing is involved in the progression from local colorectal tumors towards metastatic disease (Li & Chen, 2011). Since the miR-34 family can be induced by p53, mutation of p53 would presumably cause a down-regulation or inability to induce *miR-34a*. Therefore, one would assume that *miR-34a* methylation would only be advantageous for tumors with an intact p53 pathway. This mutual exclusiveness was shown in a previous study (Vogt et al, 2011). Contrary to these data, the *miR-34* inactivation was independent of the p53 expression pattern in the present study. The differences in cohort composition and location might partially explain the contradictory results: in this study, tumors from the right-sided colon were analyzed, whereas the previous study included mainly left-sided colorectal cancer. Another possible explanation might be that promoter methylation occurs early in tumor development and therefore is an independent event that precedes p53 inactivation, which occurs relatively late during tumorigenesis (Fearon & Vogelstein, 1990; Feinberg et al, 2006). Interestingly, there were indications for p53-independent *miR-34* regulations before, like shown for MK5, which activates miR-34b/c expression via phosphorylation of FOXO3a, thereby enabling it to arrest proliferation (Kress et al, 2011). Another study showed that p63 can directly bind to p53-consensus sites in both *miR-34a* and *miR-34c* regulatory regions and inhibited their activity (Antonini et al, 2010). Moreover, it was shown, that ELK1 can up-regulate *miR-34a* expression as a consequence of BRAF induced senescence (Christoffersen et al, 2010). In accordance with this study, significantly elevated miR-34a levels were observed in tumors carrying the activating BRAF mutation V600E in this study. This and potentially more

so far unknown mechanisms might explain the independence of miR-34 inactivation and expression of the p53 status.

Interestingly, decreased levels of miR-34a expression correlate with relapse of non–small cell lung cancer, as well as recurrence of breast cancer and poor patient survival (Gallardo et al, 2009; Peurala et al, 2011). Therefore, it is likely that CpG-methylation of *miR-34a* in colon cancer is also associated with shorter survival and recurrence, presumably due to the associated increase of distant metastases detected here. However, our analysis was based on a case–control design, using the presence or absence of distant metastases within a follow-up period of five years after surgical resection of the primary tumor as endpoint. Therefore, the chosen patients do not represent a population-based clinical collective. The analyzed markers and marker combinations could not be correlated with the overall and disease-free survival of the patients. The relevance of the present findings for overall and disease-free survival should be the subject of future analyses.

Another aspect of this study is an almost ubiquitary methylation of the *miR-34b/c* promoter (approximately 92%) in this tumor collection, which does not allow any correlation with p53 alterations. Similar frequencies of *miR-34b/c* methylation in colorectal cancer have been previously reported by others: 90% by Toyota and colleagues, 99% by Vogt and colleagues, and 97.5% by Kalimutho and colleagues (Toyota et al, 2008; Vogt et al, 2011; Kalimutho et al, 2011). On the contrary, data obtained by Lujambio and colleagues contradict these observations (Lujambio et al, 2008): although using the same MSP primer sets only about 35% of the colorectal tumor samples from their study were positive for *miR-34b/c* methylation, which was associated with metastases formation. Obviously, the extremely high frequency of *miR-34b/c* methylation in the present study of colon cancer cases did not allow any association with other parameters. Besides unknown biological mechanisms the differences might be explained by technical reasons like sensitivity of the MSP assay.

6.2.2) Limiting factors for the correlations between the expression of miR-34 and its targets

In contrast to other studies the correlations between low miR-34a and elevated target expression was, though being significant, relatively weak. This may be due to the fact that miR-34a negatively regulates a variety of targets, besides the ones reported herein, each of which has been shown to be involved in the promotion of metastases, such as CD44, c-Myc, Axl, TPD52, LEF1, or MTA2 (Christoffersen et al, 2010; Kaller et al, 2011; Liu et al, 2011; Mudduluru et al, 2011). This multiplicity of potential regulations suggests that the entire miR-34-regulated signature of genes is important for the prevention of metastases, rather than single targets.

Like mentioned before, the expression of the EMT-TF Slug is significantly associated with distant metastases in CRC (Shioiri et al, 2006). Due to the similarity of the DNA-binding motifs of Snail and Slug it is likely that Slug also regulates the expression of *miR-34a/b/c.* Therefore, it should be addressed in future studies, whether Slug is able to repress of *miR-34* genes and whether this regulation occurs in CRC, since this would be an alternative mechanism for cancer cells to gain a selective advantage besides Snail-mediated repression of the miR-34 family.

Additionally, all of the miR-34a targets in this study are inter-connected with several signaling pathways. Snail, for instance, can be induced by a broad spectrum of signaling pathways among them Wnt, TGF-β, Hedgehog, EGF/FGF, hypoxia, hepatocyte growth factor (HGF) and NFκB signaling (Nieto, 2011; Peinado et al, 2007). All of these possibly influence the expression pattern of Snail protein in patient samples and therefore prevent detection of potential correlations. The same is true for c-Met and β-catenin, which are regulated by different factors as well (Kim et al, 2013; Sadiq & Salgia, 2013).

6.2.3) Association of miR-34a with other parameters besides metastases

Though the cohort analyzed here was not designed to address this question, we found strong evidence that mature miR-34a levels are decreased in N+ compared with N0 tumor samples and the proportion of cases showing a methylated *miR-34a* promoter was significantly higher in samples with lymph node metastases. This is supported by a study showing that ectopic miR-34a prevents the formation of lymph node metastases in a murine model of hepatocellular carcinoma (Guo et al, 2011). Therefore, suppression of lymph node metastasis by miR-34a in CRC should be addressed in the future.

The genome-wide assessment of methylated genes in CRC has revealed a unique molecular subgroup of tumors with the so-called CpG island methylator phenotype (CIMP). These tumors exhibit a particularly high frequency of methylated genes and account for 30% to 40% of right-sided colon cancer (Fearon, 2011). In sporadic colon cancer the DNA mismatch repair gene *hMLH1* is among these methylated genes, which in turn leads to high-grade microsatellite instability (MSI-H; Weisenberger et al, 2006). Furthermore, CIMP-positive colon cancers usually show either mutation of BRAF or KRAS. Our finding that high miR-34a expression, and therefore the absence of CpG-methylation at *miR-34a* promoters, correlates with loss of hMLH1 protein expression, MSI-H and the presence of BRAF-mutations, indicates that miR-34a is not a "target" of CIMP-associated hyper-methylation. This was unexpected, since miR-34a is thought to have tumor suppressive activities and represents an important effector of p53 activity. Upon its methylation-dependent silencing tumor cells are expected to gain a selective advantage. The silencing of other genes may be more relevant for tumor progression in CIMP-positive tumors.

6.2.4) Application of miR-34a as diagnostic biomarker

Since the patient's prognosis after surgical removal of the primary tumor mainly depends on disease recurrence, which is associated with distant metastasis, the quest for prognostic markers, which identify patients with high risk of recurrence and metastasis, is very important for patient management (Mina & Sledge, 2011). The results of the present study indicate that *miR-34*a is preferentially down-regulated via CpG-methylation of its promoter in primary colon cancers, which metastasize to the liver. *miR-34* silencing was shown to be associated with increased expression of several selected miR-34 target molecules, which may be part of a larger set of miR-34 targets, which are up-regulated in tumors. But what might be the clinical consequences and how could these findings influence current treatment strategies? The results of this study suggest that detection of miR-34a expression and *miR-34a* CpG-methylation could be used as a biomarker for metastasizing colorectal tumors, which might improve the decisions regarding follow-up treatment of patients after resection of primary tumors.

Within the last years several prognostic markers have been found to be predictive for colorectal cancer outcome and/or distant spread (Neumann et al, 2011; Neumann et al, 2012b; Walther et al, 2009; Zlobec & Lugli, 2008). Most of them are based on immuno-histochemical detection of certain proteins which can be derived from dissected tissue. In contrast, analysis of *miR-34a* methylation and/or expression entails isolation of DNA and/or RNA, which would make diagnosis more time and money consuming. However, there are arguments, which justify this effort: First, the isolation of nucleic acids, either DNA or RNA, offers a much broader insight into the genetic/molecular background of the tumor. While tissue sections usually can only be stained for one marker at a time, the analysis of nucleic acids provides an opportunity to analyze several markers in parallel. In particular, several miRNAs have recently been found to be associated with metastatic outcome of colorectal cancer (de Krijger et al, 2011). Among these are up-regulated onco-miRs, such as miR-17-92 and miR-21, as well as down-regulated tumor suppressing miRNAs like let-7, miR-200b and c. Therefore,

the diagnostic detection of expression of a whole panel of miRNAs, including miR-34a, is conceivable.

Since promoter methylation is a common mechanism of miRNA silencing in cancer, the simultaneous analyses of multiple, silenced promoters would be beneficial as well. This idea is further supported by recent trials, which described the detection of *miR-34a* CpG-methylation in mucosal wash fluids from patients undergoing colonoscopy and isolating DNA from stool samples (Kamimae et al, 2011; Ahlquist et al, 2012). This detection of *miR-34a* methylation in released tumor cells could help to determine whether an elevated risk for distant metastases of the patients is given. According to our theoretical risk assessment, this prognostic value may be further increased by the simultaneous analysis of miR-34 targets and might identify sub-groups of patients, which should receive an intensified follow-up observation and treatment after surgery. This approach is supported by a recent study, which analyzed 148 patients with lung adenocarcinomas (Akagi et al, 2013). Here, the combined detection of miR-21 expression and a set of four protein coding mRNAs was superior to either classifier alone, with regards to the significance of the patients prognosis.

However, in order to establish miR-34 as a biomarker in the clinic, the findings obtained here should be confirmed in further studies using larger cohorts of patients. The case-control study design used here allows to draw insightful conclusions about the association between factors and the clinical condition using a relative small number of investigated cases, but case numbers for this study were comparatively low and should be confirmed in further studies using larger cohorts of patients. As discussed above, the promoters of *miR-34b* and *miR-34c* were almost completely silenced by CpG-methylation. Although this constellation makes detection of methylation useless for prognostic purposes regarding distant spread, it may allow early detection of colon cancer. For example, it was shown that *miR-34b/c* methylation in stool DNA can be used for early detection of colorectal cancer (Kalimutho et al, 2011).

6.2.5) Application of miR-34 for therapeutic purposes

In the present study miR-34a down-regulation was shown to correlate with metastases to the liver and the lymph nodes. Besides representing a potential diagnostic biomarker, miR-34 recently emerged as a potential therapeutic agent to prevent/treat metastases: first results obtained from human cell lines in this and previous publications indicate a suppression of cellular migration by miR-34 (Yamazaki et al, 2012; Yang et al, 2012b).

Moreover, a recent publication demonstrated that miR-34-based therapy might be efficient even independent of the p53 status in breast and colorectal cancer cell lines (Zhao et al, 2013). The authors report that miR-34-mediated repression of HDAC1 leads to an induction of $p21^{CIP1/WAF1}$, while depletion of $p21^{CIP1/WAF1}$ specifically interfered with the ability of miR-34 to inhibit cancer cell proliferation. First, these data suggest that miR-34 controls a tumor suppressor pathway previously assigned to p53. Second, the results provide an attractive therapeutic strategy for cancer patients irrespective of the p53 status and third, show an alternative mechanism of miR-34 to mediate growth arrest and cellular senescence besides targeting for instance the previously described Bcl-2, CDK4, CDK6, Cyclin D1, Cyclin E2 and E2F3 (reviewed in Hermeking 2010).

These results obtained in cell lines coincide with an anti-cancer effect of miR-34 mimetics in several *in vivo* studies. The ectopic expression of miR-34a, for instance, was shown to prevent lymph node metastasis in a murine model of hepatocellular carcinoma (Guo et al, 2011). This is in accordance with the presence of *miR-34* methylation and its diminished expression in N+ cases, which was found in this study. Moreover, systemic delivery of miR-34a was shown to reduce tumor burden and growth of xenografts in mice and led to reduced metastases formation. While some researchers used nano particles to deliver the synthetic miRNAs (Chen et al, 2010; Pramanik et al, 2011), others made use of lipid-based vehicles (Trang et al, 2011; Wiggins et al, 2010), lentiviral systems (Kasinski & Slack, 2012) or commercial agents, such as siPORT and RNALancerII (Liu et al, 2011). Beyond its impact on solid tumors miR-34a delivery was shown to abrogate the *in vivo* growth of large B-

cell lymphomas (Craig et al, 2012). Taken together, a therapeutic role for miR-34 in the clinic is more than conceivable, but the emphasis should now be on applicability in higher species and man (Bader, 2012; Kasinski & Slack, 2011). Recently miR-34 entered a phase 1 trial in patients with primary liver cancer or metastatic cancer with liver involvement (Bouchie, 2013). The miR-34 mimics are delivered using liposomes, which naturally accumulate in the liver, making liver cancer the first realistic indication for therapy. Preferential targeting of tumor cells is achieved by pH sensitive binding of the liposomes. On the basis of the data presented here, miR-34 therapy might prevent the formation of metastases in liver and lymph nodes in colorectal cancer patients.

6.3) miR-34a regulates c-Kit and thereby interferes with several cancer relevant processes

In this study c-Kit was identified as a new target of the miR-34 family. Since c-Kit plays a role in numerous cancer-associated pathways, these results extend the knowledge of tumor suppressive mechanisms of miR-34.

The findings from this sub-chapter are summarized in Figure 51: A variety of stresses can result in DNA damage, leading to activation of p53, which in turn promotes the transcription of the primary *miR-34a* transcript. Once the pri-miRNA is processed, the mature miR-34a can target *c-Kit* via its 3'-UTR and thereby down-regulate the expression of the mature receptor protein. This effect mediates several, different responses depending on the cell line/type. For instance, miR-34-mediated down-regulation of c-Kit resulted in diminished Erk phosphorylation levels, which was associated with decreased anchorage-independent colony formation in soft agar. Furthermore, low endogenous c-Kit protein levels or a decrease of c-Kit expression, caused by ectopic miR-34, were associated with increased chemosensitivity. Moreover, miR-34a inhibited migration and invasion and also SCF-mediated enhancement of these processes in a c-Kit-dependent manner. Finally, activation of c-Kit induced several stemness markers in CRC cell lines and was associated with

their expression in primary CRC tumors, whereas activation of miR-34a in CRC cell lines resulted in a down-regulation of c-Kit and c-Kit-induced markers, and suppressed sphere-formation of CRC cells, indicating that CRC stemness may be controlled by the miR-34/c-Kit axis.

Another group recently reported that miR-34a is able to determine the cell-fate of early-stage dividing colon cancer stem cells (CCSCs) by degradation of *Notch1* mRNA (Bu et al, 2013). Elevated miR-34a levels were found in differentiating progeny, whereas low levels of miR-34a demarcate self-renewing CCSCs. Moreover, miR-34a loss of function and gain of function altered the balance between self-renewal versus differentiation both *in vitro* and *in vivo* by generating a sharp threshold response where a bimodal Notch signal specifies the choice between self-renewal and differentiation. This is in particular interesting, since it is the first evidence for a gradient-dependent mechanism that converts noisy input into a toggle switch for robust cell-fate decisions. The same principle would for instance be conceivable for the regulation of c-Kit, which like Notch1 also represents a trans-membrane receptor molecule.

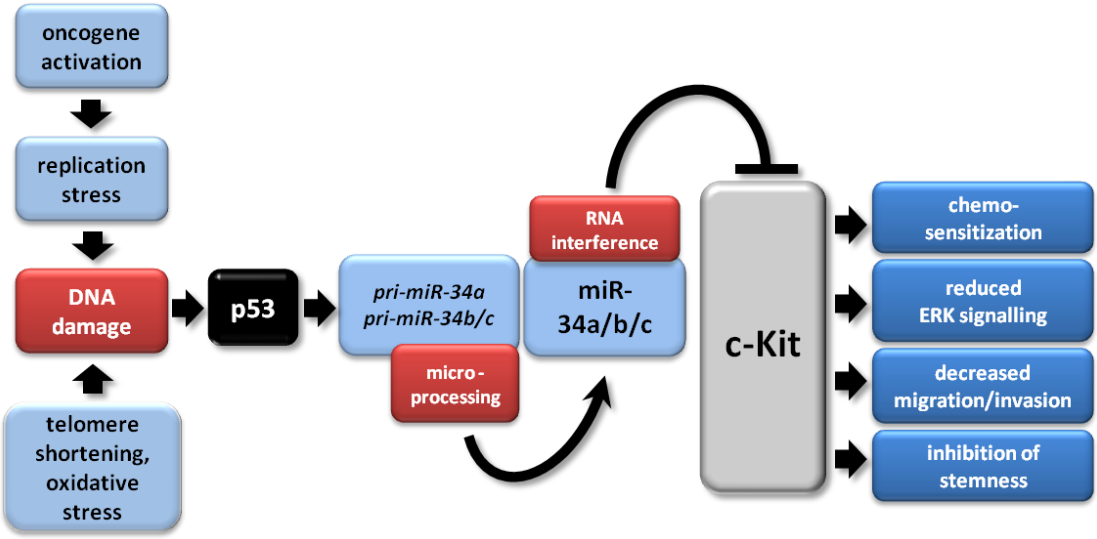

Figure 51: The p53/miR-34/c-Kit axis. The model summarizes the different effects of miR-34a directly targeting c-Kit in different colorectal cancer cells which are presented in this study. Moreover, it links them to mechanisms upstream of this cascade (light blue). p53 (black) activity is induced upon DNA damage which may be generated by numerous factors/stresses, and results in increased miR-34a expression. This in turn leads to reduced c-Kit levels by directly targeting the *c-Kit* 3'-UTR. Lowered c-Kit results in multiple effects depicted on the right in dark blue. Figure modified from Hermeking, 2007.

6.3.1) The c-Kit/miR-34 axis in cancer

Our studies were mainly carried out in colorectal cancer cells, which have previously been shown to be feasible for studies on c-Kit (Bellone et al, 2001; Yasuda et al, 2007). However, the role of c-Kit in CRC is unclear and former studies described contradictory results regarding the importance of c-Kit expression in CRC: Friedrichs and colleagues found that c-Kit expression is rare (17.1%) in colorectal carcinomas, which was in accordance with other studies reporting that c-Kit was expressed at very low frequencies in colorectal cancer samples (Friederichs et al, 2010; Reed et al, 2002; Yorke et al, 2003). Further studies found c-Kit expression in CRC samples in 59% of stage II colorectal cancer patients (El-Serafi et al, 2010), in 90% of normal colon mucosas and 30% of neoplastic tissue (Sammarco et al, 2004), and in 15% of primary colorectal tumors and 14% of distant metastases (Preto et al, 2007).

Though these patient-derived results appear to be very heterogeneous, cell culture experiments suggested that c-Kit presumably has a function in colorectal cancer cells, since the c-Kit receptor as well as its ligand are expressed at elevated levels in colorectal cancer cell lines (Lahm et al, 1995). In support of this, Bellone and colleagues demonstrated that SCF was able to stimulate anchorage independent growth in four out of five CRC cell lines. Besides, the c-Kit receptor staining was found to be over-represented in colon cancer tissue compared with normal mucosa from patients. Furthermore, aberrant activation of the c-Kit axis was shown to have anti-apoptotic and invasion-stimulating effects on DLD1 CRC cells (Bellone et al, 2001; Bellone et al, 1997). Moreover, an increased invasion upon addition of SCF was documented in Colo320 cells (Yasuda et al, 2007). Our study supports these findings and reveals that c-Kit-dependent cancer cell properties can be compromised by miR-34: a SCF-mediated increase in the invasive capacities of Colo320 cells was found to occur to the same extent in this study as reported before. In addition, we found that SCF also increases migration of Colo320 cells. Furthermore, this study shows that miR-34a diminishes the effects of SCF, presumably by targeting c-Kit, and therefore interrupts the SCF signaling pathways, which are responsible for the changes in cell behavior.

As mentioned above, replacement therapy with miR-34a mimetics was successfully tested in several preclinical studies using mouse models of cancer and may therefore represent a therapeutic option for the treatment of several tumor entities in the future (Guo et al, 2011; Kasinski & Slack, 2011; Liu et al, 2011; Pramanik et al, 2011; Wiggins et al, 2010). Our results indicate that c-Kit may be up-regulated due to inactivation of miR-34 either by CpG-methylation or p53 mutations/inhibition. Such tumors may be especially sensitive to a replacement of miR-34 using mimetics.

6.3.2) Role of c-Kit in stemness, chemoresistance and angiogenesis

Our results indicate that c-Kit is able to endow cancer cells with properties of chemoresistance, which can be partially reverted by miR-34a. This is reminiscent of the effect of Imatinib (STI571), which also targets c-Kit and was shown to be therapeutically effective against gastrointestinal stromal tumors/GISTs (Attoub et al, 2002; van Oosterom et al, 2001). Imatinib rendered DLD1 cells, which express high c-Kit levels, more responsive to the cytotoxic effect of 5-FU [0.03-1 mM] (Bellone et al, 2004). Therefore, the additive effect of c-Kit inhibition and 5-FU has precedence and should be studied further, since this potentially allows a dose reduction of chemotherapeutic compounds in the future. miR-34 mimetics were previously shown to sensitize cell lines derived from other types of tumors, such as breast, prostate and lung cancer towards chemotherapy (Fujita et al, 2008; Li et al, 2012; Wang et al, 2012) and elevated miR-34a was associated with chemosensitivity in patients with gastric cancer (Kim et al, 2011a). Therefore, miR-34 mimetics are promising candidates for clinical applications (Bader, 2012).

Furthermore, we found that c-Kit activation results in the up-regulation of several stemness markers in colorectal cancer cells and primary tumors. This is in accordance with previous findings, which show that colorectal cancer stem cells display increased resistance towards chemotherapeutics such as 5-FU (Bitarte et al, 2011; Hsu et al, 2013). A potential mechanism how c-Kit mediates chemoresistance was proposed by Chau and colleagues (Chau et al, 2012). In their study c-Kit activation was shown to up-regulate ABCG2 to confer chemoresistance in ovarian cancer. This membrane-bound protein is a member of the ATP-binding cassette (ABC) transporter super-family. The authors report, that this effect was mediated via Phosphatidylinositol-3-kinase (PI3K)/Akt signaling and β-catenin/TCF-mediated transcriptional activation of ABCG2. They discuss that this is in particular interesting, since this pathway was shown to be involved in the regulation of ABC drug transporters before, which might explain why stem cells are resistant to a variety of agents, rather than towards a single chemotherapeutic agent (Scotto, 2003; Kemper et al,

2010). Since β-catenin/TCF signaling is frequently altered in colorectal cancer as well, this mechanism might also apply to this entity and should be addressed in further studies (Brabletz et al, 2005). The correlation between β-catenin and c-Kit expression in colorectal tumor samples, shown within this study, further supports this assumption.

Interestingly, previous publications revealed that miR-221 and 222 regulate angiogenic processes via targeting c-Kit (Poliseno et al, 2006). Tumor-angiogenesis is an important step in tumorigenesis, since solid tumors have to be supplied with nutrients from the blood stream to exceed a certain size. Since miR-34a targets c-Kit as well, effects of p53 on tumor-angiogenesis may be mediated, at least in part, via miR-34.

6.3.3) miR-34a targets multiple receptor tyrosine kinases

In this study c-Kit was identified and characterized as a new miR-34a target. Interestingly, several other studies recently reported other receptor tyrosine kinases, which are regulated via miR-34a, among them c-Met, Axl and PDGFRα (Corney et al, 2010; Mudduluru et al, 2011; Silber et al, 2012). Therefore, miR-34 seems to specifically target this class of signaling molecules, which are of central importance for cancer, since they regulate processes essential for tumor initiation and progression. By suppression of RTKs, miR-34 may be able to effectively mediate tumor suppression by p53. In the future, additional studies may reveal whether additional RTKs represent targets of the miR-34 family.

6.4) Potential relevance for non-cancerous processes

All of the sub-projects reported in this work addressed the biology or clinical applications of miR-34 related to human cancer. Nevertheless, some interesting findings emerged during these studies, which might be of relevance to other diseases as well.

6.4.1) Additional findings from the M0/M1 patient collection

As discussed above, the patient collection, which was analyzed here, was designed to determine factors, which are important for the formation of distant metastases in colon cancer. However, the expression of the mature miRNA in patients revealed some interesting associations. For instance, the expression of the mature miRNA was significantly elevated in tumors of older patients. This is consistent with recent studies, which reported elevated mature miR-34a during aging in rat liver and fruit flies, senescence of human diploid fibroblast, as well as during senescence of the eye and cardiac aging in humans (Boon et al, 2013; Chien et al, 2013; Li et al, 2011; Liu et al, 2012; Maes et al, 2009). Interestingly, a recent publication reported that c-Kit positive stem cells are necessary and sufficient for functional cardiac regeneration and repair (Ellison et al, 2013). In combination with the results obtained in the present study, this suggests that the influence of miR-34a on aging might be mediated via inhibition of c-Kit, since down-regulation of c-Kit would result in diminished regeneration and therefore enable miR-34 to promote aging.

However, it remains largely unclear why older patients, which have a higher risk for cancer, in general show increased levels of miR-34a, which is supposed to be protective against cancer. One plausible explanation is increased p53 activity in aged tissues due to accumulation of DNA damage caused by e.g. telomere shorting, exogenous DNA damaging insults, such as irradiation or endogenous free radicals (Sharpless & DePinho, 2002; Vogelstein et al, 2000). However, as other variables also change with age, additional processes may lead to an up-regulation of miR-34.

6.4.2) The miR-34/c-Kit axis in allergic disorders

The role of c-Kit as a new miR-34a target was elucidated in this study. Since both, miR-34a and c-Kit, share an interface with a multitude of signaling pathways, more detailed analyses are necessary in order to illuminate the different aspects and consequences, which are inherent in this regulation. For instance activation of c-Kit is not only associated with cancer, but seems to play a role in allergic asthma as well (Krishnamoorthy et al, 2008). Recently, miR-34a was shown to interfere with a component of the mTOR signaling pathway and thereby to play a role in mast cell survival – a process critical in allergic disorders (Shin et al, 2012). Moreover, TGF-β was reported to suppress miR-34 thereby leading to secretion of the chemokine CCL22, which is a direct target of miR-34, and recruitment of regulatory T cells (Yang et al, 2012a). In line with this, miR-34/449 family members were shown to be repressed in airway epithelial cells of asthmatic patients compared to healthy controls (Solberg et al, 2012). These findings place miR-34 in the context of allergic disorders and miR-34-dependent down-regulation of c-Kit might therefore be important for these diseases as well. Interestingly, inhibition of different RTKs and particularly c-Kit seems to affect asthma via decreasing histamine levels, infiltration of mast cells and eosinophils, interleukin (IL)-4 production and airway hyper-responsiveness *in vivo* (Guntur & Reinero, 2012; Jensen et al, 2007; Reber et al, 2006). Since miR-34a was successfully tested as a potential new therapeutic agent in the lung and other organs using mouse models, it will be interesting to see, whether miR-34-based therapies can also be applied to treat immune dysregulations such as allergic asthma (Guo et al, 2011; Kasinski & Slack, 2011; Liu et al, 2011; Pramanik et al, 2011; Wiggins et al, 2010).

7) Summary

Over the last years miR-34 emerged as a major down-stream effector of the tumor suppressor p53. In particular, miR-34 was shown to trigger several cancer suppressive processes like apoptosis, cell cycle arrest and senescence by targeting the mRNAs of different target genes such as the survival factor Bcl-2 or different CDKs.

During this study, we could show that the EMT-TF Snail was regulated by miR-34. This amplifies the miR-34-mediated tumor suppressive effect by stabilizing the epithelial phenotype, and was associated with reduced migration and invasion and inhibition of stemness. Furthermore, Snail was shown to target miR-34, thereby forming a regulatory feedback loop controlling the transition between epithelial and mesenchymal traits, which is also important for metastases formation.

In further experiments on colorectal cancer tissue samples, miR-34 was shown to be significantly repressed in primary tumors, which were associated with metastases to the liver within five years after removal. Further analyses suggested that this was probably due to epigenetic silencing, since a significant proportion of the cases with low miR-34a expression showed a CpG-methylation of the *miR-34a* promoter region. Subsequent immunohistochemical analyses of the miR-34a targets Snail, c-Met and β-catenin revealed that detection of *miR-34a* silencing in resected primary colon cancer is of prognostic value for the prediction of distant metastases, especially in combination with detection of c-Met and β-catenin expression.

Additionally, the receptor tyrosine kinase c-Kit was identified as a new miR-34 target in this study. First results in different cell lines indicate that this regulation can have implications for cancer related cell properties like sensitivity to chemotherapeutic agents, migration and stemness.

Taken together the results obtained in this study improve the understanding of miR-34 and support its role as tumor suppressor. Furthermore, the results suggest that detection of the loss of miR-34 can be used for diagnostic

purposes. In addition, the results are in favor of current activities, which aim to bring miR-34 to the clinic as a therapeutic agent.

8) Zusammenfassung

In den vergangenen Jahren zeichnete sich miR-34 als einer der Haupteffektoren des Tumorsuppressors p53 ab. Im Einzelnen wurde gezeigt, dass miR-34 verschiedene, einer Krebserkrankung vorbeugende Prozesse wie Apoptose, Zellzyklus-Arrest und Seneszenz vermittelt, indem sie die mRNAs verschiedener Zielgene herunter reguliert, darunter zum Beispiel der Überlebensfaktor Bcl-2 oder verschiedene Cyclin-abhängige Kinasen (CDKs).

Im Laufe dieser Studie konnten wir zeigen, dass der EMT-induzierende Transkriptionsfaktor Snail ebenso von miR-34 reguliert wird. Dadurch verstärkt sich der miR-34-vermittelte Tumor-supprimierende Effekt indem der epitheliale Phänotyp stabilisiert, zelluläre Migration und Invasion reduziert und Stammzelligkeit inhibiert werden. Darüber hinaus wurde gezeigt, dass Snail selbst die Expression von miR-34 hemmt, womit es eine regulatorische Rückkopplungsschleife bildet, die den Übergang zwischen epithelialen und mesenchymalen Eigenschaften einer Zelle kontrolliert, der für die Bildung von Metastasen wichtig ist.

In weiteren Analysen wurde anhand von kolorektalem Tumorgewebe gezeigt, dass miR-34 präferenziell in Primärtumoren reprimiert wurde, die innerhalb von fünf Jahren nach ihrer Entfernung mit Lebermetastasen einher gingen. Weitere Analysen legten nahe, dass dies wahrscheinlich auf epigenetischer Promotor-Inaktivierung beruhte, da ein signifikanter Anteil der schwach miR-34 exprimierenden Tumoren eine CpG-Methylierung am *miR-34a* Promotor aufwiesen. Weiterführende immunhistochemische Analysen der Proteine Snail, c-Met und β-catenin, deren mRNAs Zielstrukturen von miR-34a sind, ergaben, dass der Nachweis von *miR-34a* Inaktivierung und Zielgen-Expression bei operativ entfernten, kolorektalen Karzinomen von prognostischem Wert für die Vorhersage von Fernmetastasen sein kann. Dies galt im Speziellen für den Nachweis der Kombination aus *miR-34a* Promotor Hyper-Methylierung und erhöhter Expression von c-Met und β-catenin.

Zudem wurde in dieser Studie auch die Rezeptor-Tyrosin-Kinase c-Kit als eine neue Zielstruktur von miR-34 identifiziert. Erste Ergebnisse in

verschiedenen Zelllinien zeigen, dass diese Regulation auf Krebs-assoziierte Zell-Eigenschaften Einfluss nehmen kann. Darunter fallen die Sensitivität gegenüber Chemotherapeutika, gesteigerte Migration und Invasion und Stammzelligkeit.

Zusammengefasst verbessern die Ergebnisse, welche im Laufe der vorliegenden Studie erhoben wurden, das Verständnis für die Funktion von miR-34 und unterstützen seine Rolle als Tumorsuppressor. Darüber hinaus lassen die Ergebnisse vermuten, dass der Nachweis des Verlustes von *miR-34* künftig für diagnostische Zwecke verwendet werden kann. Die Ergebnisse unterstützen zudem gegenwärtige Aktivitäten, die darauf abzielen miR-34 als Therapeutikum klinisch einzusetzen.

9) Publications

The results of this thesis have been published in the following articles:

Original articles:

- **Siemens H***, Jackstadt R*, Hünten S*, Kaller M*, Menssen A*, Götz U and Hermeking H (2011). miR-34 and SNAIL form a double-negative feedback loop to regulate epithelial-mesenchymal transitions. Cell Cycle 10 (24), 4256-71.
  (IF 2011: 5.359)

- **Siemens H***, Neumann J*, Jackstadt R, Mansmann U, Horst D, Kirchner T and Hermeking H (2013). Detection of miR-34a promoter methylation in combination with elevated expression of c-Met and β-catenin predicts distant metastasis of colon cancer. Clinical Cancer Research 19 (3), 710-20.
  (IF 2012: 7.837)

- **Siemens H**, Jackstadt R, Kaller M and Hermeking H (2013). Repression of c-Kit by p53 is mediated by miR-34 and is associated with reduced chemoresistance, migration and stemness. Oncotarget 4 (9), advance online publications
  (IF 2012: 6.636)

Review/book chapter:

- Hünten S*, **Siemens H***, Kaller M*, Hermeking H (2013). The p53/microRNA network in cancer: experimental and bioinformatics approaches. Advances in Experimental Medicine and Biology 2013; 774: 77-101.

* These authors contributed equally to this work

In addition, I made contributions to the following submitted manuscripts, which are not further described here:

Original articles:

- Hahn S, Jackstadt R, **Siemens H**, Hünten S and Hermeking H (2013). SNAIL and miR-34a feed-forward regulation of ZNF281/ZBP99 promotes epithelial-mesenchymal-transition. (The EMBO Journal, manuscript under revision)

- Shi L, Jackstadt R, **Siemens H**, Li H, Kirchner T and Hermeking H (2013). p53-induced miR-15a/16-1 and AP4 form a double-negative feedback loop to regulate epithelial-mesenchymal transition and metastasis in colorectal cancer. (Cancer Research, manuscript under revision)

10) References

Abbas HA, Pant V, Lozano G (2011) The ups and downs of p53 regulation in hematopoietic stem cells. *Cell Cycle* 10: 3257-3262

Ahlquist DA, Zou H, Domanico M, Mahoney DW, Yab TC, Taylor WR, Butz ML, Thibodeau SN, Rabeneck L, Paszat LF, Kinzler KW, Vogelstein B, Bjerregaard NC, Laurberg S, Sorensen HT, Berger BM, Lidgard GP (2012) Next-generation stool DNA test accurately detects colorectal cancer and large adenomas. *Gastroenterology* 142: 248-256

Akagi I, Okayama H, Schetter AJ, Robles AI, Kohno T, Bowman ED, Kazandjian D, Welsh JA, Oue N, Saito M, Miyashita M, Uchida E, Takizawa T, Takenoshita S, Skaug V, Mollerup S, Haugen A, Yokota J, Harris CC (2013) Combination of protein coding and noncoding gene expression as a robust prognostic classifier in stage I lung adenocarcinoma. *Cancer Res* 73**:** 3821-3832

Anderson DM, Lyman SD, Baird A, Wignall JM, Eisenman J, Rauch C, March CJ, Boswell HS, Gimpel SD, Cosman D, et al. (1990) Molecular cloning of mast cell growth factor, a hematopoietin that is active in both membrane bound and soluble forms. *Cell* 63: 235-243

Antonini D, Russo MT, De Rosa L, Gorrese M, Del Vecchio L, Missero C (2010) Transcriptional repression of miR-34 family contributes to p63-mediated cell cycle progression in epidermal cells. *J Invest Dermatol* 130: 1249-1257

Attoub S, Rivat C, Rodrigues S, Van Bocxlaer S, Bedin M, Bruyneel E, Louvet C, Kornprobst M, Andre T, Mareel M, Mester J, Gespach C (2002) The c-kit tyrosine kinase inhibitor STI571 for colorectal cancer therapy. *Cancer Res* 62: 4879-4883

Bader AG (2012) miR-34 - a microRNA replacement therapy is headed to the clinic. *Front Genet* 3: 120

Bae Y, Yang T, Zeng HC, Campeau PM, Chen Y, Bertin T, Dawson BC, Munivez E, Tao J, Lee BH (2012) miRNA-34c regulates Notch signaling during bone development. *Hum Mol Genet* 21: 2991-3000

Bartel DP (2009) MicroRNAs: target recognition and regulatory functions. *Cell* 136: 215-233

Batlle E, Sancho E, Franci C, Dominguez D, Monfar M, Baulida J, Garcia De Herreros A (2000) The transcription factor snail is a repressor of E-cadherin gene expression in epithelial tumour cells. *Nat Cell Biol* 2: 84-89

Bellone G, Carbone A, Sibona N, Bosco O, Tibaudi D, Smirne C, Martone T, Gramigni C, Camandona M, Emanuelli G, Rodeck U (2001) Aberrant activation of c-kit protects colon carcinoma cells against apoptosis and enhances their invasive potential. *Cancer Res* 61: 2200-2206

Bellone G, Ferrero D, Carbone A, De Quadros MR, Gramigni C, Prati A, Davidson W, Mioli P, Dughera L, Emanuelli G, Rodeck U (2004) Inhibition of cell survival and invasive potential of colorectal carcinoma cells by the tyrosine kinase inhibitor STI571. *Cancer Biol Ther* 3: 385-392

Bellone G, Silvestri S, Artusio E, Tibaudi D, Turletti A, Geuna M, Giachino C, Valente G, Emanuelli G, Rodeck U (1997) Growth stimulation of colorectal carcinoma cells via the c-kit receptor is inhibited by TGF-beta 1. *J Cell Physiol* 172: 1-11

Bellone G, Smirne C, Carbone A, Buffolino A, Scirelli T, Prati A, Solerio D, Pirisi M, Valente G, Nano M, Emanuelli G (2006) KIT/stem cell factor expression in premalignant and malignant lesions of the colon mucosa in relationship to disease progression and outcomes. *Int J Oncol* 29: 851-859

Bernardo BC, Gao XM, Winbanks CE, Boey EJ, Tham YK, Kiriazis H, Gregorevic P, Obad S, Kauppinen S, Du XJ, Lin RC, McMullen JR (2012) Therapeutic inhibition of the miR-34 family attenuates pathological cardiac remodeling and improves heart function. *Proc Natl Acad Sci U S A* 109: 17615-17620

Besmer P, Murphy JE, George PC, Qiu FH, Bergold PJ, Lederman L, Snyder HW, Jr., Brodeur D, Zuckerman EE, Hardy WD (1986) A new acute transforming feline retrovirus and relationship of its oncogene v-kit with the protein kinase gene family. *Nature* 320: 415-421

Bird A (2007) Perceptions of epigenetics. *Nature* 447: 396-398

Bitarte N, Bandres E, Boni V, Zarate R, Rodriguez J, Gonzalez-Huarriz M, Lopez I, Javier Sola J, Alonso MM, Fortes P, Garcia-Foncillas J (2011) MicroRNA-451 is involved in the self-renewal, tumorigenicity, and chemoresistance of colorectal cancer stem cells. *Stem Cells* 29: 1661-1671

Bommer GT, Gerin I, Feng Y, Kaczorowski AJ, Kuick R, Love RE, Zhai Y, Giordano TJ, Qin ZS, Moore BB, MacDougald OA, Cho KR, Fearon ER (2007) p53-mediated activation of miRNA34 candidate tumor-suppressor genes. *Curr Biol* 17: 1298-1307

Boon RA, Iekushi K, Lechner S, Seeger T, Fischer A, Heydt S, Kaluza D, Treguer K, Carmona G, Bonauer A, Horrevoets AJ, Didier N, Girmatsion Z, Biliczki P, Ehrlich JR, Katus HA, Muller OJ, Potente M, Zeiher AM, Hermeking H, Dimmeler S (2013) MicroRNA-34a regulates cardiac ageing and function. *Nature* 495: 107-110

Bou Kheir T, Futoma-Kazmierczak E, Jacobsen A, Krogh A, Bardram L, Hother C, Gronbaek K, Federspiel B, Lund AH, Friis-Hansen L (2011) miR-449 inhibits cell proliferation and is down-regulated in gastric cancer. *Mol Cancer* 10: 29

Bouchie A (2013) First microRNA mimic enters clinic. *Nat Biotechnol* 31: 577

Brabletz S, Brabletz T (2010) The ZEB/miR-200 feedback loop--a motor of cellular plasticity in development and cancer? *EMBO Rep* 11: 670-677

Brabletz T (2012a) MiR-34 and SNAIL: another double-negative feedback loop controlling cellular plasticity/EMT governed by p53. *Cell Cycle* 11: 215-216

Brabletz T (2012b) To differentiate or not--routes towards metastasis. *Nat Rev Cancer* 12: 425-436

Brabletz T, Hlubek F, Spaderna S, Schmalhofer O, Hiendlmeyer E, Jung A, Kirchner T (2005) Invasion and metastasis in colorectal cancer: epithelial-mesenchymal transition, mesenchymal-epithelial transition, stem cells and beta-catenin. *Cells Tissues Organs* 179: 56-65

Bracken CP, Gregory PA, Kolesnikoff N, Bert AG, Wang J, Shannon MF, Goodall GJ (2008) A double-negative feedback loop between ZEB1-SIP1 and the microRNA-200 family regulates epithelial-mesenchymal transition. *Cancer Res* 68: 7846-7854

Breslow NE, Day NE (1987) Statistical methods in cancer research. Volume II--The design and analysis of cohort studies. *IARC Sci Publ*: 1-406

Bronner CE, Baker SM, Morrison PT, Warren G, Smith LG, Lescoe MK, Kane M, Earabino C, Lipford J, Lindblom A, et al. (1994) Mutation in the DNA mismatch repair gene homologue hMLH1 is associated with hereditary non-polyposis colon cancer. *Nature* 368: 258-261

Brownawell AM, Macara IG (2002) Exportin-5, a novel karyopherin, mediates nuclear export of double-stranded RNA binding proteins. *J Cell Biol* 156: 53-64

Bu P, Chen KY, Chen JH, Wang L, Walters J, Shin YJ, Goerger JP, Sun J, Witherspoon M, Rakhilin N, Li J, Yang H, Milsom J, Lee S, Zipfel W, Jin MM, Gumus ZH, Lipkin SM, Shen X (2013) A microRNA miR-34a-Regulated Bimodal Switch Targets Notch in Colon Cancer Stem Cells. *Cell Stem Cell* 12: 602-615

Bunz F, Dutriaux A, Lengauer C, Waldman T, Zhou S, Brown JP, Sedivy JM, Kinzler KW, Vogelstein B (1998) Requirement for p53 and p21 to sustain G2 arrest after DNA damage. *Science* 282: 1497-1501

Burk U, Schubert J, Wellner U, Schmalhofer O, Vincan E, Spaderna S, Brabletz T (2008) A reciprocal repression between ZEB1 and members of the miR-200 family promotes EMT and invasion in cancer cells. *EMBO Rep* 9: 582-589

Camp RL, Rimm EB, Rimm DL (1999) Met expression is associated with poor outcome in patients with axillary lymph node negative breast carcinoma. *Cancer* 86: 2259-2265

Cantwell-Dorris ER, O'Leary JJ, Sheils OM (2011) BRAFV600E: implications for carcinogenesis and molecular therapy. *Mol Cancer Ther* 10: 385-394

Catalano A, Rodilossi S, Rippo MR, Caprari P, Procopio A (2004) Induction of stem cell factor/c-Kit/slug signal transduction in multidrug-resistant malignant mesothelioma cells. *J Biol Chem* 279: 46706-46714

Chang CJ, Chao CH, Xia W, Yang JY, Xiong Y, Li CW, Yu WH, Rehman SK, Hsu JL, Lee HH, Liu M, Chen CT, Yu D, Hung MC (2011) p53 regulates epithelial-mesenchymal transition and stem cell properties through modulating miRNAs. *Nat Cell Biol* 13: 317-323

Chang TC, Wentzel EA, Kent OA, Ramachandran K, Mullendore M, Lee KH, Feldmann G, Yamakuchi M, Ferlito M, Lowenstein CJ, Arking DE, Beer MA, Maitra A, Mendell JT (2007) Transactivation of miR-34a by p53 broadly influences gene expression and promotes apoptosis. *Mol Cell* 26: 745-752

Chau WK, Ip CK, Mak AS, Lai HC, Wong AS (2012) c-Kit mediates chemoresistance and tumor-initiating capacity of ovarian cancer cells through activation of Wnt/beta-catenin-ATP-binding cassette G2 signaling. *Oncogene* 32: 2767-81

Chen X, Hu H, Guan X, Xiong G, Wang Y, Wang K, Li J, Xu X, Yang K, Bai Y (2012) CpG island methylation status of miRNAs in esophageal squamous cell carcinoma. *Int J Cancer* 130: 1607-1613

Chen Y, Zhu X, Zhang X, Liu B, Huang L (2010) Nanoparticles modified with tumor-targeting scFv deliver siRNA and miRNA for cancer therapy. *Mol Ther* 18: 1650-1656

Chien KH, Chen SJ, Liu JH, Chang HM, Woung LC, Liang CM, Chen JT, Lin TJ, Chiou SH, Peng CH (2013) Correlation between microRNA-34a levels and lens opacity severity in age-related cataracts. *Eye (Lond)* 27: 883-888

Chim CS, Wong KY, Qi Y, Loong F, Lam WL, Wong LG, Jin DY, Costello JF, Liang R (2010) Epigenetic inactivation of the miR-34a in hematological malignancies. *Carcinogenesis* 31: 745-750

Choi YJ, Lin CP, Ho JJ, He X, Okada N, Bu P, Zhong Y, Kim SY, Bennett MJ, Chen C, Ozturk A, Hicks GG, Hannon GJ, He L (2011) miR-34 miRNAs provide a barrier for somatic cell reprogramming. *Nat Cell Biol* 13: 1353-1360

Christoffersen NR, Shalgi R, Frankel LB, Leucci E, Lees M, Klausen M, Pilpel Y, Nielsen FC, Oren M, Lund AH (2010) p53-independent upregulation of miR-34a during oncogene-induced senescence represses MYC. *Cell Death Differ* 17: 236-245

Corney DC, Hwang CI, Matoso A, Vogt M, Flesken-Nikitin A, Godwin AK, Kamat AA, Sood AK, Ellenson LH, Hermeking H, Nikitin AY (2010) Frequent downregulation of miR-34 family in human ovarian cancers. *Clin Cancer Res* 16: 1119-1128

Craig VJ, Tzankov A, Flori M, Schmid CA, Bader AG, Muller A (2012) Systemic microRNA-34a delivery induces apoptosis and abrogates growth of diffuse large B-cell lymphoma in vivo. *Leukemia* 26: 2421-2424

de Krijger I, Mekenkamp LJ, Punt CJ, Nagtegaal ID (2011) MicroRNAs in colorectal cancer metastasis. *J Pathol* 224: 438-447

Duensing A, Medeiros F, McConarty B, Joseph NE, Panigrahy D, Singer S, Fletcher CD, Demetri GD, Fletcher JA (2004) Mechanisms of oncogenic KIT signal transduction in primary gastrointestinal stromal tumors (GISTs). *Oncogene* 23: 3999-4006

Eger A, Aigner K, Sonderegger S, Dampier B, Oehler S, Schreiber M, Berx G, Cano A, Beug H, Foisner R (2005) DeltaEF1 is a transcriptional repressor of E-cadherin and regulates epithelial plasticity in breast cancer cells. *Oncogene* 24: 2375-2385

Ellison GM, Vicinanza C, Smith AJ, Aquila I, Leone A, Waring CD, Henning BJ, Stirparo GG, Papait R, Scarfo M, Agosti V, Viglietto G, Condorelli G, Indolfi C, Ottolenghi S, Torella D, Nadal-Ginard B (2013) Adult c-kit(pos) Cardiac Stem Cells Are Necessary and Sufficient for Functional Cardiac Regeneration and Repair. *Cell* 154: 827-842

El-Serafi MM, Bahnassy AA, Ali NM, Eid SM, Kamel MM, Abdel-Hamid NA, Zekri AR (2010) The prognostic value of c-Kit, K-ras codon 12, and p53 codon 72 mutations in Egyptian patients with stage II colorectal cancer. *Cancer* 116: 4954-4964

Fabian MR, Sonenberg N, Filipowicz W (2010) Regulation of mRNA translation and stability by microRNAs. *Annu Rev Biochem* 79: 351-379

Fearon ER (2011) Molecular genetics of colorectal cancer. *Annu Rev Pathol* 6: 479-507

Fearon ER, Vogelstein B (1990) A genetic model for colorectal tumorigenesis. *Cell* 61: 759-767

Feil R, Fraga MF (2011) Epigenetics and the environment: emerging patterns and implications. *Nat Rev Genet* 13: 97-109

Feinberg AP (2007) Phenotypic plasticity and the epigenetics of human disease. *Nature* 447: 433-440

Feinberg AP, Ohlsson R, Henikoff S (2006) The epigenetic progenitor origin of human cancer. *Nat Rev Genet* 7: 21-33

Felli N, Fontana L, Pelosi E, Botta R, Bonci D, Facchiano F, Liuzzi F, Lulli V, Morsilli O, Santoro S, Valtieri M, Calin GA, Liu CG, Sorrentino A, Croce CM, Peschle C (2005) MicroRNAs 221 and 222 inhibit normal erythropoiesis and erythroleukemic cell growth via kit receptor down-modulation. *Proc Natl Acad Sci U S A* 102: 18081-18086

Fijneman RJ, Carvalho B, Postma C, Mongera S, van Hinsbergh VW, Meijer GA (2007) Loss of 1p36, gain of 8q24, and loss of 9q34 are associated with stroma percentage of colorectal cancer. *Cancer Lett* 258: 223-229

Filipowicz W (2005) RNAi: the nuts and bolts of the RISC machine. *Cell* 122: 17-20

Fire A, Xu S, Montgomery MK, Kostas SA, Driver SE, Mello CC (1998) Potent and specific genetic interference by double-stranded RNA in Caenorhabditis elegans. *Nature* 391: 806-811

Friederichs J, von Weyhern CW, Rosenberg R, Doll D, Busch R, Lordick F, Siewert JR, Sarbia M (2010) Immunohistochemical detection of receptor tyrosine kinases c-kit, EGF-R, and PDGF-R in colorectal adenocarcinomas. *Langenbecks Arch Surg* 395: 373-379

Friedman RC, Farh KK, Burge CB, Bartel DP (2009) Most mammalian mRNAs are conserved targets of microRNAs. *Genome Res* 19: 92-105

Fujita S, Sugano K (1997) Expression of c-met proto-oncogene in primary colorectal cancer and liver metastases. *Jpn J Clin Oncol* 27: 378-383

Fujita Y, Kojima K, Hamada N, Ohhashi R, Akao Y, Nozawa Y, Deguchi T, Ito M (2008) Effects of miR-34a on cell growth and chemoresistance in prostate cancer PC3 cells. *Biochem Biophys Res Commun* 377: 114-119

Gallardo E, Navarro A, Vinolas N, Marrades RM, Diaz T, Gel B, Quera A, Bandres E, Garcia-Foncillas J, Ramirez J, Monzo M (2009) miR-34a as a prognostic marker of relapse in surgically resected non-small-cell lung cancer. *Carcinogenesis* 30: 1903-1909

Galli SJ, Zsebo KM, Geissler EN (1994) The kit ligand, stem cell factor. *Adv Immunol* 55: 1-96

Gao XN, Lin J, Gao L, Li YH, Wang LL, Yu L (2011a) MicroRNA-193b regulates c-Kit proto-oncogene and represses cell proliferation in acute myeloid leukemia. *Leuk Res* 35: 1226-1232

Gao XN, Lin J, Li YH, Gao L, Wang XR, Wang W, Kang HY, Yan GT, Wang LL, Yu L (2011b) MicroRNA-193a represses c-kit expression and functions as a methylation-silenced tumor suppressor in acute myeloid leukemia. *Oncogene* 30: 3416-3428

Genovese G, Ergun A, Shukla SA, Campos B, Hanna J, Ghosh P, Quayle SN, Rai K, Colla S, Ying H, Wu CJ, Sarkar S, Xiao Y, Zhang J, Zhang H, Kwong L, Dunn K, Wiedemeyer WR, Brennan C, Zheng H, Rimm DL, Collins JJ, Chin L (2012) microRNA regulatory network inference identifies miR-34a as a novel regulator of TGF-beta signaling in glioblastoma. *Cancer Discov* 2: 736-749

Giroldi LA, Bringuier PP, de Weijert M, Jansen C, van Bokhoven A, Schalken JA (1997) Role of E boxes in the repression of E-cadherin expression. *Biochem Biophys Res Commun* 241: 453-458

Gregory PA, Bert AG, Paterson EL, Barry SC, Tsykin A, Farshid G, Vadas MA, Khew-Goodall Y, Goodall GJ (2008) The miR-200 family and miR-205 regulate epithelial to mesenchymal transition by targeting ZEB1 and SIP1. *Nat Cell Biol* 10: 593-601

Griffiths-Jones S (2004) The microRNA Registry. *Nucleic Acids Res* 32: D109-111

Grimson A, Farh KK, Johnston WK, Garrett-Engele P, Lim LP, Bartel DP (2007) MicroRNA targeting specificity in mammals: determinants beyond seed pairing. *Mol Cell* 27: 91-105

Gunaratne PH (2009) Embryonic stem cell microRNAs: defining factors in induced pluripotent (iPS) and cancer (CSC) stem cells? *Curr Stem Cell Res Ther* 4: 168-177

Guntur VP, Reinero CR (2012) The potential use of tyrosine kinase inhibitors in severe asthma. *Curr Opin Allergy Clin Immunol* 12: 68-75

Guo Y, Li S, Qu J, Wang S, Dang Y, Fan J, Yu S, Zhang J (2011) MiR-34a inhibits lymphatic metastasis potential of mouse hepatoma cells. *Mol Cell Biochem* 354: 275-282

He L, He X, Lim LP, de Stanchina E, Xuan Z, Liang Y, Xue W, Zender L, Magnus J, Ridzon D, Jackson AL, Linsley PS, Chen C, Lowe SW, Cleary MA, Hannon GJ (2007a) A microRNA component of the p53 tumour suppressor network. *Nature* 447: 1130-1134

He X, He L, Hannon GJ (2007b) The guardian's little helper: microRNAs in the p53 tumor suppressor network. *Cancer Res* 67: 11099-11101

Hermeking H (2007) p53 enters the microRNA world. *Cancer Cell* 12: 414-418

Hermeking H (2010) The miR-34 family in cancer and apoptosis. *Cell Death Differ* 17: 193-199

Hermeking H (2012) MicroRNAs in the p53 network: micromanagement of tumour suppression. *Nat Rev Cancer* 12: 613-626

Hibi K, Takahashi T, Sekido Y, Ueda R, Hida T, Ariyoshi Y, Takagi H (1991) Coexpression of the stem cell factor and the c-kit genes in small-cell lung cancer. *Oncogene* 6: 2291-2296

Hida T, Ueda R, Sekido Y, Hibi K, Matsuda R, Ariyoshi Y, Sugiura T, Takahashi T (1994) Ectopic expression of c-kit in small-cell lung cancer. *Int J Cancer Suppl* 8: 108-109

Hines SJ, Organ C, Kornstein MJ, Krystal GW (1995) Coexpression of the c-kit and stem cell factor genes in breast carcinomas. *Cell Growth Differ* 6: 769-779

Hoermann G, Cerny-Reiterer S, Perne A, Klauser M, Hoetzenecker K, Klein K, Mullauer L, Groger M, Nijman SM, Klepetko W, Valent P, Mayerhofer M (2011) Identification of oncostatin M as a STAT5-dependent mediator of bone marrow remodeling in KIT D816V-positive systemic mastocytosis. *Am J Pathol* 178: 2344-2356

Horst D, Chen J, Morikawa T, Ogino S, Kirchner T, Shivdasani RA (2012) Differential WNT activity in colorectal cancer confers limited tumorigenic potential and is regulated by MAPK signaling. *Cancer Res* 72: 1547-1556

Horst D, Scheel SK, Liebmann S, Neumann J, Maatz S, Kirchner T, Jung A (2009) The cancer stem cell marker CD133 has high prognostic impact but unknown functional relevance for the metastasis of human colon cancer. *J Pathol* 219: 427-434

Horvay K, Casagranda F, Gany A, Hime GR, Abud HE (2011) Wnt signaling regulates Snai1 expression and cellular localization in the mouse intestinal epithelial stem cell niche. *Stem Cells Dev* 20: 737-745

Hsu HC, Liu YS, Tseng KC, Hsu CL, Liang Y, Yang TS, Chen JS, Tang RP, Chen SJ, Chen HC (2013) Overexpression of Lgr5 correlates with resistance to 5-FU-based chemotherapy in colorectal cancer. *Int J Colorectal Dis* [Epub ahead of print]

Huntzinger E, Izaurralde E (2011) Gene silencing by microRNAs: contributions of translational repression and mRNA decay. *Nat Rev Genet* 12: 99-110

Hwang CI, Matoso A, Corney DC, Flesken-Nikitin A, Korner S, Wang W, Boccaccio C, Thorgeirsson SS, Comoglio PM, Hermeking H, Nikitin AY (2011a) Wild-type p53 controls cell motility and invasion by dual regulation of MET expression. *Proc Natl Acad Sci U S A* 108: 14240-14245

Hwang WL, Yang MH, Tsai ML, Lan HY, Su SH, Chang SC, Teng HW, Yang SH, Lan YT, Chiou SH, Wang HW (2011b) SNAIL regulates interleukin-8 expression, stem cell-like activity, and tumorigenicity of human colorectal carcinoma cells. *Gastroenterology* 141: 279-291

Iacobuzio-Donahue CA (2009) Epigenetic changes in cancer. *Annu Rev Pathol* 4: 229-249

Ichimura A, Ruike Y, Terasawa K, Shimizu K, Tsujimoto G (2010) MicroRNA-34a inhibits cell proliferation by repressing mitogen-activated protein kinase kinase 1 during megakaryocytic differentiation of K562 cells. *Mol Pharmacol* 77: 1016-1024

Ikeda H, Kanakura Y, Tamaki T, Kuriu A, Kitayama H, Ishikawa J, Kanayama Y, Yonezawa T, Tarui S, Griffin JD (1991) Expression and functional role of the proto-oncogene c-kit in acute myeloblastic leukemia cells. *Blood* 78: 2962-2968

Jackstadt R, Roh S, Neumann J, Jung P, Hoffmann R, Horst D, Berens C, Bornkamm GW, Kirchner T, Menssen A, Hermeking H (2013) AP4 is a mediator of epithelial-mesenchymal transition and metastasis in colorectal cancer. *J Exp Med* 210: 1331-1350

Jensen BM, Metcalfe DD, Gilfillan AM (2007) Targeting kit activation: a potential therapeutic approach in the treatment of allergic inflammation. *Inflamm Allergy Drug Targets* 6: 57-62

John B, Enright AJ, Aravin A, Tuschl T, Sander C, Marks DS (2004) Human MicroRNA targets. *PLoS Biol* 2: e363

Jones PA, Baylin SB (2002) The fundamental role of epigenetic events in cancer. *Nat Rev Genet* 3: 415-428

Jones PL, Veenstra GJ, Wade PA, Vermaak D, Kass SU, Landsberger N, Strouboulis J, Wolffe AP (1998) Methylated DNA and MeCP2 recruit histone deacetylase to repress transcription. *Nat Genet* 19: 187-191

Kalimutho M, Di Cecilia S, Del Vecchio Blanco G, Roviello F, Sileri P, Cretella M, Formosa A, Corso G, Marrelli D, Pallone F, Federici G, Bernardini S (2011) Epigenetically silenced miR-34b/c as a novel faecal-based screening marker for colorectal cancer. *Br J Cancer* 104: 1770-1778

Kaller M, Liffers ST, Oeljeklaus S, Kuhlmann K, Roh S, Hoffmann R, Warscheid B, Hermeking H (2011) Genome-wide characterization of miR-34a induced changes in protein and mRNA expression by a combined pulsed SILAC and microarray analysis. *Mol Cell Proteomics* 10: M111 010462

Kamimae S, Yamamoto E, Yamano HO, Nojima M, Suzuki H, Ashida M, Hatahira T, Sato A, Kimura T, Yoshikawa K, Harada T, Hayashi S, Takamaru

H, Maruyama R, Kai M, Nishiwaki M, Sugai T, Sasaki Y, Tokino T, Shinomura Y, Imai K, Toyota M (2011) Epigenetic alteration of DNA in mucosal wash fluid predicts invasiveness of colorectal tumors. *Cancer Prev Res (Phila)* 4: 674-683

Kasinski AL, Slack FJ (2011) Epigenetics and genetics. MicroRNAs en route to the clinic: progress in validating and targeting microRNAs for cancer therapy. *Nat Rev Cancer* 11: 849-864

Kasinski AL, Slack FJ (2012) miRNA-34 prevents cancer initiation and progression in a therapeutically-resistant K-ras and p53-induced mouse model of lung adenocarcinoma. *Cancer Res* 72: 5576-5587

Kemper K, Grandela C, Medema JP (2010) Molecular identification and targeting of colorectal cancer stem cells. *Oncotarget* 1: 387-395

Kent D, Copley M, Benz C, Dykstra B, Bowie M, Eaves C (2008) Regulation of hematopoietic stem cells by the steel factor/KIT signaling pathway. *Clin Cancer Res* 14: 1926-1930

Kim CH, Kim HK, Rettig RL, Kim J, Lee ET, Aprelikova O, Choi IJ, Munroe DJ, Green JE (2011a) miRNA signature associated with outcome of gastric cancer patients following chemotherapy. *BMC Med Genomics* 4: 79

Kim NH, Kim HS, Kim NG, Lee I, Choi HS, Li XY, Kang SE, Cha SY, Ryu JK, Na JM, Park C, Kim K, Lee S, Gumbiner BM, Yook JI, Weiss SJ (2011b) p53 and microRNA-34 are suppressors of canonical Wnt signaling. *Sci Signal* 4: ra71

Kim NH, Kim HS, Li XY, Lee I, Choi HS, Kang SE, Cha SY, Ryu JK, Yoon D, Fearon ER, Rowe RG, Lee S, Maher CA, Weiss SJ, Yook JI (2011c) A p53/miRNA-34 axis regulates Snail1-dependent cancer cell epithelial-mesenchymal transition. *J Cell Biol* 195: 417-433

Kim T, Veronese A, Pichiorri F, Lee TJ, Jeon YJ, Volinia S, Pineau P, Marchio A, Palatini J, Suh SS, Alder H, Liu CG, Dejean A, Croce CM (2011d) p53 regulates epithelial-mesenchymal transition through microRNAs targeting ZEB1 and ZEB2. *J Exp Med* 208: 875-883

Kim VN, Han J, Siomi MC (2009) Biogenesis of small RNAs in animals. *Nat Rev Mol Cell Biol* 10: 126-139

Kim W, Kim M, Jho EH (2013) Wnt/beta-catenin signalling: from plasma membrane to nucleus. *Biochem J* 450: 9-21

Kim WK, Park M, Kim YK, Tae YK, Yang HK, Lee JM, Kim H (2011e) MicroRNA-494 downregulates KIT and inhibits gastrointestinal stromal tumor cell proliferation. *Clin Cancer Res* 17: 7584-7594

Kitamura Y, Tsujimura T, Jippo T, Kasugai T, Kanakura Y (1995) Regulation of development, survival and neoplastic growth of mast cells through the c-kit receptor. *Int Arch Allergy Immunol* 107: 54-56

Krailo MD, Pike MC (1984) Algorithm AS 196: Conditional Multivariate Logistic Analysis of Stratified Case-Control Studies. *Journal of the Royal Statistical Society Series C (Applied Statistics)* 33: 95-103

Kress TR, Cannell IG, Brenkman AB, Samans B, Gaestel M, Roepman P, Burgering BM, Bushell M, Rosenwald A, Eilers M (2011) The MK5/PRAK kinase and Myc form a negative feedback loop that is disrupted during colorectal tumorigenesis. *Mol Cell* 41: 445-457

Krishnamoorthy N, Oriss TB, Paglia M, Fei M, Yarlagadda M, Vanhaesebroeck B, Ray A, Ray P (2008) Activation of c-Kit in dendritic cells regulates T helper cell differentiation and allergic asthma. *Nat Med* 14: 565-573

Krol J, Loedige I, Filipowicz W (2010) The widespread regulation of microRNA biogenesis, function and decay. *Nat Rev Genet* 11: 597-610

Krystal GW, Hines SJ, Organ CP (1996) Autocrine growth of small cell lung cancer mediated by coexpression of c-kit and stem cell factor. *Cancer Res* 56: 370-376

Kudo-Saito C, Shirako H, Takeuchi T, Kawakami Y (2009) Cancer metastasis is accelerated through immunosuppression during Snail-induced EMT of cancer cells. *Cancer Cell* 15: 195-206

Kurrey NK, Jalgaonkar SP, Joglekar AV, Ghanate AD, Chaskar PD, Doiphode RY, Bapat SA (2009) Snail and slug mediate radioresistance and chemoresistance by antagonizing p53-mediated apoptosis and acquiring a stem-like phenotype in ovarian cancer cells. *Stem Cells* 27: 2059-2068

Lahm H, Amstad P, Yilmaz A, Borbenyi Z, Wyniger J, Fischer JR, Suardet L, Givel JC, Odartchenko N (1995) Interleukin 4 down-regulates expression of c-kit and autocrine stem cell factor in human colorectal carcinoma cells. *Cell Growth Differ* 6: 1111-1118

Lane DP (1992) Cancer. p53, guardian of the genome. *Nature* 358: 15-16

Lee AS, Seo YC, Chang A, Tohari S, Eu KW, Seow-Choen F, McGee JO (2000) Detailed deletion mapping at chromosome 11q23 in colorectal carcinoma. *Br J Cancer* 83: 750-755

Lee RC, Feinbaum RL, Ambros V (1993) The C. elegans heterochronic gene lin-4 encodes small RNAs with antisense complementarity to lin-14. *Cell* 75: 843-854

Lennartsson J, Blume-Jensen P, Hermanson M, Ponten E, Carlberg M, Ronnstrand L (1999) Phosphorylation of Shc by Src family kinases is necessary for stem cell factor receptor/c-kit mediated activation of the Ras/MAP kinase pathway and c-fos induction. *Oncogene* 18: 5546-5553

Lennartsson J, Ronnstrand L (2012) Stem Cell Factor Receptor/c-Kit: From Basic Science to Clinical Implications. *Physiol Rev* 92: 1619-1649

Lewis BP, Burge CB, Bartel DP (2005) Conserved seed pairing, often flanked by adenosines, indicates that thousands of human genes are microRNA targets. *Cell* 120: 15-20

Lindner I, Hemdan NY, Buchold M, Huse K, Bigl M, Oerlecke I, Ricken A, Gaunitz F, Sack U, Naumann A, Hollborn M, Thal D, Gebhardt R, Birkenmeier G (2010) Alpha2-macroglobulin inhibits the malignant properties of astrocytoma cells by impeding beta-catenin signaling. *Cancer Res* 70: 277-287

Li N, Fu H, Tie Y, Hu Z, Kong W, Wu Y, Zheng X (2009) miR-34a inhibits migration and invasion by down-regulation of c-Met expression in human hepatocellular carcinoma cells. *Cancer Lett* 275: 44-53

Li N, Muthusamy S, Liang R, Sarojini H, Wang E (2011) Increased expression of miR-34a and miR-93 in rat liver during aging, and their impact on the expression of Mgst1 and Sirt1. *Mech Ageing Dev* 132: 75-85

Li Q, Chen H (2011) Epigenetic modifications of metastasis suppressor genes in colon cancer metastasis. *Epigenetics* 6: 849-852

Li XJ, Ji MH, Zhong SL, Zha QB, Xu JJ, Zhao JH, Tang JH (2012) MicroRNA-34a Modulates Chemosensitivity of Breast Cancer Cells to Adriamycin by Targeting Notch1. *Arch Med Res* 43: 514-521

Liu C, Kelnar K, Liu B, Chen X, Calhoun-Davis T, Li H, Patrawala L, Yan H, Jeter C, Honorio S, Wiggins JF, Bader AG, Fagin R, Brown D, Tang DG (2011) The microRNA miR-34a inhibits prostate cancer stem cells and metastasis by directly repressing CD44. *Nat Med* 17: 211-215

Liu N, Landreh M, Cao K, Abe M, Hendriks GJ, Kennerdell JR, Zhu Y, Wang LS, Bonini NM (2012) The microRNA miR-34 modulates ageing and neurodegeneration in Drosophila. *Nature* 482: 519-523

Lize M, Klimke A, Dobbelstein M (2011) MicroRNA-449 in cell fate determination. *Cell Cycle* 10: 2874-2882

Lize M, Pilarski S, Dobbelstein M (2010) E2F1-inducible microRNA 449a/b suppresses cell proliferation and promotes apoptosis. *Cell Death Differ* 17: 452-458

Lodygin D, Tarasov V, Epanchintsev A, Berking C, Knyazeva T, Korner H, Knyazev P, Diebold J, Hermeking H (2008) Inactivation of miR-34a by aberrant CpG methylation in multiple types of cancer. *Cell Cycle* 7: 2591-2600

Lujambio A, Calin GA, Villanueva A, Ropero S, Sanchez-Cespedes M, Blanco D, Montuenga LM, Rossi S, Nicoloso MS, Faller WJ, Gallagher WM, Eccles SA, Croce CM, Esteller M (2008) A microRNA DNA methylation signature for human cancer metastasis. *Proc Natl Acad Sci U S A* 105: 13556-13561

Lujambio A, Lowe SW (2012) The microcosmos of cancer. *Nature* 482: 347-355

Luo L, Zeng J, Liang B, Zhao Z, Sun L, Cao D, Yang J, Shen K (2011) Ovarian cancer cells with the CD117 phenotype are highly tumorigenic and are related to chemotherapy outcome. *Exp Mol Pathol* 91: 596-602

Ma Y, Liang D, Liu J, Axcrona K, Kvalheim G, Giercksky KE, Nesland JM, Suo Z (2012) Synergistic effect of SCF and G-CSF on stem-like properties in prostate cancer cell lines. *Tumour Biol* 33: 967-978

Maes OC, Sarojini H, Wang E (2009) Stepwise up-regulation of microRNA expression levels from replicating to reversible and irreversible growth arrest states in WI-38 human fibroblasts. *J Cell Physiol* 221: 109-119

Mahzouni P, Jafari M (2012) The study of CD117 expression in glial tumors and its relationship with the tumor-type and grade. *J Res Med Sci* 17: 159-163

Mani SA, Guo W, Liao MJ, Eaton EN, Ayyanan A, Zhou AY, Brooks M, Reinhard F, Zhang CC, Shipitsin M, Campbell LL, Polyak K, Brisken C, Yang J, Weinberg RA (2008) The epithelial-mesenchymal transition generates cells with properties of stem cells. *Cell* 133: 704-715

Martinho O, Goncalves A, Moreira MA, Ribeiro LF, Queiroz GS, Schmitt FC, Reis RM, Longatto-Filho A (2008) KIT activation in uterine cervix adenosquamous carcinomas by KIT/SCF autocrine/paracrine stimulation loops. *Gynecol Oncol* 111: 350-355

Melo SA, Esteller M (2011) A precursor microRNA in a cancer cell nucleus: get me out of here! *Cell Cycle* 10: 922-925

Mina LA, Sledge GW, Jr. (2011) Rethinking the metastatic cascade as a therapeutic target. *Nat Rev Clin Oncol* 8: 325-332

Montone KT, van Belle P, Elenitsas R, Elder DE (1997) Proto-oncogene c-kit expression in malignant melanoma: protein loss with tumor progression. *Mod Pathol* 10: 939-944

Mudduluru G, Ceppi P, Kumarswamy R, Scagliotti GV, Papotti M, Allgayer H (2011) Regulation of Axl receptor tyrosine kinase expression by miR-34a and miR-199a/b in solid cancer. *Oncogene* 30: 2888-2899

Mulero-Navarro S, Esteller M (2008) Epigenetic biomarkers for human cancer: the time is now. *Crit Rev Oncol Hematol* 68: 1-11

Muzny (2012) Comprehensive molecular characterization of human colon and rectal cancer. *Nature* 487: 330-337

Natali PG, Nicotra MR, Winkler AB, Cavaliere R, Bigotti A, Ullrich A (1992) Progression of human cutaneous melanoma is associated with loss of expression of c-kit proto-oncogene receptor. *Int J Cancer* 52: 197-201

Neumann J, Bahr F, Horst D, Kriegl L, Engel J, Luque RM, Gerhard M, Kirchner T, Jung A (2011) SOX2 expression correlates with lymph node metastases and distant spread in right-sided colon cancer. *BMC Cancer* 11: 518

Neumann J, Horst D, Kriegl L, Maatz S, Engel J, Jung A, Kirchner T (2012a) A simple immunohistochemical algorithm predicts the risk of distant metastases in right-sided colon cancer. *Histopathology* 60: 416-426

Neumann J, Reu S, Kirchner T (2012b) [Prognostic marker profiles for risk of distant metastases in colorectal cancer]. *Pathologe* 33: 39-44

Nieto MA (2011) The ins and outs of the epithelial to mesenchymal transition in health and disease. *Annu Rev Cell Dev Biol* 27: 347-376

Ohtani-Fujita N, Fujita T, Aoike A, Osifchin NE, Robbins PD, Sakai T (1993) CpG methylation inactivates the promoter activity of the human retinoblastoma tumor-suppressor gene. *Oncogene* 8: 1063-1067

Papadopoulos N, Nicolaides NC, Wei YF, Ruben SM, Carter KC, Rosen CA, Haseltine WA, Fleischmann RD, Fraser CM, Adams MD, et al. (1994) Mutation of a mutL homolog in hereditary colon cancer. *Science* 263: 1625-1629

Pasquinelli AE, Reinhart BJ, Slack F, Martindale MQ, Kuroda MI, Maller B, Hayward DC, Ball EE, Degnan B, Muller P, Spring J, Srinivasan A, Fishman M, Finnerty J, Corbo J, Levine M, Leahy P, Davidson E, Ruvkun G (2000) Conservation of the sequence and temporal expression of let-7 heterochronic regulatory RNA. *Nature* 408: 86-89

Peinado H, Ballestar E, Esteller M, Cano A (2004) Snail mediates E-cadherin repression by the recruitment of the Sin3A/histone deacetylase 1 (HDAC1)/HDAC2 complex. *Mol Cell Biol* 24: 306-319

Peinado H, Olmeda D, Cano A (2007) Snail, Zeb and bHLH factors in tumour progression: an alliance against the epithelial phenotype? *Nat Rev Cancer* 7: 415-428

Peparini N, Caronna R, Tellan G, Chirletti P (2009) Expression of receptors tyrosine kinase c-kit and EGF-R in colorectal adenocarcinomas: is there a relationship with epithelial-mesenchymal transition during tumor progression? *Langenbecks Arch Surg* 394: 1131-1132; author reply 1133-1134

Perini G, Diolaiti D, Porro A, Della Valle G (2005) In vivo transcriptional regulation of N-Myc target genes is controlled by E-box methylation. *Proc Natl Acad Sci U S A* 102: 12117-12122

Perl AK, Wilgenbus P, Dahl U, Semb H, Christofori G (1998) A causal role for E-cadherin in the transition from adenoma to carcinoma. *Nature* 392: 190-193

Peurala H, Greco D, Heikkinen T, Kaur S, Bartkova J, Jamshidi M, Aittomaki K, Heikkila P, Bartek J, Blomqvist C, Butzow R, Nevanlinna H (2011) MiR-34a expression has an effect for lower risk of metastasis and associates with expression patterns predicting clinical outcome in breast cancer. *PLoS One* 6: e26122

Pillai RS, Bhattacharyya SN, Artus CG, Zoller T, Cougot N, Basyuk E, Bertrand E, Filipowicz W (2005) Inhibition of translational initiation by Let-7 MicroRNA in human cells. *Science* 309: 1573-1576

Pinho AV, Rooman I, Real FX (2011) p53-dependent regulation of growth, epithelial-mesenchymal transition and stemness in normal pancreatic epithelial cells. *Cell Cycle* 10**:** 1312-1321

Poliseno L, Tuccoli A, Mariani L, Evangelista M, Citti L, Woods K, Mercatanti A, Hammond S, Rainaldi G (2006) MicroRNAs modulate the angiogenic properties of HUVECs. *Blood* 108: 3068-3071

Polyak K, Weinberg RA (2009) Transitions between epithelial and mesenchymal states: acquisition of malignant and stem cell traits. *Nat Rev Cancer* 9: 265-273

Pramanik D, Campbell NR, Karikari C, Chivukula R, Kent OA, Mendell JT, Maitra A (2011) Restitution of tumor suppressor microRNAs using a systemic nanovector inhibits pancreatic cancer growth in mice. *Mol Cancer Ther* 10: 1470-1480

Pratt AJ, MacRae IJ (2009) The RNA-induced silencing complex: a versatile gene-silencing machine. *J Biol Chem* 284: 17897-17901

Preto A, Moutinho C, Velho S, Oliveira C, Rebocho AP, Figueiredo J, Soares P, Lopes JM, Seruca R (2007) A subset of colorectal carcinomas express c-KIT protein independently of BRAF and/or KRAS activation. *Virchows Arch* 450: 619-626

Raver-Shapira N, Marciano E, Meiri E, Spector Y, Rosenfeld N, Moskovits N, Bentwich Z, Oren M (2007) Transcriptional activation of miR-34a contributes to p53-mediated apoptosis. *Mol Cell* 26: 731-743

Reber L, Da Silva CA, Frossard N (2006) Stem cell factor and its receptor c-Kit as targets for inflammatory diseases. *Eur J Pharmacol* 533: 327-340

Reed J, Ouban A, Schickor FK, Muraca P, Yeatman T, Coppola D (2002) Immunohistochemical staining for c-Kit (CD117) is a rare event in human colorectal carcinoma. *Clin Colorectal Cancer* 2: 119-122

Riggs JW, Barrilleaux BL, Varlakhanova N, Bush KM, Chan V, Knoepfler PS (2013) Induced pluripotency and oncogenic transformation are related processes. *Stem Cells Dev* 22: 37-50

Rivas FV, Tolia NH, Song JJ, Aragon JP, Liu J, Hannon GJ, Joshua-Tor L (2005) Purified Argonaute2 and an siRNA form recombinant human RISC. *Nat Struct Mol Biol* 12: 340-349

Rothschild G, Sottas CM, Kissel H, Agosti V, Manova K, Hardy MP, Besmer P (2003) A role for kit receptor signaling in Leydig cell steroidogenesis. *Biol Reprod* 69: 925-932

Roy HK, Smyrk TC, Koetsier J, Victor TA, Wali RK (2005) The transcriptional repressor SNAIL is overexpressed in human colon cancer. *Dig Dis Sci* 50: 42-46

Sadiq AA, Salgia R (2013) MET as a possible target for non-small-cell lung cancer. *J Clin Oncol* 31: 1089-1096

Sakai T, Toguchida J, Ohtani N, Yandell DW, Rapaport JM, Dryja TP (1991) Allele-specific hypermethylation of the retinoblastoma tumor-suppressor gene. *Am J Hum Genet* 48: 880-888

Sammarco I, Capurso G, Coppola L, Bonifazi AP, Cassetta S, Delle Fave G, Carrara A, Grassi GB, Rossi P, Sette C, Geremia R (2004) Expression of the proto-oncogene c-KIT in normal and tumor tissues from colorectal carcinoma patients. *Int J Colorectal Dis* 19: 545-553

Sanchez-Tillo E, Liu Y, de Barrios O, Siles L, Fanlo L, Cuatrecasas M, Darling DS, Dean DC, Castells A, Postigo A (2012) EMT-activating transcription factors in cancer: beyond EMT and tumor invasiveness. *Cell Mol Life Sci* 69: 3429-3456

Scotto KW (2003) Transcriptional regulation of ABC drug transporters. *Oncogene* 22: 7496-7511

Shames DS, Minna JD, Gazdar AF (2007) DNA methylation in health, disease, and cancer. *Curr Mol Med* 7: 85-102

Sharpless NE, DePinho RA (2002) p53: good cop/bad cop. *Cell* 110: 9-12

Shenker N, Flanagan JM (2012) Intragenic DNA methylation: implications of this epigenetic mechanism for cancer research. *Br J Cancer* 106: 248-253

Shimono Y, Zabala M, Cho RW, Lobo N, Dalerba P, Qian D, Diehn M, Liu H, Panula SP, Chiao E, Dirbas FM, Somlo G, Pera RA, Lao K, Clarke MF (2009) Downregulation of miRNA-200c links breast cancer stem cells with normal stem cells. *Cell* 138: 592-603

Shin J, Pan H, Zhong XP (2012) Regulation of mast cell survival and function by tuberous sclerosis complex 1. *Blood* 119: 3306-3314

Shioiri M, Shida T, Koda K, Oda K, Seike K, Nishimura M, Takano S, Miyazaki M (2006) Slug expression is an independent prognostic parameter for poor survival in colorectal carcinoma patients. *Br J Cancer* 94: 1816-1822

Siemens H, Jackstadt R, Hunten S, Kaller M, Menssen A, Gotz U, Hermeking H (2011) miR-34 and SNAIL form a double-negative feedback loop to regulate epithelial-mesenchymal transitions. *Cell Cycle* 10: 4256-4271

Silber J, Jacobsen A, Ozawa T, Harinath G, Pedraza A, Sander C, Holland EC, Huse JT (2012) miR-34a repression in proneural malignant gliomas upregulates expression of its target PDGFRA and promotes tumorigenesis. *PLoS One* 7: e33844

Solberg OD, Ostrin EJ, Love MI, Peng JC, Bhakta NR, Hou L, Nguyen C, Solon M, Barczak AJ, Zlock LT, Blagev DP, Finkbeiner WE, Ansel KM, Arron JR, Erle DJ, Woodruff PG (2012) Airway epithelial miRNA expression is altered in asthma. *Am J Respir Crit Care Med* 186: 965-974

Sontheimer EJ (2005) Assembly and function of RNA silencing complexes. *Nat Rev Mol Cell Biol* 6: 127-138

Suva ML, Riggi N, Bernstein BE (2013) Epigenetic reprogramming in cancer. *Science* 339: 1567-1570

Suzuki H, Yamamoto E, Nojima M, Kai M, Yamano HO, Yoshikawa K, Kimura T, Kudo T, Harada E, Sugai T, Takamaru H, Niinuma T, Maruyama R, Yamamoto H, Tokino T, Imai K, Toyota M, Shinomura Y (2010) Methylation-associated silencing of microRNA-34b/c in gastric cancer and its involvement in an epigenetic field defect. *Carcinogenesis* 31: 2066-2073

Tanaka N, Toyooka S, Soh J, Kubo T, Yamamoto H, Maki Y, Muraoka T, Shien K, Furukawa M, Ueno T, Asano H, Tsukuda K, Aoe K, Miyoshi S (2011) Frequent methylation and oncogenic role of microRNA-34b/c in small-cell lung cancer. *Lung Cancer* 76: 32-38

Tarasov V, Jung P, Verdoodt B, Lodygin D, Epanchintsev A, Menssen A, Meister G, Hermeking H (2007) Differential regulation of microRNAs by p53

revealed by massively parallel sequencing: miR-34a is a p53 target that induces apoptosis and G1-arrest. *Cell Cycle* 6: 1586-1593

Tazawa H, Tsuchiya N, Izumiya M, Nakagama H (2007) Tumor-suppressive miR-34a induces senescence-like growth arrest through modulation of the E2F pathway in human colon cancer cells. *Proc Natl Acad Sci U S A* 104: 15472-15477

Theou-Anton N, Tabone S, Brouty-Boye D, Saffroy R, Ronnstrand L, Lemoine A, Emile JF (2006) Co expression of SCF and KIT in gastrointestinal stromal tumours (GISTs) suggests an autocrine/paracrine mechanism. *Br J Cancer* 94: 1180-1185

Thiery JP, Acloque H, Huang RY, Nieto MA (2009) Epithelial-mesenchymal transitions in development and disease. *Cell* 139: 871-890

Thorstensen L, Qvist H, Heim S, Liefers GJ, Nesland JM, Giercksky KE, Lothe RA (2000) Evaluation of 1p losses in primary carcinomas, local recurrences and peripheral metastases from colorectal cancer patients. *Neoplasia* 2: 514-522

Toyota M, Suzuki H, Sasaki Y, Maruyama R, Imai K, Shinomura Y, Tokino T (2008) Epigenetic silencing of microRNA-34b/c and B-cell translocation gene 4 is associated with CpG island methylation in colorectal cancer. *Cancer Res* 68: 4123-4132

Trang P, Wiggins JF, Daige CL, Cho C, Omotola M, Brown D, Weidhaas JB, Bader AG, Slack FJ (2011) Systemic delivery of tumor suppressor microRNA mimics using a neutral lipid emulsion inhibits lung tumors in mice. *Mol Ther* 19: 1116-1122

Uddin S, Hussain AR, Ahmed M, Al-Dayel F, Bu R, Bavi P, Al-Kuraya KS (2010) Inhibition of c-MET is a potential therapeutic strategy for treatment of diffuse large B-cell lymphoma. *Lab Invest* 90: 1346-1356

van Oosterom AT, Judson I, Verweij J, Stroobants S, Donato di Paola E, Dimitrijevic S, Martens M, Webb A, Sciot R, Van Glabbeke M, Silberman S, Nielsen OS (2001) Safety and efficacy of imatinib (STI571) in metastatic gastrointestinal stromal tumours: a phase I study. *Lancet* 358: 1421-1423

Vassilev LT, Vu BT, Graves B, Carvajal D, Podlaski F, Filipovic Z, Kong N, Kammlott U, Lukacs C, Klein C, Fotouhi N, Liu EA (2004) In vivo activation of the p53 pathway by small-molecule antagonists of MDM2. *Science* 303: 844-848

Vogelstein B, Lane D, Levine AJ (2000) Surfing the p53 network. *Nature* 408: 307-310

Vogt M, Munding J, Gruner M, Liffers ST, Verdoodt B, Hauk J, Steinstraesser L, Tannapfel A, Hermeking H (2011) Frequent concomitant inactivation of

miR-34a and miR-34b/c by CpG methylation in colorectal, pancreatic, mammary, ovarian, urothelial, and renal cell carcinomas and soft tissue sarcomas. *Virchows Arch* 458: 313-322

Walther A, Johnstone E, Swanton C, Midgley R, Tomlinson I, Kerr D (2009) Genetic prognostic and predictive markers in colorectal cancer. *Nat Rev Cancer* 9: 489-499

Wang C, Curtis JE, Geissler EN, McCulloch EA, Minden MD (1989) The expression of the proto-oncogene C-kit in the blast cells of acute myeloblastic leukemia. *Leukemia* 3: 699-702

Wang X, Dong K, Gao P, Long M, Lin F, Weng Y, Ouyang Y, Ren J, Zhang H (2012) microRNA-34a Sensitizes Lung Cancer Cell Lines to DDP Treatment Independent of p53 Status. *Cancer Biother Radiopharm* 28: 45-50

Wang Z, Chen Z, Gao Y, Li N, Li B, Tan F, Tan X, Lu N, Sun Y, Sun J, Sun N, He J (2011) DNA hypermethylation of microRNA-34b/c has prognostic value for stage non-small cell lung cancer. *Cancer Biol Ther* 11: 490-496

Wei J, Shi Y, Zheng L, Zhou B, Inose H, Wang J, Guo XE, Grosschedl R, Karsenty G (2012) miR-34s inhibit osteoblast proliferation and differentiation in the mouse by targeting SATB2. *J Cell Biol* 197: 509-521

Weisenberger DJ, Siegmund KD, Campan M, Young J, Long TI, Faasse MA, Kang GH, Widschwendter M, Weener D, Buchanan D, Koh H, Simms L, Barker M, Leggett B, Levine J, Kim M, French AJ, Thibodeau SN, Jass J, Haile R, Laird PW (2006) CpG island methylator phenotype underlies sporadic microsatellite instability and is tightly associated with BRAF mutation in colorectal cancer. *Nat Genet* 38: 787-793

Welch C, Chen Y, Stallings RL (2007) MicroRNA-34a functions as a potential tumor suppressor by inducing apoptosis in neuroblastoma cells. *Oncogene* 26: 5017-5022

Wellner U, Schubert J, Burk UC, Schmalhofer O, Zhu F, Sonntag A, Waldvogel B, Vannier C, Darling D, zur Hausen A, Brunton VG, Morton J, Sansom O, Schuler J, Stemmler MP, Herzberger C, Hopt U, Keck T, Brabletz S, Brabletz T (2009) The EMT-activator ZEB1 promotes tumorigenicity by repressing stemness-inhibiting microRNAs. *Nat Cell Biol* 11: 1487-1495

Wiesenauer CA, Yip-Schneider MT, Wang Y, Schmidt CM (2004) Multiple anticancer effects of blocking MEK-ERK signaling in hepatocellular carcinoma. *J Am Coll Surg* 198: 410-421

Wiggins JF, Ruffino L, Kelnar K, Omotola M, Patrawala L, Brown D, Bader AG (2010) Development of a lung cancer therapeutic based on the tumor suppressor microRNA-34. *Cancer Res* 70: 5923-5930

Xu Q, Seeger FH, Castillo J, Iekushi K, Boon RA, Farcas R, Manavski Y, Li YG, Assmus B, Zeiher AM, Dimmeler S (2012) Micro-RNA-34a contributes to the impaired function of bone marrow-derived mononuclear cells from patients with cardiovascular disease. *J Am Coll Cardiol* 59: 2107-2117

Yamazaki H, Chijiwa T, Inoue Y, Abe Y, Suemizu H, Kawai K, Wakui M, Furukawa D, Mukai M, Kuwao S, Saegusa M, Nakamura M (2012) Overexpression of the miR-34 family suppresses invasive growth of malignant melanoma with the wild-type p53 gene. *Exp Ther Med* 3: 793-796

Yang P, Li QJ, Feng Y, Zhang Y, Markowitz GJ, Ning S, Deng Y, Zhao J, Jiang S, Yuan Y, Wang HY, Cheng SQ, Xie D, Wang XF (2012a) TGF-beta-miR-34a-CCL22 signaling-induced Treg cell recruitment promotes venous metastases of HBV-positive hepatocellular carcinoma. *Cancer Cell* 22: 291-303

Yang S, Li Y, Gao J, Zhang T, Li S, Luo A, Chen H, Ding F, Wang X, Liu Z (2012b) MicroRNA-34 suppresses breast cancer invasion and metastasis by directly targeting Fra-1. *Oncogene* doi: 10.1038/onc.2012.432

Yang X, Feng M, Jiang X, Wu Z, Li Z, Aau M, Yu Q (2009) miR-449a and miR-449b are direct transcriptional targets of E2F1 and negatively regulate pRb-E2F1 activity through a feedback loop by targeting CDK6 and CDC25A. *Genes Dev* 23: 2388-2393

Yarden Y, Kuang WJ, Yang-Feng T, Coussens L, Munemitsu S, Dull TJ, Chen E, Schlessinger J, Francke U, Ullrich A (1987) Human proto-oncogene c-kit: a new cell surface receptor tyrosine kinase for an unidentified ligand. *EMBO J* 6: 3341-3351

Yasuda A, Sawai H, Takahashi H, Ochi N, Matsuo Y, Funahashi H, Sato M, Okada Y, Takeyama H, Manabe T (2007) Stem cell factor/c-kit receptor signaling enhances the proliferation and invasion of colorectal cancer cells through the PI3K/Akt pathway. *Dig Dis Sci* 52: 2292-2300

Yorke R, Chirala M, Younes M (2003) c-kit proto-oncogene product is rarely detected in colorectal adenocarcinoma. *J Clin Oncol* 21: 3885-3887

Yu F, Yao H, Zhu P, Zhang X, Pan Q, Gong C, Huang Y, Hu X, Su F, Lieberman J, Song E (2007) let-7 regulates self renewal and tumorigenicity of breast cancer cells. *Cell* 131: 1109-1123

Yu J, Zhang L, Hwang PM, Rago C, Kinzler KW, Vogelstein B (1999) Identification and classification of p53-regulated genes. *Proc Natl Acad Sci U S A* 96: 14517-14522

Zamore PD, Tuschl T, Sharp PA, Bartel DP (2000) RNAi: double-stranded RNA directs the ATP-dependent cleavage of mRNA at 21 to 23 nucleotide intervals. *Cell* 101: 25-33

Zhang J, Espinoza LA, Kinders RJ, Lawrence SM, Pfister TD, Zhou M, Veenstra TD, Thorgeirsson SS, Jessup JM (2012) NANOG modulates stemness in human colorectal cancer. *Oncogene* doi: 10.1038/onc.2012.461.

Zhao J, Lammers P, Torrance CJ, Bader AG (2013) TP53-independent Function of miR-34a via HDAC1 and p21. *Mol The;.* doi: 10.1038/mt.2013.148

Zlobec I, Lugli A (2008) Prognostic and predictive factors in colorectal cancer. *J Clin Pathol* 61: 561-569

11) Abbreviations

5-FU	5-fluorouracil
ABCG2	ATP-binding cassette sub-family G member 2
Ago	argonaute protein
APS	ammonium peroxodisulfate
Bcl-2	B-cell lymphoma 2
bp	basepairs
BTG4	B-cell translocation gene 4
CD	cluster of differentiation
CDC20	cell-division cycle protein 20
CDK	cyclin-dependent kinase
cDNA	complementary DNA
(q)ChIP	(quantitative) chromatin immunoprecipitation
CI	confidence interval
c-Kit	v-kit Hardy-Zuckerman 4 feline sarcoma viral oncogene homolog
c-Met/HGFR	hepatocyte growth factor receptor
c-Myc	v-MYC avian myelocytomatosis viral oncogene homologue
CpG	cytidine-phosphate-guanidin
CRC	colorectal cancer
CSC	cancer stem cell
Cy3	cyanine 3
DAPI	2-(4-amidinophenyl)-6-indolecarbamidine dihydrochloride
DMEM	Dulbecco`s modified Eagles medium
DMSO	dimethyl-sulfoxide
DNA	deoxyribonucleic acid
DNMT	DNA-methyltransferase
DOX	doxycycline
E.coli	*Escherichia coli*
E-box	enhancer box
ELK1	ETS-like gene 1
EMT	epithelial-mesenchymal transition
Erk	extracellular signal-regulated kinase
ETS	E-twenty six
FACS	fluorescence-activated cell sorting
FBS	fetal bovine serum
FOXO3	forkhead box O3
GAPDH	glyceraldehyde 3-phosphate dehydrogenase
gDNA	genomic DNA
GFP	green fluorescent protein
GIST	gastrointestinal stromal tumor
HBSS	Hanks`balanced salt solution

HDAC	histone deacetylase
HDF	human diploid fibroblast
HGF	hepatocyte growth factor
HRP	horseradish peroxidase
IF	immunofluorescence
IHC	immunohistochemistry
LEF1	lymphoid enhancer-binding factor 1
Lgr5	leucine rich repeat containing G protein coupled receptor 5
MAPK	mitogen-activated protein kinase
MBP	methyl-CpG-binding domain protein
MDM2	mouse double minute 2 homolog
MEK1/MAP2K1	dual specificity mitogen-activated protein kinase kinase 1
MET	mesenchymal-epithelial transition
miR(NA)	microRNA
MK5	MAP kinase-activated protein kinase 5
mRNA	messenger RNA
MSP	methylation specific PCR
MTA2	metastasis-associated protein MTA2
mTOR	mammalian target of rapamycin
OR	odds ratio
ORF	open reading frame
PARP	poly (ADP-ribose) polymerase
PBS	phosphate buffered saline
(q)PCR	(quantitative) polymerase chain reaction
PDGF	platelet-derived growth factor
PDGFR	platelet-derived growth factor receptor
PI3K	phosphoinositide-3-kinase
pri-miR(NA)	primary microRNA transcript
Rb	retinoblastoma protein
RFP	red fluorescent protein
RISC	RNA induced silencing complex
RNA	ribonucleic acid
RNAi	RNA interference
RNAPol	RNA polymerase
RT	room temperature
RTK	receptor tyrosine kinase
SATB2	special AT-rich sequence-binding protein 2
SCF	stem cell factor
SD	standard deviation
SDS	sodium dodecyl sulfate
SBS	Snail binding site
STAT	signal transducers and activators of transcription
TAR	transactivation-responsive
TCF	T cell transcription factor

Temed	tetramethylethylenediamine
Tet	tetracycline
TF	transcription factor
TRBP	(TAR) RNA binding protein
TSS	transcription start site
tTa	tetracycline-controlled transactivator
U	unit
UTR	untranslated region
VSV	vesicular stomatitis virus (tag)
WB	Western blot
ZEB	zinc finger E-box-binding homeobox protein

Acknowledgement

There are many people, who I owe a debt of deep gratitude as they have made this work possible:

First of all, I am sincerely grateful to Prof. Dr. Heiko Hermeking for giving me the opportunity to work on a fascinating project, for accompanying my work with his scientific interest, discussions and ideas, for arranging successful collaborations with other scientists and for the great support with all the smaller and bigger problems that arose in the years I spent in his laboratory.

I also want to thank the reviewers of my thesis for taking the time and effort to evaluate my writing.

I would like to thank all the past and present members of the group for helpfulness, scientific suggestions and discussions. In particular, I want to thank Stefanie Hahn, Sabine Hünten, Rene Jackstadt and Dr. Markus Kaller for the excellent scientific help, constructive and interesting discussions, and for being more than just bench neighbors. Moreover, I am grateful to Dr. Antje Menssen for important and essential scientific suggestions and ideas. I also want to include Ursula Götz for the exquisite technical support.

I would like to thank Dr. Jens Neumann for the great collaboration on the M0/M1 collection, especially the selection and evaluation of clinical samples, his advices and for sharing his enthusiasm for histopathology. I also would like to acknowledge the technical assistants Mona Melz, Anja Heyer and Andrea Sendelhofert, who performed the immunohistochemical staining of the samples. Moreover, it was also a great pleasure to work with Prof. Dr. Ulrich Mansmann, who helped me a lot with the analysis and interpretation of the data.

I am deeply grateful to my fantastic family for their patience and support during the past years and who I can count on in every second. And last but not least I want to thank Diana for her permanent and unconditional support.